

FLOOD PROPAGATION COMPUTATION BY MUSKINGUM METHODS

*A Thesis Submitted
in Partial Fulfilment of the Requirement
for the Degree of*
MASTER OF TECHNOLOGY

by

KANDUKURI NARESH BABU

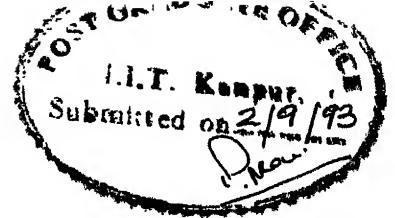
to the

**DEPARTMENT OF CIVIL ENGINEERING
INDIAN INSTITUTE OF TECHNOLOGY KANPUR
SEPTEMBER, 1993**

CE-1993-M- BAB-FLO

09 OCT 1993 / CE
CENTRAL LIBRARY
I. I. T. KANPUR
Inv. No. A.116521

-TH
627.4
B 119 f



CERTIFICATE

It is certified that the work contained in the thesis entitled, " FLOOD PROPAGATION COMPUTATION BY MUSKINGUM METHODS " by Mr. Kandukuri Naresh Babu, has been carried out under my supervision and this work has not been submitted elsewhere for a degree.

K. Subramanya
(Dr. K. Subramanya)

Professor

Civil Engineering Deptt.

ABSTRACT

In this study, the basic Muskingum method, the Muskingum-Cunge method (MC) and the various improvements of MC method are discussed. At first, MC method of flood routing is compared with that of the implicit Preissmann scheme. It has been found that the MC method has less attenuation and more translation of outflow peak discharge. The MC method predicts more initial flows than the implicit Preissmann scheme.

To improve the MC method, an attempt is made by changing its forward finite difference scheme into a Leap frog finite difference scheme, named MCLF model. It has been found that this proposed model is of second order accurate scheme and the numerical diffusion is eliminated considerably. Further, the solution approaches the analytical solution of the kinematic wave equation, creating very less attenuation of peak discharge and hence do not adequately represent the physical phenomena.

To predict the better initial flows by the MC method, a method of segregating IH which uses the MC method called SMC model is proposed. The SMC model predicts the flows upto the first Q_{50} more accurately than the MC method.

A different approach is made to improve the MC method by using the Laplace transform solution of a step input function for Muskingum equation with the relevant boundary conditions. This model is named as MLT model. In the MLT model, the given IH is approximated to a input staircase function and routed explicitly. The MLT method predicts outflow peaks to the same degree of accuracy as the MC method. The time of occurrence of the routed peak outflow is also predicted to the same degree of accuracy as in the MC method. The MLT method is thus a viable alternative to the MC method.

ACKNOWLEDGEMENTS

I express my greatest appreciation to my supervisor, Professor *K.Subramanya*. He has always given me freedom to pursue my own interest and at the same time provided all the support, guidance and encouragement I needed. Learning how to do research from him and discussing problems with him have become some of my most joyful experiences at IITK. Furthermore, I am greatly indebted to *Dr.B.S.Murty* for giving me many needed suggestions and help during my study at IITK. I also like to thank Professors Rama Seshan, Surya Rao, Gangadharaiah and Bithin Datta for the excellent courses offered by them.

I would like to thank Alok, Malhal, Ravi Motwani, Sitharam, Jiwa, Sai and Manish with whom I discussed, shared my joys and worries. I owe a great deal to my sibs Anita, Rohini and Srinu. Their inspiration, expectation and confidence have been a great source of support to me.

To, my Parents with Love

Table of Contents

	Page
CERTIFICATE.....	ii
ABSTRACT.....	iii
Acknowledgements.....	v
List of Figures.....	ix
Notation.....	xii
1. Introduction.....	1
2. Literature Review	
2.1 Kinematic wave model.....	4
2.2 Muskingum method of Flood Routing.....	5
2.3 Muskingum-Cunge method.....	11
2.4 Muskingum-Cunge method with Variable Parameters..	14
2.5 Simplified Muskingum Routing Equation	17
2.6 Muskingum method as proposed by Koussis.....	17
2.7 Least Squares Parameter Estimation for Muskingum Flood Routing.....	19
2.8 Muskingum method with Variable Parameters of V.P.Singh.....	21
3. Analysis of Kinematic Routing	
3.1 First order Differential Equation for one-to-one Stage-Discharge Relationship.....	26

3.2 Leap-Frog Finite Difference Scheme.....	29
3.3 Stability analysis.....	30
3.4 Method of Routing.....	31
3.5 Discussion.....	36
4. Modification of MC method Through Segregation of Input Hydrograph	
4.1 Earlier Studies.....	37
4.2 Segregation Model.....	40
4.3 Numerical Experimentation.....	41
4.4 Conclusion.....	55
5. Laplace Transform Method	
5.1 Routing of a Step Input.....	57
5.2 Routing of Inflow Hydrograph by Step Input Functions.....	61
5.3 Estimation of Parameters K and θ	62
5.4 Proposed Algorithm of Muskingum-Laplace-Transform	64
5.5 Numerical Experimentation.....	65
5.6 Conclusion.....	79
6. Conclusions and Recommendations.....	83
References.....	7
Appendix-1 Preissmann Scheme for Numerical Solution of St.Venant Equations.....	90
Appendix-2 Input Data.....	96

Fig. 2.1	<i>x-t</i> Plane: Finite difference grid For Muskingum-Cunge Model.....	11
Fig. 2.2	Curve for Stability.....	15
Fig. 2.3	Computational cell.....	16
Fig. 2.4	Comparison of results from Preissmann and Moin - Triangular IH.....	25
Fig. 2.5	Comparison of results from Preissmann and Moin - Log Pearson type III IH.....	25
Fig. 3.1	A River reach.....	28
Fig. 3.2	<i>x-t</i> Plane: Finite difference grid for a Leap Frog Scheme.....	29
Fig. 3.3	Comparison of results from the MC and MCLF methods - Normal IH.....	34
Fig. 3.4	Attenuation of peak discharge in MC and MCLF methods - Normal IH.....	34
Fig. 3.5	Comparison of results from MC and MCLF methods - Steep rise IH.....	35
Fig. 3.6	Attenuation of peak discharge in MC and MCLF methods - Steep rise IH.....	35
Fig. 4.1	Inflow hydrograph.....	39
Fig. 4.2	Complex hydrograph.....	39
Fig. 4.3	Stratification of a IH.....	38
Fig. 4.4a	Segregation of IH.....	40
Fig. 4.4b	Segregation of Complex IH.....	42

Fig. 4.5	Comparison of SMC model with the MC and Preissmann models --- Normal IH.....	46
Fig. 4.6	Flows upto Q_{50} in the SMC, MC and the Preissmann models ---- Normal IH.....	46
Fig. 4.7	Comparison of SMC model with the MC and Preissmann models --- Steep rise IH.....	47
Fig. 4.8	Flows upto Q_{50} in the SMC, MC and the Preissmann models ---- Steep rise IH.....	47
Fig. 4.9	Comparison of SMC model with the MC and Preissmann models --- Complex IH.....	50
Fig. 4.10	Flows upto Q_{50} in the SMC, MC and the Preissmann models ---- Complex IH.....	50
Fig. 4.11	Comparison of SMC model with the MC and Preissmann models --- Complex IH.....	53
Fig. 4.12	Flows upto Q_{50} in the SMC, MC and the Preissmann models ---- Complex IH.....	53
Fig. 4.13	Comparison of SMC model with the MC and Preissmann models --- Complex IH.....	54
Fig. 4.14	Flows upto Q_{50} in the SMC, MC and the Preissmann models ---- Complex IH.....	54
Fig. 5.0	Definition Sketch.....	59
Fig. 5.1	Stair case approximation of a IH.....	61
Fig. 5.2	Comparison of MLT model with the MC and the Preissmann models - Normal IH.....	68
Fig. 5.3	Attenuation of peak discharge in MLT, MC and the Preissmann models - Normal IH.....	68

Fig. 5.4	Comparison of MLT model with the MC and the Preissmann models - Steep rise IH.....	71
Fig. 5.5	Attenuation of peak discharge in MLT,MC and the Preissmann models - Steep rise IH.....	71
Fig. 5.6	Comparison of MLT model with the MC and the Preissmann models - Triangular IH.....	74
Fig. 5.7	Attenuation of peak discharge in MLT,MC and the Preissmann models - Triangular IH.....	74
Fig. 5.8	Comparison of MLT model with the MC and the Preissmann models - Log Pearson Type III IH.....	78
Fig. 5.9	Attenuation of peak depth in MLT,MC and the Preissmann models - Log Pearson type III IH.....	78
Fig. 5.10	Comparison of DMLT model with the MLT and Preissmann models - Normal IH.....	80
Fig. 5.11	Negative Flows in DMLT.....	80
Fig. A.1	Definition Sketch.....	90
Fig. A.2	Computational grid.....	93

NOTATION

A	cross-sectional area
B	breadth of channel
c	celerity
CN	Courant number
g	acceleration due to gravity
i	distance node
I_0	Inflow ordinate at time $t = 0$
I	inflow at any time
j	time node
K	average reach travel time
L	length of reach
n	Manning's roughness coefficient
P	variable to transform time domain to Laplace domain
Q	outflow at any time
Q_p	peak discharge
S	Storage
s_0	bed slope
t	time
v	flow velocity
x	distance in direction of flow
y	depth of flow
Δt	time increment
Δx	distance increment
θ	Coefficient reflecting effect of Inflow and outflow

CHAPTER-1

INTRODUCTION

Flood routing is the technique of determining the flood hydrograph at a section of river by utilizing the data of flood flow at one or more upstream sections. The hydrologic analysis of problems such as flood forecasting, flood protection, reservoir design and spillway design invariably include flood routing. In these applications, two broad categories of routing can be recognized. These are:

1. Reservoir routing.
2. Channel routing.

In reservoir routing the effect of flood wave entering a reservoir is studied. In channel routing the changes in the shape of a hydrograph as it travels down a channel is studied. Flood routing for channels may be done by using the systems approach, also called as hydrologic flood routing. If flood routing is done by a process approach, it is called hydraulic flood routing. The hydrologic modeling involves a conceptual modeling whereas the later is done by mathematical modeling. Hydrologic channel routing is based on the storage concept. The hydraulic models are based on the solution of a pair of non-linear partial differential equations, the Saint Venant equations, based on the principles of

CHAPTER-1

INTRODUCTION

Flood routing is the technique of determining the flood hydrograph at a section of river by utilizing the data of flood flow at one or more upstream sections. The hydrologic analysis of problems such as flood forecasting, flood protection, reservoir design and spillway design invariably include flood routing. In these applications, two broad categories of routing can be recognized. These are:

1. Reservoir routing.
2. Channel routing.

In reservoir routing the effect of flood wave entering a reservoir is studied. In channel routing the changes in the shape of a hydrograph as it travels down a channel is studied. Flood routing for channels may be done by using the systems approach, also called as hydrologic flood routing. If flood routing is done by a process approach, it is called hydraulic flood routing. The hydrologic modeling involves a conceptual modeling whereas the later is done by mathematical modeling. Hydrologic channel routing is based on the storage concept. The hydraulic models are based on the solution of a pair of non-linear partial differential equations, the Saint Venant equations, based on the principles of

mass and momentum conservation.

There are broadly two techniques to solve the hydrodynamic Saint-Venant equations

1. Approximate methods which are based on equations of continuity and on a drastically curtailed equations of motion.
2. Complete Numerical methods which solve the basic Saint-Venant equations through numerical modeling[23].

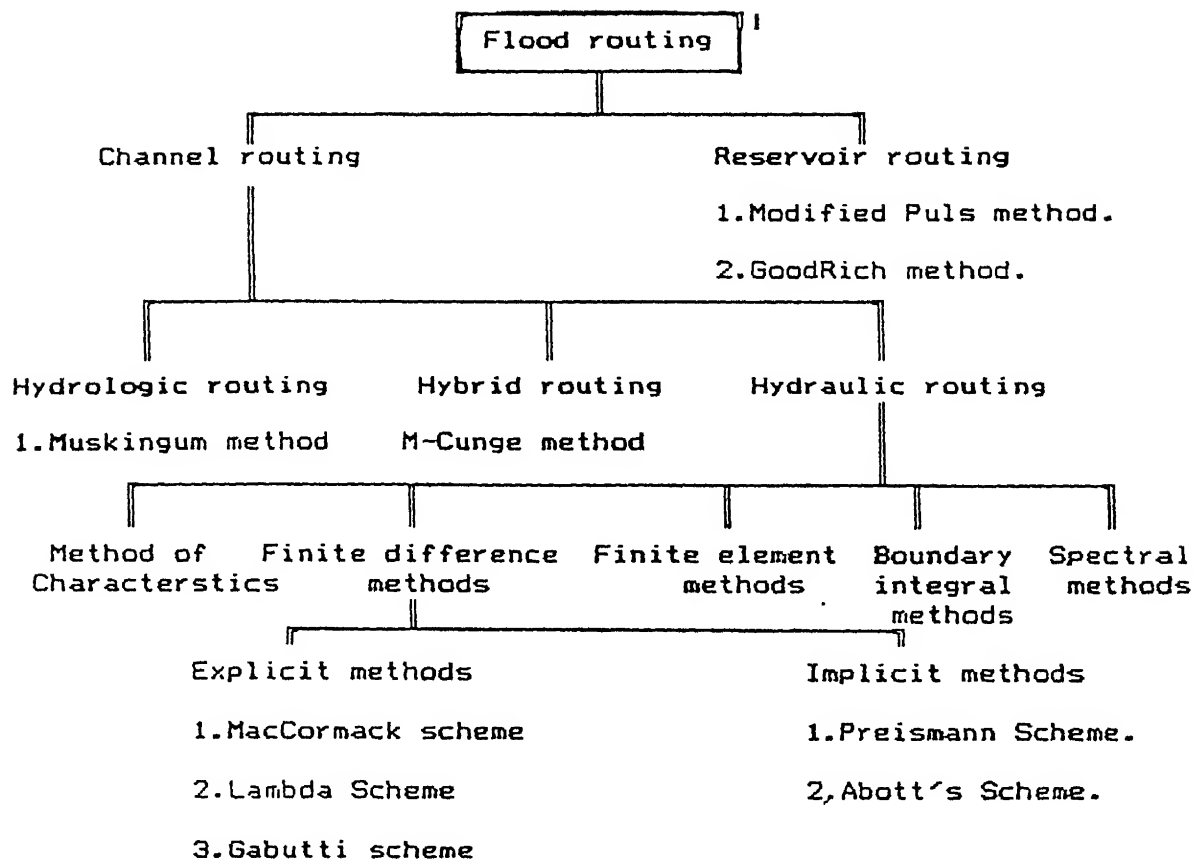
There is a hybrid approach which is similar in nature to hydrologic routing methods, yet contains sufficient physical information to compare favorably with the more complex hydraulic routing techniques. This hybrid approach is the basis of Muskingum-Cunge method of flood routing.

The Muskingum method is a hydrologic model which is more a conceptual model with empirically determined storage functions. The direct relationship between the steady flow rating function $Q = F(y)$ and the storage function provides a basis for this mode.

The Muskingum-Cunge method is a hybrid model in which the routing parameters are calculated as a function of the following physical properties:

- 1) Reach length Δx
- 2) Peak discharge Q_p
- 3) Kinematic wave celerity c
- 4) Bottom slope s_0 .

The various flood routing methods are shown in the Flow chart-1.



Note: 1, 2, 3 are examples only

Flow Chart for methods of flood routing

The basic Muskingum method, the Muskingum-Cunge method and its various variations (improvements) are discussed in Chapter 2. In Chapter 3, an analytical method which is developed by using a Leap-frog scheme is presented. A technique of Muskingum-Cunge routing by segregating the input hydrograph is developed and its characteristics are discussed in Chapter 4. An approach for routing the flood by a lumped model is empirically developed by making use of the solution to a step input function of Muskingum equation with suitable boundary conditions in Chapter 5. Chapter 6 discusses the significant conclusions of this study.

CHAPTER-2

LITERATURE REVIEW

2.0 INTRODUCTION:

A general form of the resistance formulas, such as Chezy or Manning may be written as

$$Q = C' A R^m \sqrt{s_f} \quad (2.1)$$

where C' is the empirical constant, R is the hydraulic radius, m is an exponent and s_f is the slope of the energy grade line. In Chezy's formula, $C' = C$, $m = 0.5$. For steady uniform flows, Q is the normal discharge Q_n and $s_f = s_o$.

2.1 KINEMATIC WAVE MODEL:

For steady uniform flows Eq(2.1) becomes

$$Q_n = C' A R^m \sqrt{s_o} \quad (2.2)$$

Eliminating $C'AR^m$ from Eq(2.1) and Eq(2.2), we obtain

$$Q = \frac{Q_n}{\sqrt{s_o}} \sqrt{s_f} \quad (2.3)$$

From the dynamic equation

$$s_f = s_o - \frac{dy}{dx} - \frac{V}{g} \frac{dV}{dx} - \frac{1}{g} \frac{dV}{dt} \quad (2.4)$$

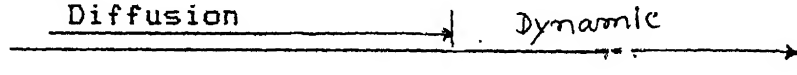
Substitution of expression for s in Eq(2.3) yields

$$Q = Q_n \sqrt{1 - \frac{1}{s_o} \frac{dy}{dx} - \frac{V}{s_o g} \frac{dV}{dx} - \frac{1}{s_o g} \frac{dV}{dt}} \quad (2.5)$$

Kinematic

Diffusion

Dynamic



The Eq(2.5) demonstrates the distinguishing characteristic of the kinematic wave model, that the (Eq A1-2) discharge is always equal to the normal discharge and is thus a single valued function of depth. The St. Venant equations(Eqs..A1-2) reduce to

$$\frac{\partial A}{\partial t} + \frac{\partial Q}{\partial x} = q \quad (2.6)$$

and $Q = Q_n = C A R^m \sqrt{s_o}$ (2.7)

This system can be combined into a single equation commonly referred to as kinematic wave equation, as

$$\frac{1}{c} \frac{\partial Q}{\partial t} + \frac{\partial Q}{\partial x} = q \quad (2.8)$$

in which the coefficient $1/c$ is either a constant (linear models) or a variable (non linear models). The parameter c , describing the travel speed of flood wave is called the kinematic wave speed, and may, at a particular cross-section and for a given Q , can be evaluated from Kleitz- Seddon's law as

$$c = \left(\frac{dQ}{dA} \right)_x = \frac{1}{B} \left(\frac{dQ}{dy} \right)_x \quad (2.9)$$

2.2 MUSKINGUM-METHOD OF FLOOD ROUTING:

In the Muskingum method of routing, the form of continuity equation used in the lumped model states that, for a given time interval, the difference between the inflow to a reach and the outflow from the reach must be equal to the change of storage within the reach. Mathematically, the storage equation is

$$\frac{dS}{dt} = I(t) - Q(t) \quad (2.10)$$

and storage - discharge relationship is given by a linear relationship.

$$S = K [\theta I + (1 - \theta)Q] \quad (2.11)$$

where K and θ are routing parameters. Physically, K is considered as the average reach travel time in the reach, and θ is a coefficient reflecting the relative effects of inflow and outflow on each storage.

Expressing Eq(2.10) in the finite-difference form and then substituting Eq(2.11)

$$\left(\frac{I_t + I_{t+\Delta t}}{2} \right) \Delta t - \left(\frac{Q_t + Q_{t+\Delta t}}{2} \right) = K \left[\theta (I_{t+\Delta t} - I_t) + (1-\theta) (Q_{t+\Delta t} - Q_t) \right] \quad (2.12)$$

in which Δt is routing period or descretization time interval.

Rearranging and solving for $Q_{t+\Delta t}$

$$Q_{t+\Delta t} = C_0 I_{t+\Delta t} + C_1 I_t + C_2 Q_t \quad (2.13)$$

$$C_0 = - \frac{K \theta + 0.5 \Delta t}{C_3} \quad (2.14a)$$

$$C_1 = \frac{K \theta + 0.5 \Delta t}{C_3} \quad (2.14b)$$

$$C_2 = \frac{K (1-\theta) - 0.5 \Delta t}{C_3} \quad (2.14c)$$

$$\text{where } C_3 = K(1-\theta) + 0.5 \Delta t \quad (2.14d)$$

The coefficients C_0 , C_1 and C_2 are such that $C_0 + C_1 + C_2 = 1.0$

2.2.0 ESTIMATION OF PARAMETERS:

There are a number of methods available for estimating the parameters K and θ of the Muskingum method. The available techniques are

- 1) Graphical estimation

- 2) Moment matching technique
- 3) Optimization technique
- 4) Least squares estimation.

2.2.1 GRAPHICAL ESTIMATION:

In graphical estimation, a trial value of θ is chosen, values of storage S at any time t are plotted against the corresponding $[\theta I + (1-\theta)Q]$ values. If the value of θ is chosen correctly, a straight line relationship will be resulting. If an incorrect value of θ is used, the plotted points will trace a looping curve. By trial and error, a value of θ is so chosen that the data very nearly describe a straight line. The inverse of this straight line will give the value of K . Details are available in Subramanya[24].

2.2.2 METHOD OF MOMENTS:

This method is based on first determining the moments of the Instantaneous unit hydrograph (IUH), $h(t)$ of the reach and then expressing these moments in terms of the moments of inflow and outflow. The parameters K and θ are then estimated as [22]:

$$h(t) = \frac{1}{K(1-\theta)^2} e^{-t/(K(1-\theta))} - \frac{\theta}{1-\theta} \delta(t)$$

where $h(t)$ is the IUH of the reach

$\delta(t)$ is the Dirac δ function or impulse inflow.

$$K = M_1^O(Q) - M_1^O(I) \quad (2.15)$$

$$\theta = 0.5 \times \left\{ 1 - \frac{M_2(Q) - M_2(I)}{K^2} \right\} \quad (2.16)$$

In this $M_1^O(Q)$, $M_1^O(I)$ are the first moments of the outflow and

inflow hydrographs about the origin.

$M_2(Q)$, $M_2(I)$ are the second moments of outflow and inflow hydrographs about their respective centre of gravity.

2.2.3 OPTIMIZATION TECHNIQUE:

The direct optimization method [22] is based on directly determining the coefficients C_0 , C_1 , C_2 in Eq(2.13) without first estimating K and θ in Eq(2.14). This would involve minimizing the error function in comparing observed hydrograph with computed hydrograph. Again, the error function can be defined in a least squares sense or differently. There are in fact only two unknowns, since the third can be obtained from $C_0 + C_1 + C_2 = 1.0$. Let us consider C_1 and C_2 to be the unknowns. Then Eq(2.13) reduces to

$$Q_{t+\Delta t} - I_{t+\Delta t} = C_1 (I_{t+\Delta t} - I_t) + C_2 (I_{t+\Delta t} - Q_t) \quad (2.17)$$

The coefficients C_1 and C_2 can be derived by comparing flows of a known inflow hydrograph with flows of the corresponding outflow hydrograph.

Let us define

$$R = Q_{t+\Delta t} - I_{t+\Delta t}$$

$$F = I_{t+\Delta t} - I_t$$

$$G = I_{t+\Delta t} - Q_t$$

Eq(2.17) can be rewritten as

$$R = C_1 F + C_2 G$$

which is identical in form to Eq(2.13) with $C_0 = 0.0$.

Therefore,

$$C_1 = \left(\frac{\sum R_o F \sum G^2 - \sum R_o G \sum FG}{\sum F^2 \sum G^2 - (\sum FG)^2} \right)$$

$$C_2 = \left(\frac{\sum R_o G \sum F^2 - \sum R_o F \sum FG}{\sum F^2 \sum G^2 - (\sum FG)^2} \right)$$

Where R_o is observed R . Then C_o can be computed from $C_o = 1 - C_1 - C_2$.

It can be obtained

$$\theta = \frac{C_1 + 0.5 C_2 - 0.5}{C_1 + C_2} \quad (2.18)$$

$$K = \frac{\Delta t (C_1 + C_2)}{1 - C_2} \quad (2.19)$$

2.2.4 LEAST SQUARES METHOD:

The least squares method is based on minimizing the sum of deviations between observed storage and estimated storage for a given inflow and outflow sequence. That is,

$$E = \sum_{j=1}^N [S_o(j) - S_e(j)]^2 \rightarrow \min \quad (2.20)$$

where E is the error function to be minimized, $S_o(j)$ is the observed storage for the j^{th} time interval, $S_e(j)$ is the estimated storage for the j^{th} time interval, and N is the number of observations or data.

The estimated storage should be given by Eq(2.11) can be modified to incorporate the difference C between relative and absolute storage.

$$S = K [\theta I + (1-\theta) Q] + C \quad (2.21)$$

If the flood wave is starting on a dry river bed, the parameter C will vanish. First considering the case $c \neq 0$. Substituting Eq(2.21) into Eq(2.22) and dropping the index for brevity,

$$E = \sum_{j=1}^N [S_o - K \theta I - K(1-\theta) Q - C]^2 \rightarrow \min \quad (2.22)$$

Differentiating Eq(2.22) with respect to A, B, C equating each time to zero, and re-arranging,

$$\sum S_o I = A \sum I^2 + B \sum QI + C \sum I$$

$$\sum S_o Q = A \sum IQ + B \sum Q^2 + C \sum Q$$

$$\sum S_o = A \sum I + B \sum Q + CN$$

Solving for A, B, C

$$A = \frac{y_1}{y_2} - \frac{y_3}{y_2} \quad B = \frac{y_1 z_2 - y_2 z_1}{y_3 z_2 - y_2 z_3}$$

$$C = \frac{\sum S_o - A \sum I - B \sum Q}{N} \quad (2.23)$$

$$y_1 = \sum S_o I - \frac{\sum S_o - \sum I}{N}$$

$$y_2 = \sum I - \frac{(\sum I)^2}{N}$$

$$y_3 = \sum IQ - \frac{\sum Q \sum I}{N}$$

$$z_1 = \sum S_o Q - \frac{\sum S_o \sum Q}{N}$$

$$z_2 = \sum IQ - \left(\frac{\sum I \sum Q}{N} \right)$$

$$z_3 = \sum Q^2 - \frac{(\sum Q)^2}{N}$$

Therefore, $K = A+B$ (2.24a)

$$\theta = \frac{A}{K} \quad (2.24b)$$

Equations (2.23) and (2.24) give the parameters K, θ and C for a known inflow-outflow sequence.

If C = 0, then the error function E follows:

$$E = \sum_1^N [S_o - K \theta I - (1-\theta) KQ]^2 \Rightarrow \min \quad (2.25)$$

Using A and B as defined before, differentiating E with respect to A and B and equating each time to zero.

$$\sum S_o I = A \sum I^2 + B \sum IQ$$

$$\sum S_o Q = A \sum IQ + B \sum Q^2$$

Solving for A and B,

$$A = \frac{\sum S_o I \sum Q^2 - \sum S_o Q \sum I Q}{\sum I^2 \sum Q^2 - (\sum I Q)^2} \quad (2.26)$$

$$B = \frac{\sum S_o Q \sum I^2 - \sum S_o I \sum I Q}{\sum I^2 \sum Q^2 - (\sum I Q)^2} \quad (2.27)$$

Therefore, $K = A + B$, $\theta = \frac{A}{K}$.

COMMENT: Of all the above four methods, the moment matching technique is easily adoptable and simple to use. In this study, the moment matching technique is used, to estimate the routing parameters K and θ when the inflow and outflow hydrographs are given.

2.3 MUSKINGUM-CUNGE METHOD:

In the Muskingum-Cunge[6] method (MC method), for the kinematic wave model an explicit finite difference scheme had been proposed. The space time grid is as follows :

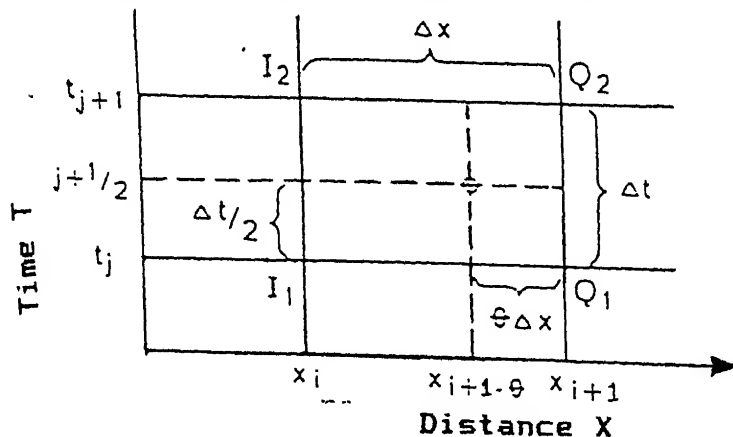


Fig. 2.1 x-t Plane: Finite difference grid for
Muskingum-Cunge Model

In the above Fig. 2.1, the scheme introduces a weighing coefficient θ , in the finite difference representation of the time

derivative. Evaluating the finite difference quotients for the space and time derivatives at the point $i+1-\theta$, $j+1/2$, the kinematic wave equation for the zero lateral inflow, may be written in finite difference form as

$$\left\langle \frac{1}{c} \right\rangle \frac{\theta(I_2 - I_1) + (1-\theta)(Q_2 - Q_1)}{\Delta t} + \frac{Q_1 + Q_2 - I_1 - I_2}{2 \Delta x} = 0.0 \quad (2.28)$$

in which $\langle 1/c \rangle \neq f(t)$; and $\langle c \rangle$ is an average value of c for the reach.

Introducing the travel time parameters $K = \frac{\Delta x}{\langle c \rangle}$, the solution of Eq(2.28) for Q_2 can be reduced to form identical to the classical Muskingum coefficient equation.

$$Q_2 = C_1 I_1 + C_2 I_2 + C_a Q_1 \quad (2.29a)$$

where ,

$$C_1 = \frac{K\theta + \frac{\Delta t}{2}}{K(1-\theta) + \frac{\Delta t}{2}} \quad (2.29b)$$

$$C_2 = \frac{-K\theta + \frac{\Delta t}{2}}{K(1-\theta) + \frac{\Delta t}{2}} \quad (2.29c)$$

$$C_a = \frac{K(1-\theta) - \frac{\Delta t}{2}}{K(1-\theta) + \frac{\Delta t}{2}} \quad (2.29d)$$

Cunge[6] showed that the Muskingum scheme is a second -order approximation of the diffusion equation if the parameters are evaluated as

$$K = \frac{\Delta x}{\langle c \rangle} \quad (2.30)$$

$$\theta = 0.5 \times \left(1 - \frac{Q}{B s_o \frac{Q}{c \Delta x}} \right) \quad (2.31)$$

and $0 < \theta < 0.5$.

This Eq(2.31) for the weighting coefficient θ was obtained

from the Taylor series expansion of $Q(x_j, y_j)$ in the finite difference form of Eq(2.28) and a comparison with the coefficients of the diffusion equations for regular channels.

2.3.2. Raudikivi's Algorithm For Estimation Of Parameters:

Raudikivi [20] has given a simplified technique for routing of a flood using MC method. The algorithm for calculating the values of K and θ as suggested by Raudikivi is as follows :

Given the reach length L , peak discharge Q_p whose time of occurrence is T_p , breadth of channel B , whose bed slope s_o ,

1. Determine or assume L/T_p , the wave celerity c .
2. Select the sub reach length Δx .
3. Calculate $\alpha_p = \frac{1}{2} \frac{L}{B s_o}$.
4. Calculate the radius of curvature at peak

$$\frac{d^2 Q_p}{dt^2} = \frac{Q_{-1} + Q_1 - 2 Q_p}{(\Delta t)^2}$$

where Q_{-1} and Q_1 are the discharges on either side of the peak discharges and Δt is the time period of given inflow hydrograph.

$$5. \text{ Calculate } Q^* = \frac{\alpha_p}{(L/T_p)^3} Q_p \left| \frac{d^2 Q_p}{dt^2} \right|$$

If $Q^* \leq 0.1 Q_p$; then $c = L/T_p$

If $Q^* > 0.1 Q_p$ redefine Q^* as

$$Q_{\text{new}}^* = Q_p \left[1 - \exp \left(- \frac{Q^*}{Q_p} \right) \right]$$

$$c = \frac{L}{T_p} - \frac{2 \alpha_p}{L^2} Q_{\text{new}}^*$$

$$6. \bar{Q}_p = Q_p - 0.5 Q^* \text{ if } (Q^* < 0.1 Q_p)$$

$$\bar{Q}_p = Q_p - 0.5 Q_{new}^* \text{ if } (Q^* > 0.1 Q_p)$$

7. The parameters K and θ are calculated as

$$K = \frac{\Delta x}{\langle c \rangle} \quad \text{and} \quad \theta = \frac{1}{2} - \frac{\alpha \bar{Q}_p}{L \Delta x \langle c \rangle}$$

where $\frac{\Delta x}{c \Delta t}$ must be less than the value given by the curve in

Fig. 2.2 which can be approximated as

If θ is less than 0.10

$$y = 1422.55 \theta^3 - 283.10 \theta^2 + 20.08 \theta$$

If θ is greater than or equal to 0.10

$$y = -1.665 \theta^2 + 2 \theta + 0.417$$

$$\text{where } y = \frac{\Delta x}{c \Delta t}$$

8. Estimate C_1 , C_2 and C_3 by Eqns (2.18)

2.4 MUSKINGUM-CUNGE METHOD WITH VARIABLE PARAMETERS:

Ponce and Yevjevich [18] have modified the MC method by defining the Courant number and cell Reynolds number in the following way.

The equation for Q_2 is as given below:

$$Q_2 = C_1 I_1 + C_2 I_2 + C_3 Q_1$$

On re-arranging the coefficients C_1 , C_2 , C_3 such that $C = \frac{c \Delta t}{\Delta x}$

which is the Courant number and $D = \left(\frac{Q}{B s_0} / c \Delta x \right)$ a type of cell

Reynolds number. They obtained the coefficients in terms of C and D as

$$C_1 = \frac{1 + C - D}{1 + C + D} \quad (2.32a)$$

$$C_2 = \frac{-1 + C + D}{1 + C + D} \quad (2.32b)$$

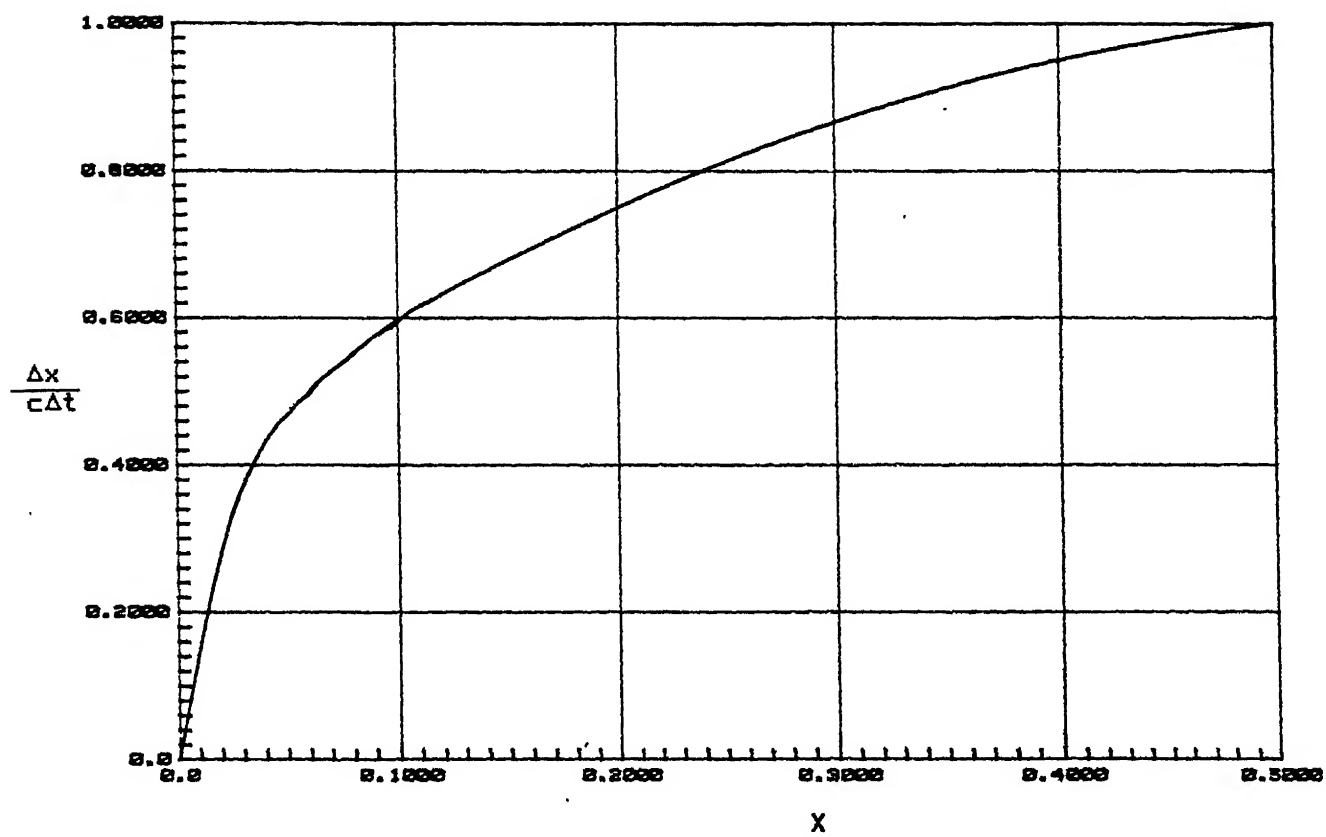


Fig. 2.2, Curve for Stability

$$C_a = \frac{1-C+D}{1+C+D} \quad (2.32c)$$

Usually, Δt is fixed, and Δx and s_o are specified for each computational cell consisting of grid points.

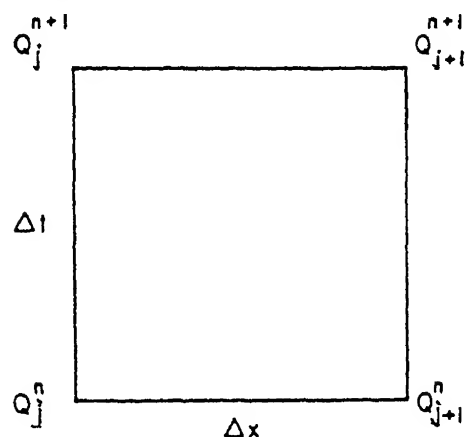


Fig. 2.3 Computational cell

Therefore, it is necessary to determine the flood wave celerity c and width discharge, q for each computational cell. The values of c and q at grid point (j,n) are defined by

$$c = \left. \frac{\partial Q}{\partial A} \right|_{j,n} \quad (2.33a)$$

$$q = \left. \frac{Q}{B} \right|_{j,n} \quad (2.33b)$$

in which Q = discharge; A = Flow area; B = top width. The values of C and D are calculated from which the routing coefficients C_1 , C_2 , C_3 are calculated.

COMMENT: This method is a slight modification of MC method in which the routing parameters are estimated for each computational cell. This way, it becomes cumbersome, to calculate the routing coefficients for each cell. The data at each grid point may not be available. Further, it loses the simplicity of MC method.

2.5 SIMPLIFIED MUSKINGUM ROUTING EQUATION:

Ponce[19] modified the MC method to make the calculations simple. The calculations for the lumped parameter mode can be proceeded in one of two ways. The conventional way is to specify space and time intervals Δx and Δt ; parameters K and θ are calculated therefrom. An alternate way is to specify K and θ and to calculate Δt and Δx from them. The proper choice of parameters can lead to a considerable simplification in the routing equation. For calculating the routing coefficients of MC if $\Delta t/K$ and θ are specified as

$$\frac{\Delta t}{K} = 1.0 \quad (2.34)$$

$$\text{and } \theta = 0 ; \quad (2.35)$$

It follows that $C_1 = C_2 = C_3 = 1/3$.

Leading to the simplified form of the Muskingum routing equation as follows:

$$Q_2 = \frac{I_1 + I_2 + Q_1}{3} \quad (2.36)$$

COMMENT: With this method it is not possible to calculate at the desired subreach. When one uses the a computer it loses its significance of easy calculations.

2.6 MUSKINGUM METHOD AS PROPOSED BY KOUSSIS:

Koussis[13] has partially modified the MC method. In the continuity equation he has carried out discretization in space only and retaining continuous functions for the time derivatives. Using

the time derivative the weighted scheme indicated in Fig. 2.1, the above kinematic wave equation, may be written as an partial differential equation as follows:

$$\frac{\partial Q}{\partial t} + \frac{1}{[1/c] \Delta x (1-\theta)} Q = \frac{1}{[1/c] \Delta x (1-\theta)} I - \frac{\theta}{1-\theta} \frac{\partial I}{\partial t} \quad (2.37)$$

with the same assumption for $\langle 1/c \rangle$ as for Eq(2.28) and assuming linear variation of Q over the time interval, Δt , the solution may be written in a form convenient for computation, i.e. as a coefficient equation of the following Muskingum type:

$$Q_2 = C_1 I_1 + C_2 I_2 + C_3 Q_1$$

where the coefficients are now

$$C_1 = \frac{\Delta x}{[c] \Delta t} (1-\beta) - \beta ; \quad (2.38a)$$

$$C_2 = 1 - \frac{\Delta x}{[c] \Delta t} (1-\beta) ; \quad (2.38b)$$

$$C_3 = \beta \quad (2.38c)$$

where
$$\beta = \exp \left[- \frac{[c] \Delta t}{\Delta x (1-\theta)} \right] \quad (2.38d)$$

Koussis demonstrated that this model is a second-order approximation to the diffusion analogy model if

$$\theta = 1 - \frac{r}{\left(\frac{\lambda + 1 + r}{\lambda + 1 - r} \right)} ; \text{ and } 0 < \theta < 0.5 \quad (2.39)$$

where $r = \frac{c \Delta t}{\Delta x}$ and $\lambda = \frac{Q}{B S_o c \Delta x}$. (2.40)

2.7 LEAST SQUARES PARAMETER ESTIMATION FOR MUSKINGUM FLOOD ROUTING:

Aldama[1] has examined the available least square parameter estimation techniques for the Muskingum routing. Gill involves the direct use of Eq(2.11) in estimation of K and θ . Absolute values of storage are rarely available in practice. Gill modified Eq(2.11) by setting $S = S_r - \sigma$; $\alpha = K\theta$; $\beta = K(1-\theta)$; where S_r is relative storage and $-\sigma$ may be interpreted as the initial storage. Hence, the storage - discharge relation may be written as $\hat{S}_{rj} = \sigma + \alpha I_j + \beta Q_j$, where the circumflex denotes estimated. Accordingly, the sum of the squares of the relative storage estimation errors becomes

$$E_s = \sum_{j=1}^N (\hat{S}_{rj} - S_{rj})^2 = \sum_{j=1}^N (\sigma + \alpha I_j + \beta Q_j - S_{rj})^2 \quad (2.41)$$

where S_{rj} = the actual value of relative storage at time $j \Delta t$; and N = the total number of time steps. The minimization of E_s leads to the following explicit expressions for α and β ;

$$\alpha = D^{-1} \left\{ \left(\sum_{j=1}^N I_j Q_j - \frac{\sum_{j=1}^N I_j \sum_{j=1}^N Q_j^2}{\sum_{j=1}^N I_j} \right) \sum_{j=1}^N S_{rj} + \left[N \sum_{j=1}^N Q_j^2 - \left(\sum_{j=1}^N Q_j \right)^2 \right] \cdot \frac{\sum_{j=1}^N I_j S_{rj}}{\sum_{j=1}^N I_j} + \left(\sum_{j=1}^N I_j \sum_{j=1}^N Q_j - N \frac{\sum_{j=1}^N I_j \sum_{j=1}^N Q_j}{\sum_{j=1}^N I_j} \right) \sum_{j=1}^N Q_j S_{rj} \right\} \quad (2.42)$$

and

$$\beta = D^{-1} \left\{ \left(\sum_{j=1}^N I_j - \frac{\sum_{j=1}^N I_j \sum_{j=1}^N I_j Q_j}{\sum_{j=1}^N I_j^2} \right) \sum_{j=1}^N S_{rj} + \left(\sum_{j=1}^N I_j \sum_{j=1}^N Q_j - N \frac{\sum_{j=1}^N I_j \sum_{j=1}^N Q_j}{\sum_{j=1}^N I_j} \right) \sum_{j=1}^N I_j S_{rj} + \left[N \sum_{j=1}^N I_j^2 - \left(\sum_{j=1}^N I_j \right)^2 \right] \sum_{j=1}^N Q_j S_{rj} \right\} \quad (2.43)$$

where

$$D = N \left[\sum_{j=1}^N I_j^2 \sum_{j=1}^N Q_j^2 - \left(\sum_{j=1}^N I_j Q_j \right)^2 \right] + 2 \sum_{j=1}^N I_j \sum_{j=1}^N Q_j \sum_{j=1}^N I_j Q_j \\ - \left(\sum_{j=1}^N I_j \right)^2 \sum_{j=1}^N Q_j^2 - \sum_{j=1}^N I_j^2 \left(\sum_{j=1}^N Q_j \right)^2 \quad (2.44)$$

once α and β are computed, K and θ can be determined as

$$K = \alpha + \beta; \quad \theta = \frac{\alpha}{\alpha + \beta} \quad (2.45)$$

but the estimated outflow, through recursive use of Eq(2.13) as

$$\hat{Q}_{j+1} = I_{j+1} + \sum_{k=0}^{j-1} C_2^k C_a (I_{j-k} - I_{j-k+1})$$

$$\text{where } C_a = C_1 + C_2 \quad (2.46)$$

Thus, minimization of the sum of squares of the outflow rate estimation error leads to

$$\left(\sum_{j=1}^N F_{j+1} \sum_{k=0}^{j-1} C_2^k G_{jk} \right) \left[\sum_{j=1}^N \left(\sum_{k=0}^{j-1} C_2^k G_{jk} \right) \left(\sum_{k=0}^{j-1} K C_2^{k-1} G_{jk} \right) \right] \\ - \left(\sum_{j=1}^N F_{j+1} \sum_{k=0}^{j-1} K C_2^{k-1} G_{jk} \right) \left[\sum_{j=1}^N \left(\sum_{k=0}^{j-1} C_2^k G_{jk} \right)^2 \right] = 0 \quad (2.47)$$

and

$$C_a = - \frac{\sum_{j=1}^N F_{j+1} \sum_{k=0}^{j-1} C_2^k G_{jk}}{\sum_{j=1}^N \left(\sum_{k=0}^{j-1} C_2^k G_{jk} \right)^2} \quad (2.48)$$

$$\text{where } F_j = I_j - Q_j \quad (2.49)$$

$$\text{and } G_{jk} = I_{j-k} - I_{j-k+1} \quad (2.50)$$

Eq(2.47) can be solved iteratively for C_2 and then C_a can be computed. K and θ may be obtained in terms of C_2 and C_a as

$$K = \frac{C_a \Delta t}{(1 - C_2)} \quad (2.51)$$

$$\theta = 1 - \frac{1 + C_2}{2 C_a} \quad (2.52)$$

COMMENT: To route a flood with the above method, considerable

computation effort is involved. Further, the method loses the simplicity of Muskingum and Muskingum-Cunge methods.

2.8 Muskingum Method With Variable Parameters of V.P.Singh[25]:

In this model, the routing parameters of the Muskingum-Cunge equation are evaluated at every discrete point on $x-t$ plane. Considering on $(i+1)^{th}$ period, let $I(i+1)$ be the inflow, $Q(i+1)$ the outflow, $w(i+1)$ the storage, and $K(i+1)$ the corresponding travel time for that period.

$$K(i+1) = \frac{\beta_1 w(i+1)}{[Q(i+1)]^{\alpha(2m+1)/(1+\alpha)}} \quad (2.53)$$

where

$$\beta_1 = \frac{a C^{(1-2m\alpha)/(1+\alpha)} (S_o + S_\Delta)^{(2m+1)/(2(1+\alpha))}}{S^m P^{\alpha(2m+1)/(1+\alpha)}} \quad (2.54)$$

For the Chezy formula $\alpha = 0.5$

S_o = bottom slope

S = water surface slope

For the period i^{th} period

$$K(i) = \frac{\beta_1 w(i)}{[Q(i)]^{\alpha(2m+1)/(1+\alpha)}} \quad (2.55)$$

By dividing Eq(2.53) by Eq(2.55) the following is obtained:

$$\frac{K(i+1)}{K(i)} = \frac{w(i+1)}{w(i)} \left[\frac{Q(i)}{Q(i+1)} \right]^{\alpha(2m+1)/(1+\alpha)} = \frac{w(i+1)}{w(i)} \left[\frac{Q(i)}{Q(i+1)} \right]^\gamma \quad (2.56)$$

where $\gamma = [\alpha(2m+1)]/(1+\alpha)$. From the kinematic wave approximation.

$$Q = \alpha_2 A^{\beta_2}$$

Then

$$\frac{Q(i+1)}{Q(i)} = \left[\frac{\alpha_2 A(i+1)}{\alpha_2 A(i)} \right]^{\beta_2} = \left[\frac{L A(i+1)}{L A(i)} \right]^{\beta_2} = \left[\frac{w(i+1)}{w(i)} \right]^{\beta_2} \quad (2.57)$$

By substituting Eq(2.57) into Eq(2.56)

$$\begin{aligned} \frac{K(i+1)}{K(i)} &= \frac{w(i+1)}{w(i)} \left[\frac{w(i)}{w(i+1)} \right]^{\alpha(2m+1)\beta_2/(1+\alpha)} \\ &= \left[\frac{w(i+1)}{w(i)} \right]^{1 - [\alpha(2m+1)\beta_2/(1+\alpha)]} \end{aligned} \quad (2.58)$$

Dimensionless weighting coefficient

For the Muskingum method, θ can be represented as

$$\theta = \frac{1}{2} - \frac{1}{2L} \quad (2.59)$$

where l is the characteristic length which can be expressed as

$$l = \frac{Q_o}{S_o} \left(\frac{\partial H}{\partial Q_o} \right) = \frac{Q_o}{S_o} \left[\frac{\partial(H - H_o)}{\partial Q_o} \right] \quad (2.60)$$

where H_o is the bottom elevation, H is the water level, and Q_o is the flow discharge.

For steady flow, the relationship between the water level and the discharge is

$$H - H_o = h = b_o Q_o^\beta \quad (2.61)$$

where h is the water depth, b_o is the constant, and β is an exponent. Taking the derivative of Eq(2.60)

$$\frac{\partial(H - H_o)}{\partial Q_o} = \frac{\partial}{\partial Q_o} [b_o Q_o^\beta] = b_o \beta Q_o^{\beta-1} \quad (2.62)$$

and substituting into Eq(2.59) yield

$$l = \frac{Q_o}{S_o} \frac{\partial(H - H_o)}{\partial Q_o} = \frac{Q_o}{S_o} b_o \beta Q_o^{\beta-1} = \frac{b_o \beta}{S_o} Q_o^\beta \quad (2.63)$$

Substitution of Eq(2.63) into Eq(2.59) yields

$$\theta = \frac{1}{2} - \frac{1}{2L} = 0.5 - \frac{b_o \beta Q_o^\beta}{2L S_o} \quad (2.64)$$

The relationship between steady-flow discharge Q_o and unsteady-flow discharge can be expressed as

$$Q = Q_o \left(1 + \frac{S_\Delta}{S_o} \right)^{1/2} \quad (2.65)$$

In general, $S_o \gg S_\Delta$, therefore, $Q \approx Q_o$ and Eq(2.64) becomes

$$\theta = 0.5 - \frac{b_o \beta}{2L S_o} Q^\beta = 0.5 - \alpha_1 Q^\beta \quad (2.66a)$$

when $L = \Delta x$, $h = b_o Q^\beta$, and $q/c = \beta h$ Eq(2.66a) becomes

$$\theta = 0.5 \left(1 - \frac{q}{c \Delta x S_o} \right) \quad (2.66b)$$

From Eq(2.66a), the following formula can be obtained:

$$\theta(i+1) = 0.5 - \frac{b_o \beta}{2L S_o} [Q(i+1)]^\beta \quad (2.66c)$$

$$\theta(i) = 0.5 - \frac{b_o \beta}{2L S_o} [Q(i)]^\beta \quad (2.66d)$$

On subtracting Eq(2.66c) from Eq(2.66d)

$$\theta(i+1) = \theta(i) + \frac{b_o \beta}{2L S_o} \{ [Q(i)]^\beta - [Q(i+1)]^\beta \}$$

COMMENT: Routing with this model is not possible unless we know $K(1), X(1), \gamma_1, \alpha_1, \beta, w(1)$. The field data scarcity may prevent the use of this particular model.

In the absence of outflow data for the catchment where inflow data and all the physical characteristics are known, to determine the accuracy of a routed flood by using any method a bench mark is needed. In this study, as the outflow data was not available, first a benchmark outflow hydrograph of the reach was created by using implicit Priessmann scheme[Appendix-1]. The Priessmann scheme gives

the numerical solution of complete Saint-Venant equations. The relative accuracies of the Muskingum-Cunge and various other proposed models are studied against this kind of bench mark in Chapter 4 and Chapter 5.

The implicit Priessmann scheme is first modeled and tested against the data sets 1 and 2 [Cooley,Moin[5]]. The outflow hydrograph obtained from the Preissmann scheme, the outflow hydrograph of Cooley and Moin are plotted in Figs. 2.4 and 2.5 along with the corresponding inflow hydrograph. The numerical error is calculated as

$$\% \text{ error} = \frac{E - E_m}{E_m} \times 100$$

where E represents the peak discharge or the depth of flow at peak discharge. E_m represents the peak discharge obtained by Cooley and Moin. The errors for these sets of data are shown in the Table 2.1

Table 2.1

Data set	Type	Moin	Preissmann	% ERROR
Set # 1	Qpeak	1764.71	1823.24	+ 3.33
Set # 2	Peak			
	Height	29.90	29.40	- 1.67

From the above Table 2.1, as the error is in the permissible limits (of < 5 %) , the Preissmann scheme modeled is considered to be adequate to generate the bench mark out flow hydrographs.

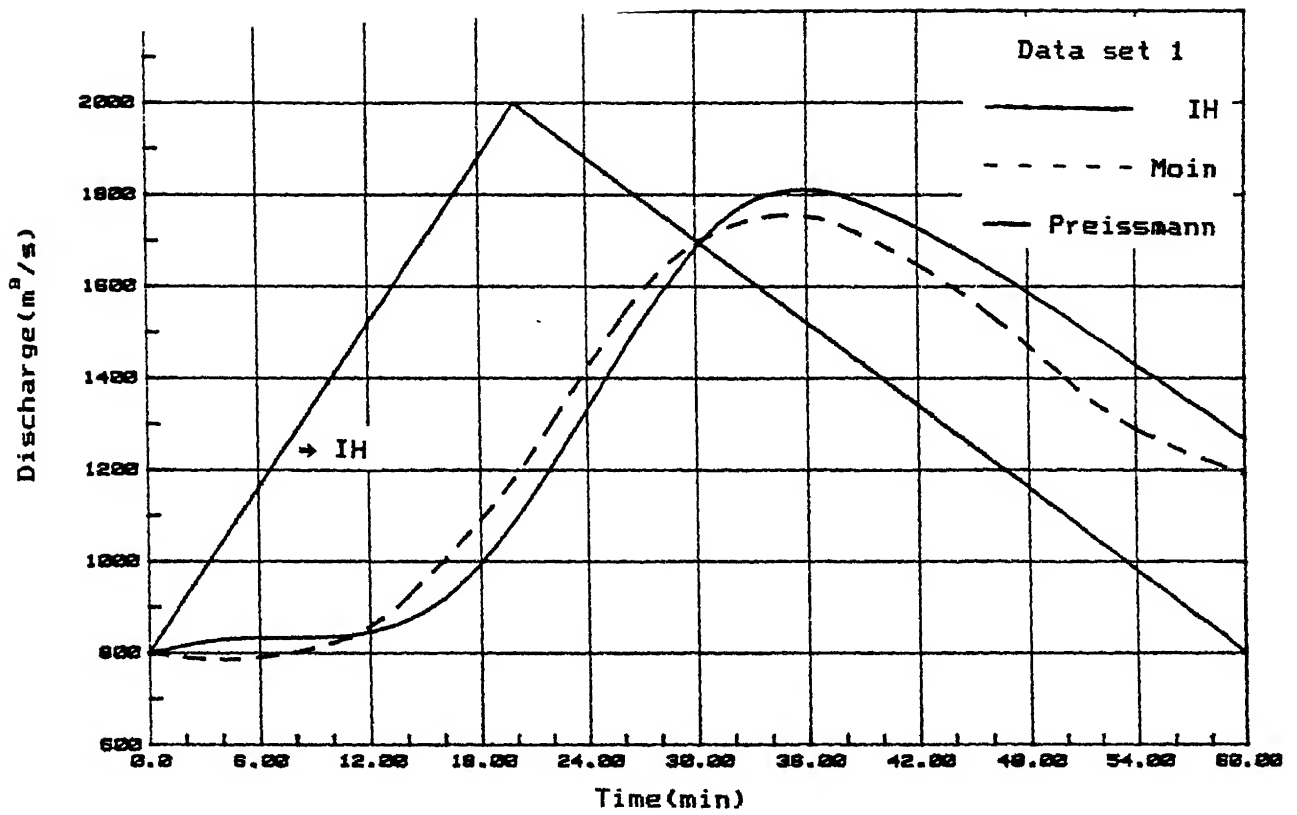


Fig. 2.4 Comparison of results from Preissmann
and Moin - Triangular IH

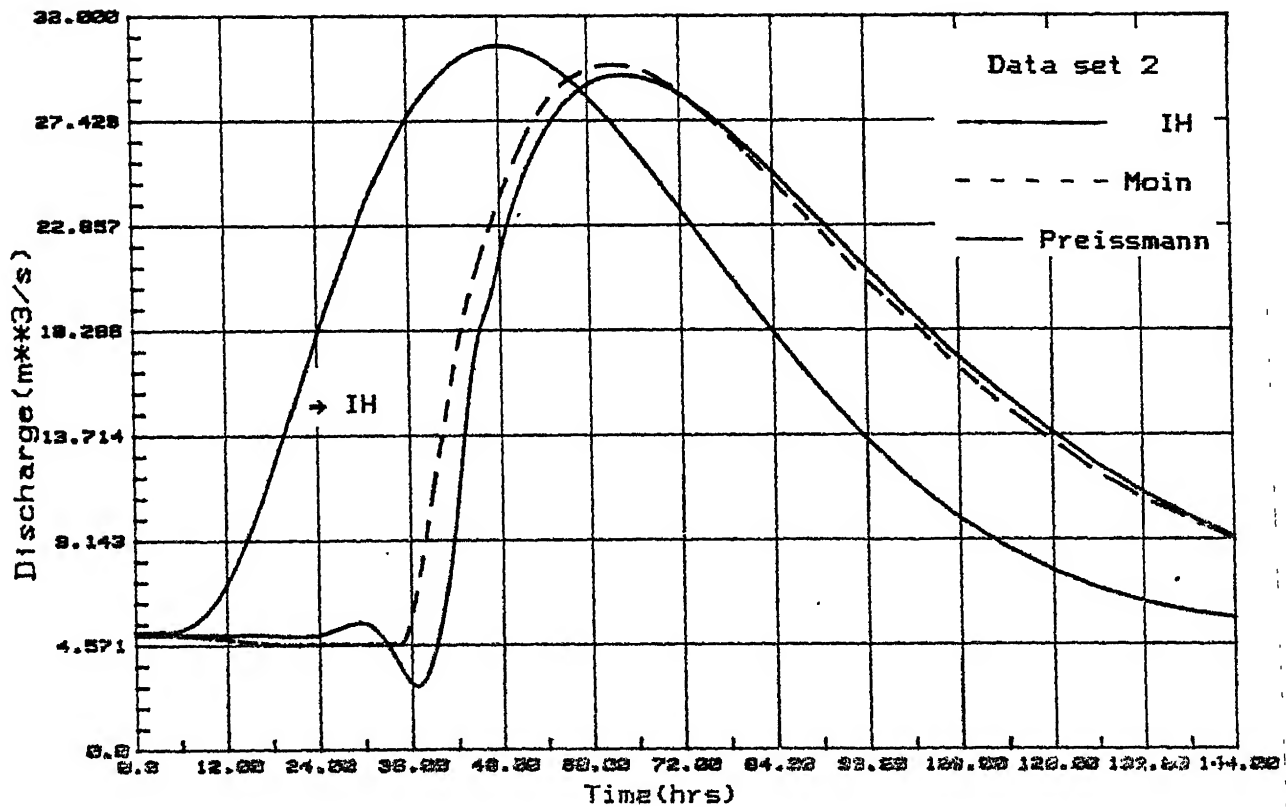


Fig. 2.5 Comparison of results from Preissmann
and Moin - Log Pearson type III IH

CHAPTER-3

ANALYSIS OF KINEMATIC ROUTING

0 INTRODUCTION:

In the Muskingum-Cunge(MC) routing the partial differential equation for continuity is approximated by implicit finite-difference scheme. In this chapter the continuity equation is approximated by Leap Frog Finite difference scheme towards achieving more accuracy in explicit routing of the flood. The order of accuracy of the leap-frog scheme is calculated and the stability analysis is also investigated. The proposed model is compared with the MC method.

3.1 FIRST ORDER DIFFERENTIAL EQUATION FOR ONE-TO-ONE STAGE DISCHARGE RELATIONSHIP :

The complete equations for gradually varying transient flow (Saint-Venant) equation for a rectangular prismatic channel are:

$$\frac{\partial y}{\partial t} + \frac{1}{B} \frac{\partial Q}{\partial x} = 0.0 \quad (3.1)$$

$$\frac{1}{g} \left[\frac{\partial v}{\partial t} + v \frac{\partial v}{\partial x} \right] = s_0 - \frac{\partial y}{\partial x} - \phi Q | Q| \quad (3.2)$$

where x = distance along the river

$y(x, t)$ = depth of water

$v(x, t)$ = mean velocity

$B(x,t)$ = width

s_o = bed slope

$Q(x,t)$ = resistance coefficient

$$\frac{1}{g} \left[\frac{\partial v}{\partial t} + v \frac{\partial v}{\partial x} \right] = \text{slope due to inertia of water}$$

Eqs.(3.1) and (3.2) are two non-linear partial differential equations are hyperbolic and their solution is subject to the following conditions:

- Two boundary conditions i.e. one upstream and one downstream of the considered river section.
- An initial state at time $t = t_o$ at each point of the considered section, consisting of a depth of water $y(x,t)$ and a velocity $v(x,t_o)$ at each cross section.

Assuming a single-valued stage/discharge curves for given points in a river, so that $x = x_o$ at a given point, then:

$Q|_{x=x_o} = Q(y)$, and hence the following relationship
 wetted area $A = A(y)$

$$\frac{\partial y}{\partial t} = \frac{\partial y}{\partial A} \frac{\partial A}{\partial t} \quad (3.3)$$

$$A|_{x=x_o} = A(Q) \quad (3.4)$$

$$\frac{\partial A}{\partial t} = \left[\frac{dA}{dQ} \right]_{x_o} \frac{\partial Q}{\partial t} \quad (3.5)$$

$$\frac{\partial y}{\partial t} = \frac{1}{B} \left[\frac{dA}{dQ} \right]_{x_o} \frac{\partial Q}{\partial t} \quad (3.6)$$

Substituting Eq(3.6) into Eq (3.1), we obtain the

$$\left[\frac{dA}{dQ} \right]_{x=x_o} \frac{\partial Q}{\partial t} + \frac{\partial Q}{\partial x} = 0 \quad (3.7)$$

The Eq(3.7) is a first order partial differential equation which is non-linear in so far as $\left(\frac{dA}{dQ}\right)_{x=x_0}$ is a function of discharge

Let AB be a river reach for which the stage-discharge relationship is assumed to be one-to-one such that Eq(3.7) can be applied.

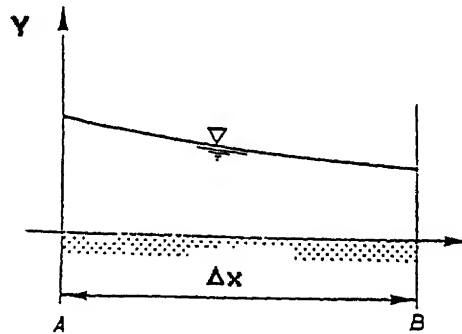


Fig. 3.1 A river reach

Then as discharge Q solely depends on distance x and time t , the following relationship holds good:

$$dQ = \frac{\partial Q}{\partial x} dx + \frac{\partial Q}{\partial t} dt \quad (3.8)$$

In order to determine the constant-discharge propagation lines dQ must be zero, hence the following relationship

$$\frac{dx}{dt} = \frac{(-\partial Q / \partial t)}{(\partial Q / \partial x)} = \frac{dQ}{dA} \quad (3.9)$$

Eq(3.9) is the characteristic equation for the Eq(3.7).

The discharge(Q) propagation rate is given by

$$c = \frac{dx}{dt} = \frac{dQ}{dA} \quad (3.10)$$

If constant celerity c is assumed irrespective of Q , the Eq(3.7) is linear as follows:

$$\frac{1}{c} \frac{\partial Q}{\partial t} + \frac{\partial Q}{\partial x} = 0.0 \quad (3.11)$$

$$\frac{dQ}{dA} = c = \text{constant} \quad (3.12)$$

$$\text{or} \quad \frac{\partial Q}{\partial t} + c \frac{\partial Q}{\partial x} = 0.0 \quad (3.13)$$

3.2 LEAP-FROG FINITE DIFFERENCE SCHEME:

The numerical solution of Eq(3.13) can be attempted by a finite difference approach assuming a finite difference in the (x,t) plane as shown in Fig. 3.2.

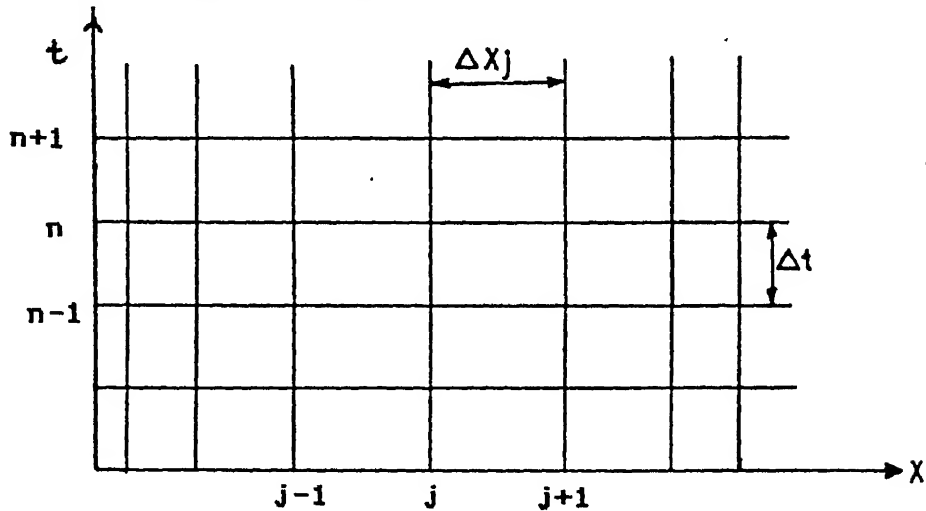


Fig. 3.2 x - t Plane: Finite difference grid for
a Leap Frog Scheme

The partial differentials are approximated by the Leap Frog finite difference scheme as :

$$\left. \begin{aligned} \frac{\partial Q}{\partial t} &\approx \frac{Q_j^{n+1} - Q_j^{n-1}}{2 \Delta t} \\ \frac{\partial Q}{\partial x} &\approx \frac{Q_{j+1}^n - Q_{j-1}^n}{2 \Delta x} \end{aligned} \right\} \quad (3.14)$$

If the resulting finite difference equation is an acceptable approximation of differential Eq(3.13) and if its solution converges with that of Eq(3.13) when Δx and Δt tend to zero.

$$LQ = \frac{\partial Q}{\partial t} + c \frac{\partial Q}{\partial x} = 0.0$$

$$L_h Q = \frac{Q_j^{n+1} - Q_j^{n-1}}{2 \Delta t} + c \frac{Q_{j+1}^n - Q_{j-1}^n}{2 \Delta x} = 0.0 \quad (3.15)$$

where L_h is differential operator based on the Eq(3.14) scheme.

On the assumption that these grid function $Q(j\Delta x, n\Delta t)$ can be expressed as a Taylor series about point $(j\Delta x, n\Delta t)$ it can be shown that the approximation error R is determined by the following formula

$$R = \frac{1}{6} \left| \left[1 - r^2 c^2 \right] \right| \left| \frac{\partial^3 Q}{\partial x^3} \right| \Delta x^2 + \text{Higher order terms} \quad (3.16)$$

$$\text{where } r = \frac{\Delta t}{\Delta x} .$$

The order of approximation by using the scheme of Eq(3.5) is 2.

$$[R = O(\Delta x^2)]$$

From the Eq(3.15) the following is obtained.

$$Q_j^{n+1} = Q_j^{n-1} - \frac{c \Delta t}{\Delta x} \left[Q_{j+1}^n - Q_{j-1}^n \right] \quad (3.17)$$

The proposed model , which is based on a Leap-Frog finite difference scheme in the MC method, is known as Muskingum-Cunge-Leap-Frog (MCLF) model in the rest of the chapter.

3.3 STABILITY ANALYSIS :

For the stability analysis in the continuity equation , the finite difference form of differential equation can be written of the following form,

$$Q_j^n = Q^* e^{i(\beta n \Delta t + \alpha j \Delta x)} \quad (3.18a)$$

$$Q_j^{n+1} = Q^* e^{i(\beta(n+1)\Delta t + \alpha j \Delta x)} \quad (3.18b)$$

$$Q_j^{n-1} = Q^* e^{i(\beta(n-1)\Delta t + \alpha_j \Delta x)} \quad (3.18c)$$

$$Q_{j+1}^n = Q^* e^{i(\beta n \Delta t + \alpha(j+1)\Delta x)} \quad (3.18d)$$

$$Q_{j-1}^n = Q^* e^{i(\beta n \Delta t + \alpha(j-1)\Delta x)} \quad (3.18e)$$

Substituting these set of Eqs(3.18) in Eq(3.15), and re-arranging we have

$$Q_j^n (e^{i\beta \Delta t} - e^{-i\beta \Delta t}) + \frac{C \Delta t}{\Delta x} Q_j^n (e^{i\alpha \Delta x} - e^{-i\alpha \Delta x}) = 0.0$$

If we define $CN = \frac{C \Delta t}{\Delta x}$ and solving for $e^{i\alpha \Delta x}$.

$$e^{2i\alpha \Delta x} + \frac{e^{i\alpha \Delta x}}{CN} (e^{i\beta \Delta t} - e^{-i\beta \Delta t}) - 1.0 = 0.0$$

The expression for $e^{i\alpha \Delta x}$ can be obtained by solving Eq(3.20).

In the resulting expression substitute $\alpha = \alpha_1 + i\alpha_2$. Equating the real and imaginary terms on both the sides in the expression, it is found that for the real term, α_2 value lies between 0 and 1.0 for all values of $\beta \Delta t$, which implies that the scheme chosen is stable.

3.4 Method of Routing:

The given reach length L , is sub-divided into n number of reaches depending on the Δx chosen. In the MCLF method a minimum number of three reaches are required. The discharges at all times at the next sub reach from the origin are obtained by using the MC method as explained in Section 2.2 in Chapter 2. Then Eq(3.17) is used to get the discharges at all reaches with respect to different times.

Case 1:

In this study, a inflow hydrograph(IH) of data set3(Fig. 3.3) is considered. The rectangular channel has a width of 50 m. The given IH is routed over a reach length of 18000 m, on a longitudinal bed slope of 0.0005. The Manning's roughness coefficient was chosen as $n = 0.03$. A Courant number of 0.85 is used for the MCLF and MC methods. A value of $\Delta x = 4500$ was used for the MCLF and MC methods. The given IH is routed by the MCLF and the MC methods. The outflow hydrographs obtained by the MCLF and the MC methods in this study are plotted in Fig. 3.3 along with the corresponding IH. Fig. 3.4 is an enlarged plot to show the attenuation of peak discharge by the MCLF and the MC methods. Some of the salient routing data are tabulated in Table 3.1.

From Figs. 3.3 and 3.4 and table 3.1 it is found that:

1. The attenuation of peak discharge is very little in MCLF method.
2. The wave translation of the peak discharge is of the same order as that of the MC method.

Case 2:

An IH of data set 4 (Fig. 3.5) with a a steep rise in the initial flows was considered next. The physical characteristics of the channel are same as that of case 1. A Courant number of 0.85 is used for the MCLF and the MC methods. A value of $\Delta x = 4500$ was used for the MCLF and the MC methods. The IH of data set 4 is routed by the MCLF and the MC methods. The outflow hydrographs obtained by the MCLF and the MC methods are shown in Fig. 3.5 along with the corresponding IH. Fig. 3.6 shows the attenuation of the peak discharge in MCLF and MC methods. Some of the salient routing data

are presented in Table 3.2.

Table 3.1 SOME SALIENT ROUTING DATA FOR DATA SET 3

Time (hrs)	ord. of	Ord. of output hydrograph (m^3/s)	
	Input hydrograph m^3/s	MC	MCLF
0.0	10.0	10.0	10.00
2.0	18.0		
2.28		10.68	10.16
4.0	50.0		
4.56		21.77	19.32
6.0	107.0		
6.08		45.77	40.14
8.0	147.0		
8.36		105.10	106.90
9.0	150.0*		
10.0	146.0		
10.64		144.24	147.35
11.4068		146.259*	149.9972
12.0	105.0		
12.16		142.93	147.41
14.0	59.0		
14.44		102.51	104.45
16.0	33.0		
16.72		55.88	52.57
18.0	17.0		
18.25		35.91	33.86
20.0	10.0		
20.53		17.21	16.53
22.0	10.0		
22.05		11.47	10.56
24.0	10.0		
24.33		10.03	10.00
25.85		10.00	10.00
28.0	10.0		
28.13		10.00	10.00

* represents peak values.

From the Figs 3.5 and 3.6 and Table 3.2, the same observations of case 1 are noted.

Table 3.2 SOME SALIENT ROUTING DATA FOR DATA SET 4

Time (hrs)	Ord. of	Ord. of output hydrograph (m^3/s)	
	Input hydrograph m^3/s	MC	MCLF
0.0	10.0	10.0	10.00
2.0	52.0		
2.28		11.68	10.77
4.0	141.0		
4.56		48.93	52.34
6.0	144.0		
6.08		122.74	125.52
7.48		142.96*	149.965*
8.0	114.0		
8.36		139.78	143.96
10.0	86.0		
10.64		121.44	110.08
12.0	61.0		
12.16		88.44	90.51
14.0	41.0		
14.44		62.54	60.91
16.0	25.0		
16.72		39.88	37.31
18.0	14.0		
18.25		24.91	24.06
20.0	10.0		
20.53		14.21	13.73
22.0	10.0		
22.05		11.47	10.08
24.0	10.0		
24.33		10.03	10.00
25.85		10.00	10.00
26.0	10.0		
28.0	10.0		
28.13		10.00	10.00

* represents peak values.

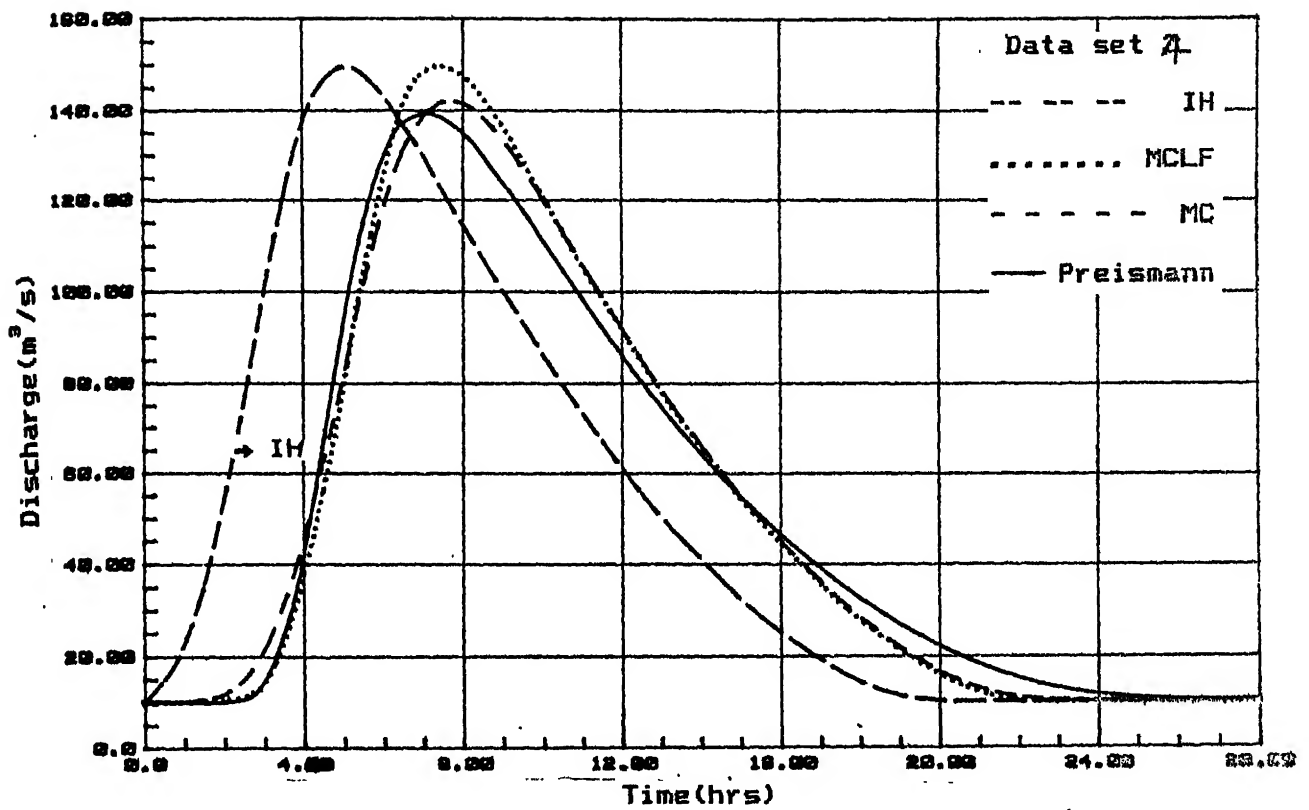


Fig. 3.5 Comparison of results from MC and
MCLF methods - Steep rise IH

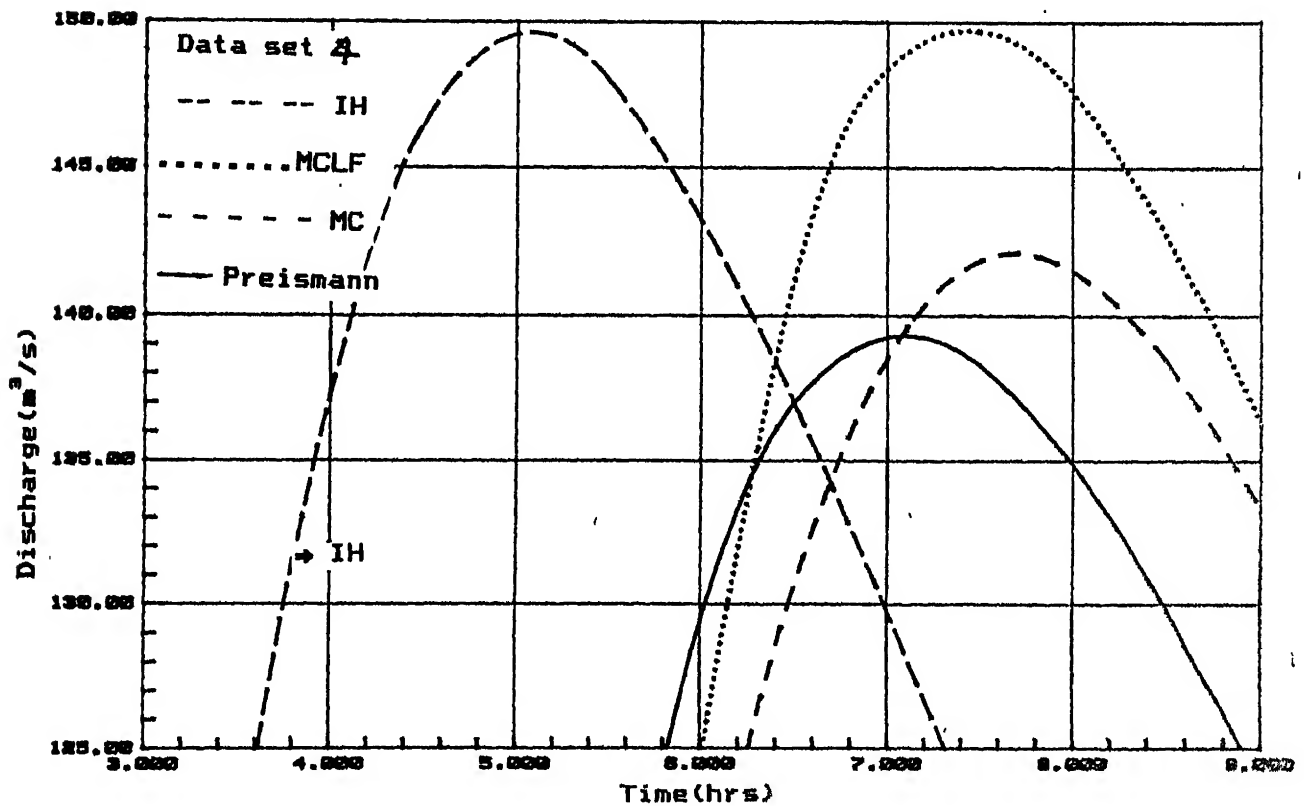


Fig. 3.6 Attenuation of peak discharge in
MC and MCLF methods - Steep rise IH

3. 5 DISCUSSION:

From this study as above it has been observed that the MCLF method creates very little attenuation of peak discharge and the translation of peak discharge is of the same order as the MC method. In the MC method, the error is introduced into the analytical solution of the continuity equation by the assumed first order finite difference scheme. In the actual flood wave there is a attenuation in the peak discharge due to the frictional effects. The numerical diffusion caused due to the finite difference operation fairly matches with that of the actual flood wave. In the MCLF method, in which there is a second order accurate finite difference scheme, the numerical diffusion is eliminated considerably and the solution approaches the analytical solution of the kinematic wave equation. Thus the attenuation of peak discharge in the MCLF method is minimal. This is in agreement with the Cunge[6] statement *whenever a closer approximation of the differential equation is obtained, this eliminates the wave attenuation (or amplifications as the case may be)* . Thus, the higher order schemes are not desirable in the MC method and no improvement of the MC method can be achieved by this way.

CHAPTER-4

MODIFICATION OF MC METHOD THROUGH SEGREGATION OF INPUT HYDROGRAPH

4.0 INTRODUCTION:

To improve the Muskingum-Cunge(MC)method without losing its simplicity and to simulate the flows which are considerably away from the range of peak discharges with more accuracy, a segregation technique of the inflow hydrograph for use in the MC method is proposed. The number of segregations depends on the range of the discharges and shape of the inflow hydrograph. The results from the proposed method are compared with those of the Preissman and MC methods.

4.1 EARLIER STUDIES:

Cunge [6] obtained the following expressions for the routing parameters K and θ as function of the physical characteristics of the channel and inflow hydrograph as

$$K = \frac{\Delta x}{\langle C \rangle} \quad (4.1)$$

and
$$\theta = 0.5 \left(1 - \frac{Q_P}{B \langle C \rangle s_0 \Delta x} \right) \quad (4.2)$$

The outflow hydrograph is obtained by routing the inflow hydrograph by using these parameters over a reach length L . The procedure of routing is explained in Section 2.3 of Chapter 2.

In certain cases, such as (i) in Fig. 4.1 , in which there is a vast difference between the initial flows at which the flood starts to build up and the peak discharge it attains and (ii) in Fig. 4.2 , when there is a rise after the flood started receding , it is felt that the determination of K and θ by considering only the peak discharge as taken by Cunge[6], may not simulate the actual conditions in the downstream adequately. To overcome this shortcoming, Ponce[18] has developed the variable parameter model in which the routing parameters K and θ are calculated for each grid cell. This procedure requires data which outwits the simplicity of the MC method.

Karmegam[12], in his stratified approach , has divided the inflow hydrograph into several strata as shown in Fig. 4.3. The relevant routing parameters K and θ for each strata are calculated with the help of past inflow and outflow data through an optimization technique.

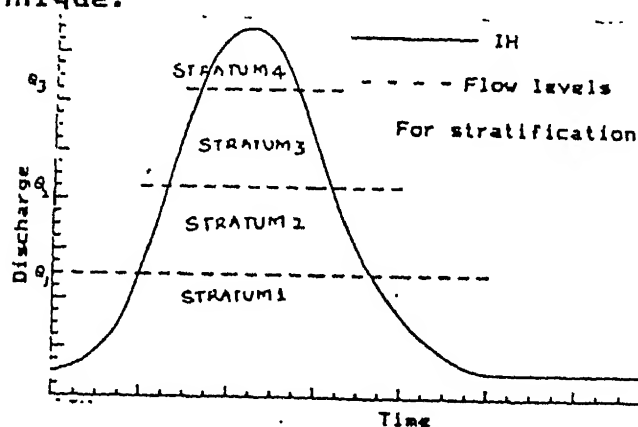


Fig. 4.3 Stratification of a IH

It is felt that this approach of Karmegam[12] is physically unconvincing and is purely an empirical approach. Further, by using the optimization technique, the simplicity of MC method is sacrificed and the routing becomes more complex than what is warranted.

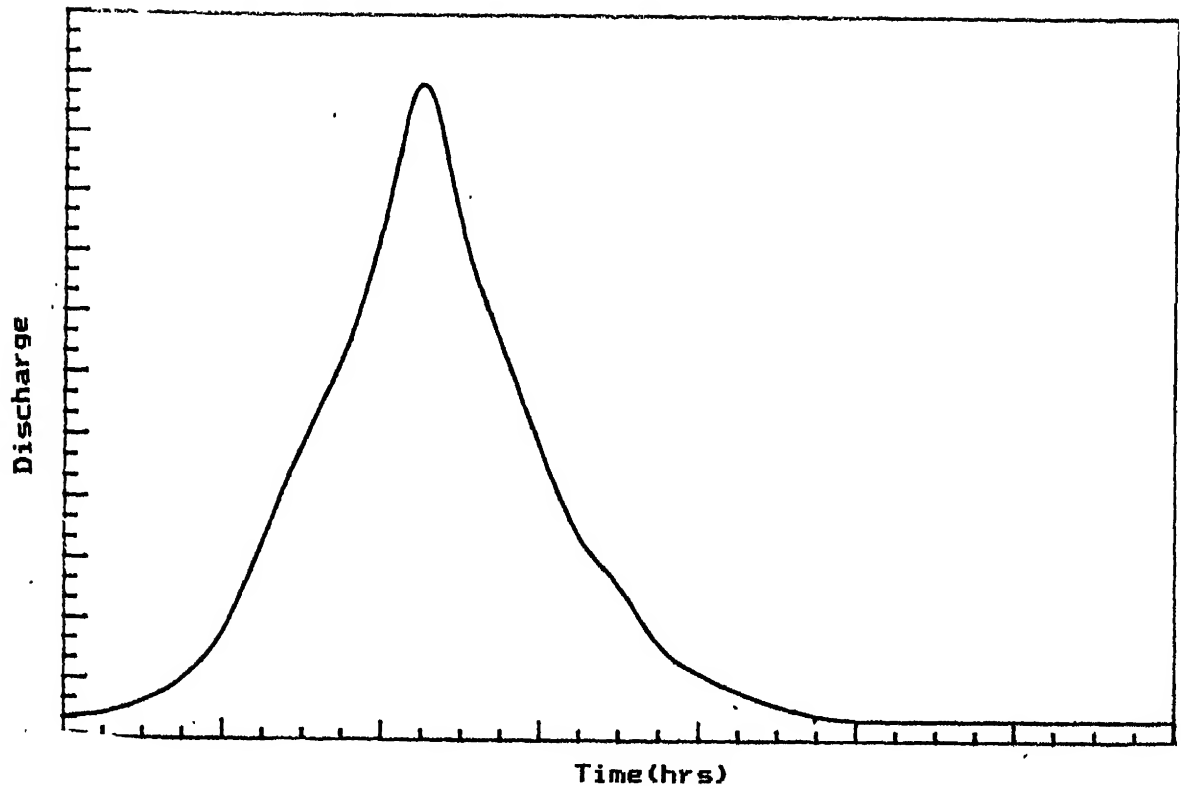


Fig. 4.1 Inflow hydrograph

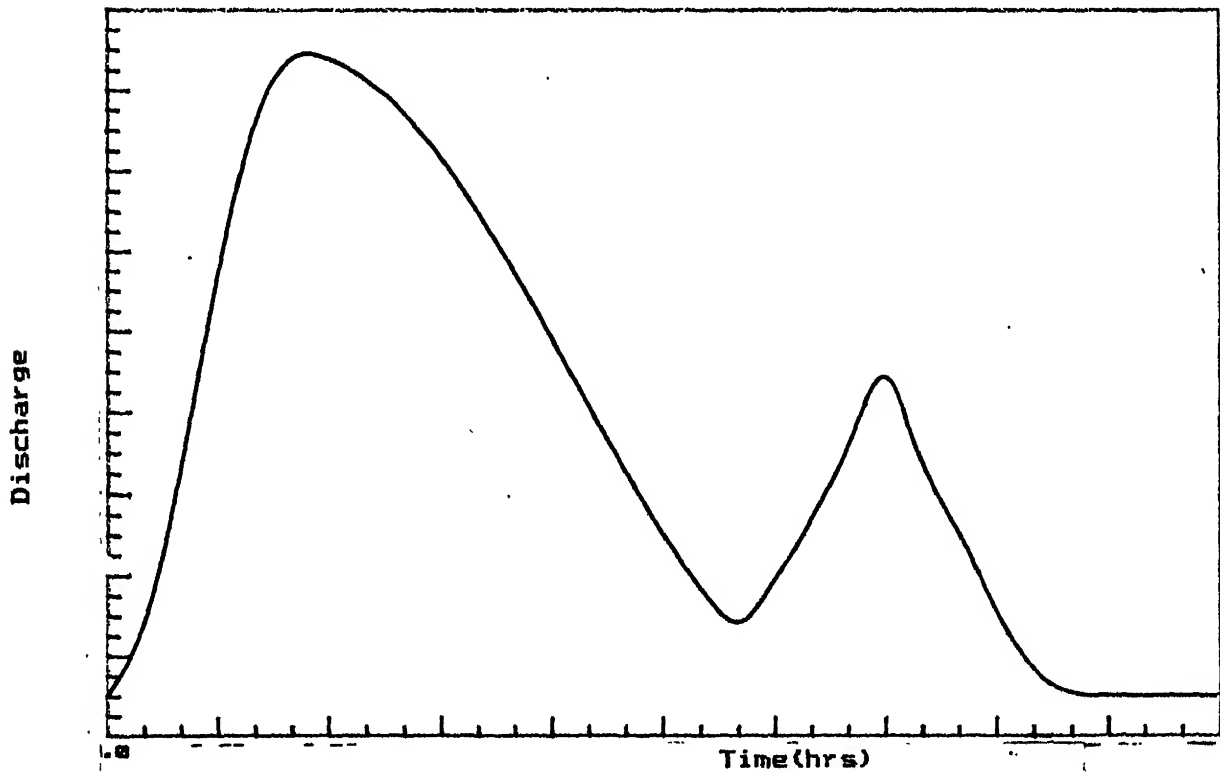


Fig. 4.2 Complex hydrograph

To overcome these shortcomings of Ponce[18] and Karmegam[12], the following Segregation model is proposed. The inflow hydrograph(IH) is divided into n number of segments depending upon the range of values. It is proposed that IH be divided into three or five segments by choosing the discharge(s) which is(/are) less than peak discharge as a basis for segregation.

Consider Fig 4.4a, where the inflow hydrograph is divided into three segments. The discharge Q_{50} which is 0.5 times the peak discharge, is taken as the basis for segregation. The resulting hydrograph now consists of three segmented hydrographs namely OBE, EBPCF and FCD. It is noted that the continuity between the hydrographs is not lost. Now it is assumed that $c \neq F(t)$ and is a constant irrespective of the discharge. This ensures the continuity equation to be linear. It may be noted that this is the basic assumption of the MC method.

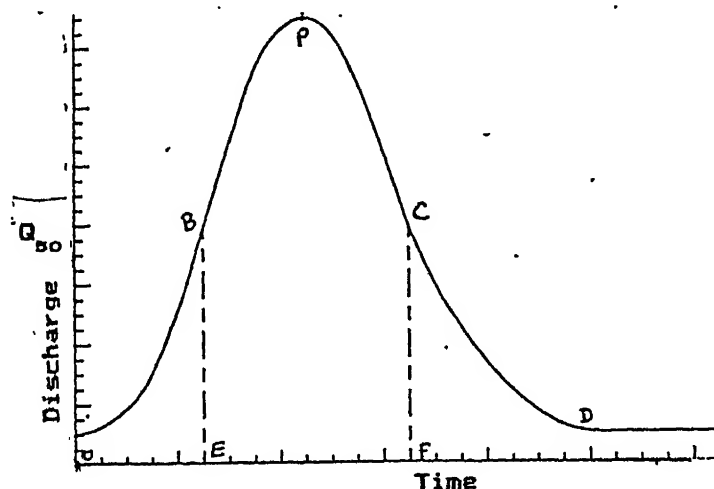


Fig. 4.4a Segregation of IH

With the above assumption, the routing parameter K is the same for all the three segregated hydrographs OBE, EBPCF and FCD, i.e.

$$K_1 = K_2 = K_3 = \frac{\Delta x}{\langle C \rangle} \quad (4.3)$$

However, the parameter θ for each segregated unit is proposed to be calculated as:

$$\text{For segment OBE} \quad \theta_1 = 0.5 \left(1 - \frac{Q_{50}}{B s_o \langle c \rangle \Delta x} \right) \quad (4.4a)$$

$$\text{For segment EBPCF} \quad \theta_2 = 0.5 \left(1 - \frac{Q_{50}}{B s_o \langle c \rangle \Delta x} \right) \quad (4.4b)$$

$$\text{For segment FCD} \quad \theta_3 = 0.5 \left(1 - \frac{Q_{50}}{B s_o \langle c \rangle \Delta x} \right) \quad (4.4c)$$

Where $Q_{50} = 0.5 Q_p$.

The IH is routed by MC method(a procedure in Section 2.3) after choosing the appropriate value of θ depending upon the class to which the discharges belong , after they are segregated.

Fig 4.4b is a complex hydrograph with two peaks. Even in this case, the IH is divided by considering Q_{50} as the basis for segregation and the values of θ are calculated by Eqs.(4.4-a,b,c).

The proposed method of segregation and routing with the MC method is designated as Segregated-Muskingum-Cunge(SMC) model in the rest of this chapter.

4.3 Numerical experimentation:

The efficacy of the proposed SMC method is compared with the implicit Preissmann scheme and the MC method through numerical experimentation. Five inflow hydrographs [set3,set4,set6,set7 and set8] were considered. For each IH, $\alpha = 0.66$ is used in the Preissmann scheme and a Courant number of 0.85 is used in MC and SMC methods.

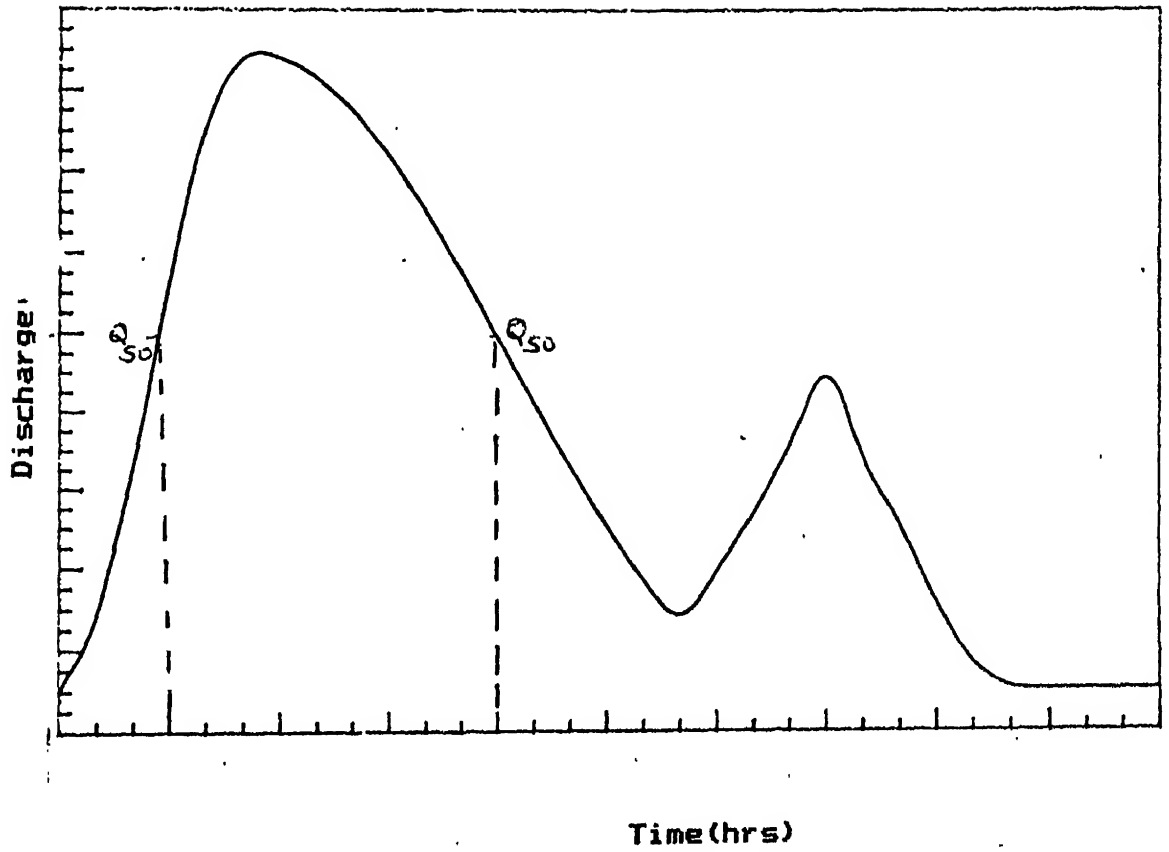


Fig. 4.4b Segregation of Complex IH

Case1:

First, the IH of data set 3 was considered. This IH was routed in a rectangular channel of 50 m wide for a reach length of 18000 m on a bed slope of 0.0005. The Manning's roughness coefficient was chosen as $n = 0.03$. The routing of IH was done by the SMC, MC and the Preissmann methods. A value of $\Delta x = 6000$ m was used in both MC and SMC methods. The IH of data set 3, and the outflow hydrographs obtained through these three models in the study are shown in Figs 4.5 and 4.6. An enlarged plot of values predicted upto Q_{50} along with the corresponding IH is shown in Fig. 4.6. Some of the salient routing data are presented in Table 4.1.

From the Figs. 4.5 and 4.6 and Table 4.1, it is seen that :

- 1) The flows predicted by the SMC method are slightly better than those of MC method up to Q_{50} . Beyond Q_{50} , both the SMC and MC methods give essentially identical results.
- 2) The attenuation of the peak in the SMC method is of the same order as that of the MC method.
- 3) The wave translation of the peak discharge for the SMC method is of the same order as that of the MC method.

Case 2:

The second IH used in the study was of data set 4 (Fig. 4.7).

The physical characteristics of the channel are the same as in Case 1. A value of $\Delta x = 6000$ m is used for the SMC and MC methods. The IH of data set 4 was routed using the SMC, MC and the Preissmann methods. The outflow hydrographs obtained through these three models are plotted in Figs. 4.7 and 4.8. Fig. 4.8 is an enlarged plot of the flows upto Q_{50} along with the corresponding IH. Some of the salient routing data are tabulated in Table 4.2.

Table 4.1 SOME SALIENT ROUTING DATA FOR DATA SET 3

Time (hrs)	Ord. of inflow	Ord. of outflow hydrograph in m^3/s		
	hydrograph (m^3/s)	MC	SMC	Preissmann
0.0	10.00	10.00	10.00	10.00
2.0	18.00			9.97
2.04		10.33	10.09	
4.0	50.00			11.00
4.08		17.58	16.59	
6.0	107.00			38.74
6.12		46.78	45.07	
8.0	147.00			109.01
8.16		99.87	99.67	
10.0	146.00			144.21
10.20		140.60	140.59	
11.0	129.00			144.44*
11.56		146.015*	146.014*	
12.0	105.00			135.62
12.24		142.24	142.24	
14.0	59.00			99.65
14.29		106.17	106.16	
16.0	33.00			65.04
16.33		62.48	61.42	
18.0	17.00			41.89
18.37		34.65	34.00	
20.0	10.00			26.71
20.41		17.91	17.41	
22.0	10.00			17.12
22.45		10.86	10.41	
23.81		10.11	10.02	
24.0	10.00			12.12
25.85		10.00	10.00	
26.0	10.00			10.51
27.89		10.00	10.00	
28.0	10.00			10.10
28.13		9.96	9.99	

* represents peak value.

Table 4.2 SOME SALIENT ROUTING DATA FOR DATA SET 4

Time (hrs)	Ord. of inflow hydrograph	Ord. of outflow hydrograph in m^3/s		
	(m^3/s)	MC	SMC	Preissmann
0.0	10.00	10.00	10.00	10.00
2.0	52.00			9.78
2.04		11.62	10.43	
4.0	141.00			38.14
4.08		47.51	43.92	
6.0	144.00			133.13
6.12		122.75	122.52	
7.0	130.00			140.85*
7.48		142.96*	142.61*	
8.0	114.00			136.66
8.16		141.30	141.29	
10.0	86.00			111.09
10.20		117.14	117.14	
12.0	61.00			86.04
12.24		88.46	88.44	
14.0	41.00			64.10
14.28		62.78	62.54	
16.32		41.78	41.68	
18.0	14.00			32.33
18.37		25.72	25.44	
20.0	10.00			22.07
20.41		14.79	14.40	
21.77		11.20	10.82	
22.0	10.00			15.06
23.81		10.06	10.00	
24.0	10.00			11.48
25.85		10.02	10.00	
26.0	10.00			10.35
27.89		10.00	10.00	
28.0	10.00			10.07

* represents the peak discharges.

From the Figs. 4.7 and 4.8 and Table 4.2, it is seen that:

The relative performance of the SMC, MC and the Preissmann methods are the same as in Case 1. The three conclusions drawn in case 1 are exactly applicable here also .

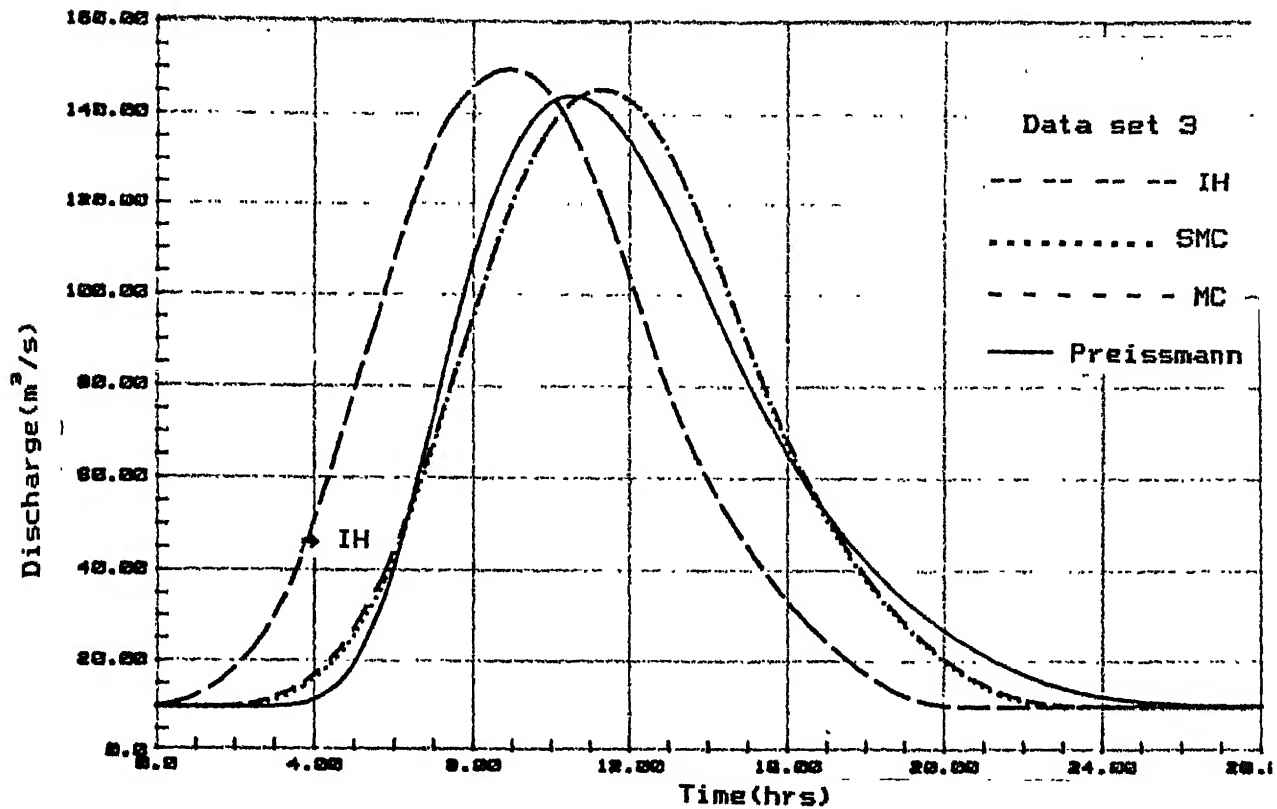


Fig. 4.5 Comparison of SMC model with the MC and Preissmann models --- Normal IH

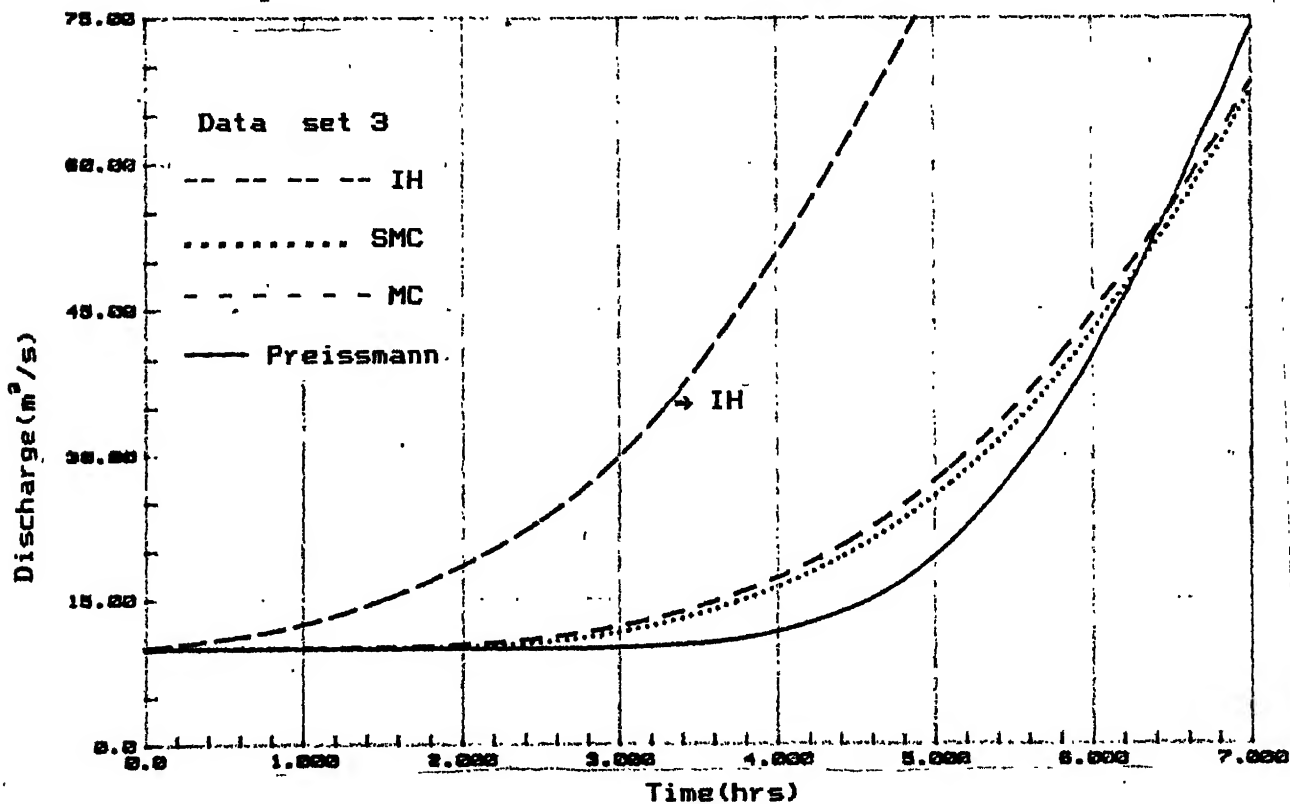


Fig. 4.6 Flows up to Q_{50} in the SMC, MC and the Preissmann models ---- Normal IH

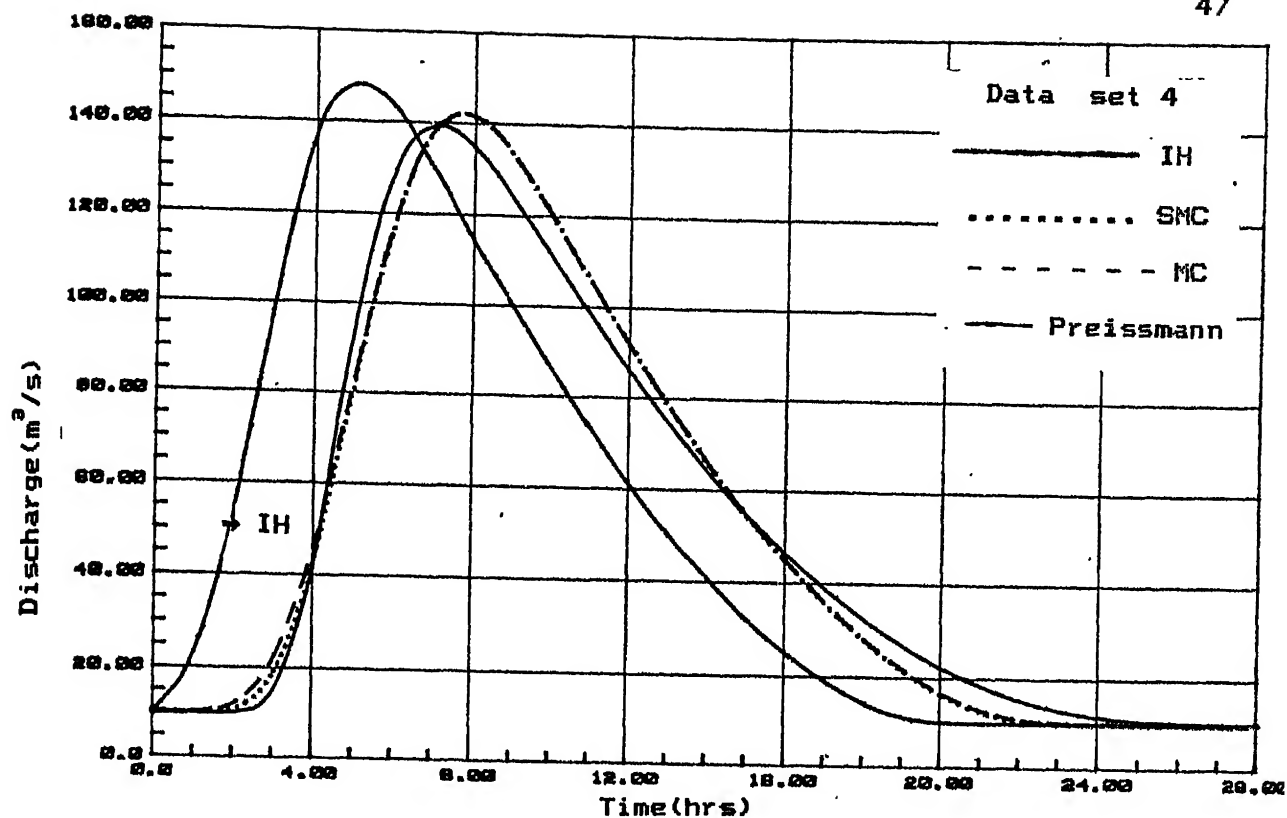


Fig. 4.7 Comparison of SMC model with the MC and Preissmann models --- Steep rise IH

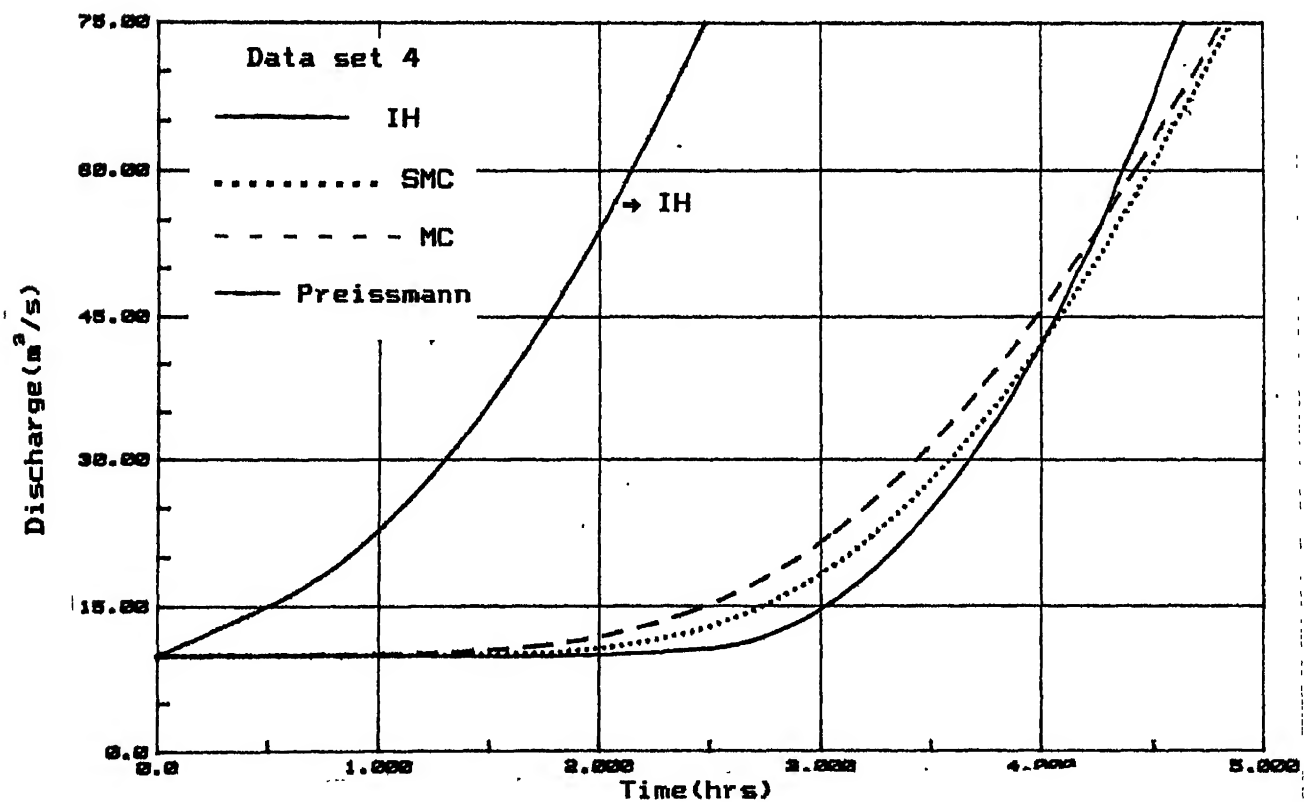


Fig. 4.8 Flows up to Q_{50} in the SMC, MC and the Preissmann models ---- Steep rise IH

Case 3:

Consider IH of data set 6 as shown in Fig.4.9. The salient feature of this IH is the presence of a second peak. The magnitude of second peak discharge is greater than Q_{50} but less than the earliest peak. The rise in IH towards the second peak occurs before the commencement of the Q_{50} in the depletion curve. This IH was routed by the SMC, MC and the Preissmann methods in a rectangular channel of 50 m wide for a reach length of 30000 m. The Longitudinal bed slope of channel is 0.0005 and $n = 0.03$. A value of $\Delta x = 7500$ m was used for the SMC and MC methods. The IH of data set 6, and outflow hydrographs obtained by these three methods are shown in Figs 4.9 and 4.10. Fig. 4.10 is an enlarged plot of the initial flows predicted upto Q_{50} , along with the corresponding IH. Some of the salient routing data are presented in Table 4.3.

From Figs. 4.9 and 4.10 and Table 4.3, it is seen that:

- 1) The flows predicted by the SMC are slightly better than that of MC model upto Q_{50} . Beyond Q_{50} both SMC and MC methods give identical results.
- 2) The attenuation of peak in the SMC method is of the same order as that of MC method.
- 3) The wave translation of peak discharge for SMC method is of the same order as that of MC method.
- 4) The predicted second peak in the SMC method is slightly higher ($\approx 13\%$) than that by the Preissmann method. However, it is of the same order as that obtained by the MC method.

Table 4.3 SOME SALIENT ROUTING DATA FOR DATA SET 6

Time (hrs)	Ord. of inflow	Ord. of	Outflow hydrograph in m ³ /s	
	hydrograph (m ³ /s)	MC	SMC	Preissmann
0.0	10.00	10.00	10.00	10.00
2.0	65.28			10.63
2.43		10.56	10.03	
4.0	154.72			6.07
4.05		22.25	17.13	
6.0	168.25			95.77
6.49		98.59	97.01	
8.0	154.72			159.55*
8.11		147.99	147.77	
9.73		162.73*	162.71*	
10.0	130.00			154.61
10.54		161.15	161.14	
12.0	140.60			136.14
12.17		148.93	148.93	
14.0	85.28			128.38
14.60		128.83	128.83	
16.0	43.48			109.44
16.22		121.16	121.12	
17.84		86.61	85.45	
18.0	17.92			74.78
20.0	10.00			48.75
20.28		38.82	37.23	
21.90		20.41	18.81	
22.0	10.0			31.22
24.0	10.0			20.04
24.33		10.95	10.38	
25.96		10.13	10.02	
26.0	10.0			14.29
28.0	10.0			11.73
28.39		10.04	10.00	

* represents the peak discharges.

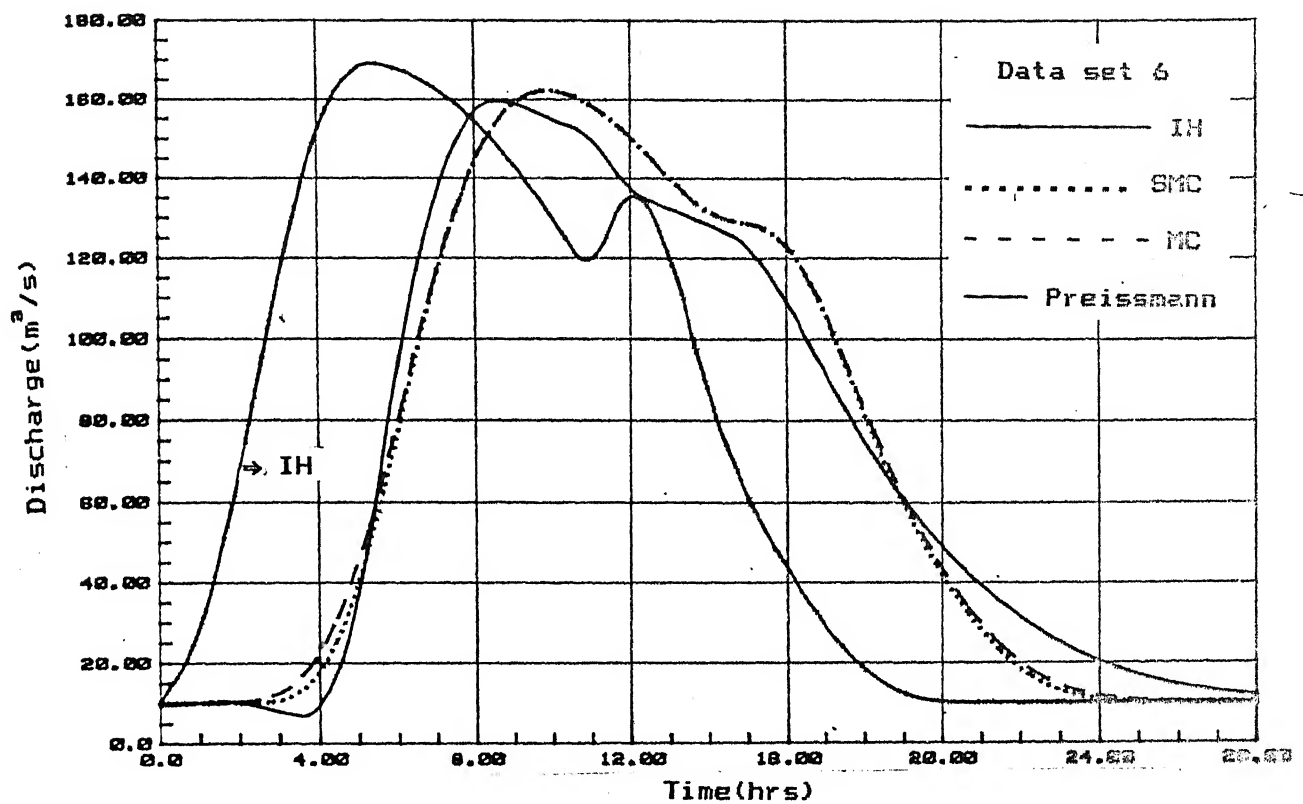


Fig. 4.9 Comparison of SMC model with the MC and Preissmann models --- Complex IH

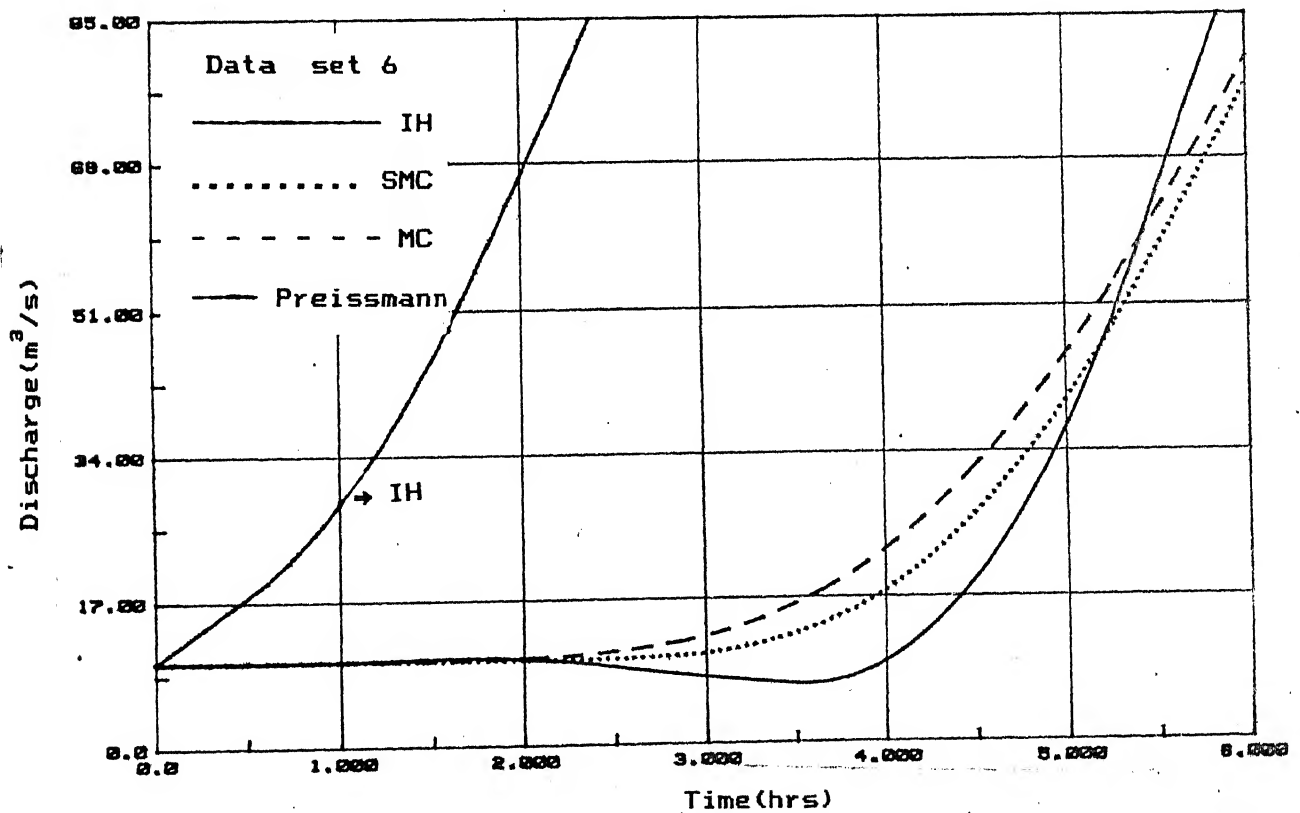


Fig. 4.10 Flows upto Q_{50} in the SMC, MC and the Preissmann models ---- Complex IH

The IH of data set 7 is shown in Fig. 4.11. In this IH, there is a second peak of magnitude $> Q_{50}$ and less than the first peak which occurs after the Q_{50} in the depletion curve has been reached. This IH was routed in the same rectangular channel as in Case 3 and the results are shown in Figs. 4.11 and 4.12. Some of the salient routing data are presented in Table 4.4.

Table 4.4 SOME SALIENT ROUTING DATA FOR DATA SET 7

Time (hrs)	Ord. of inflow hydrograph (m^3/s)	Ord. of outflow hydrograph in m^3/s		
		MC	SMC	Preissmann
0.0	10.00	10.00	10.00	10.00
2.0	65.28			10.63
2.43		10.56	10.03	
4.0	154.72			6.07
4.05		22.25	17.13	
6.0	168.25			95.77
6.49		98.59	97.01	
8.0	154.72			159.54
8.11		147.99	147.77	
9.73		162.73*	162.71*	
10.0	130.0			154.61
10.54		161.15	161.14	
12.0	98.36			135.50
12.16		148.88	148.88	
14.0	65.28			112.61
14.60		117.08	117.08	
16.0	36.47			86.34
16.22		91.36	91.32	
17.84		65.78	65.17	
18.0	70.90			62.26
20.0	65.75			54.24
20.28		53.46	49.41	
21.90		71.54	73.03	
22.0	30.60			71.57
24.0	10.00			59.75
24.33		56.72	57.84	
25.96		30.97	29.61	
26.0	10.00			40.05
28.0	10.00			24.54
28.39		12.14	10.91	

* represent peak value

LIBRARY
I. T. KANPUR
Dec. No. A. 1165

From Figs. 4.11 and 4.12 and Table 4.4, it is seen that:

The first three conclusions arrived in Case 1 (and also in Case 2 and Case 3) also hold good here. Further, the second peak is predicted well by all the three methods viz., SMC , MC and Preissmann.

Case 5:

In IH of data set 8 (Fig. 4.13) , is essentially same as that of the IH of data 7 (Case 4) , except that the magnitude of the second peak is less than the Q_{50} . The channel data are the same as in Case 4. The results of the routing of this IH are shown in Fig. 4.13, 4.14 and Table 4.5.

Table 4.5 SOME SALIENT ROUTING DATA FOR DATA SET 8

Time (hrs)	Ord. of inflow	Ord. of outflow hydrograph in m^3/s		
	hydrograph (m^3/s)	MC	SMC	Preissmann
0.0	10.00	10.00	10.00	10.00
2.0	65.28			10.63
2.43		10.56	10.03	
4.0	154.72			6.07
4.05		22.25	17.13	
6.0	168.25			95.77
6.49		98.59	97.01	
8.0	154.72			159.54*
8.11		147.99	147.77	
9.73		162.73*	162.71*	
10.0	130.0			154.61
10.54		161.15	161.14	
12.0	98.36			135.50
12.16		148.88	148.88	
14.0	65.28			112.61
14.60		117.08	117.08	
16.0	36.47			86.34
16.22		91.36	91.32	
17.84		65.78	65.17	
18.0	65.90			62.25

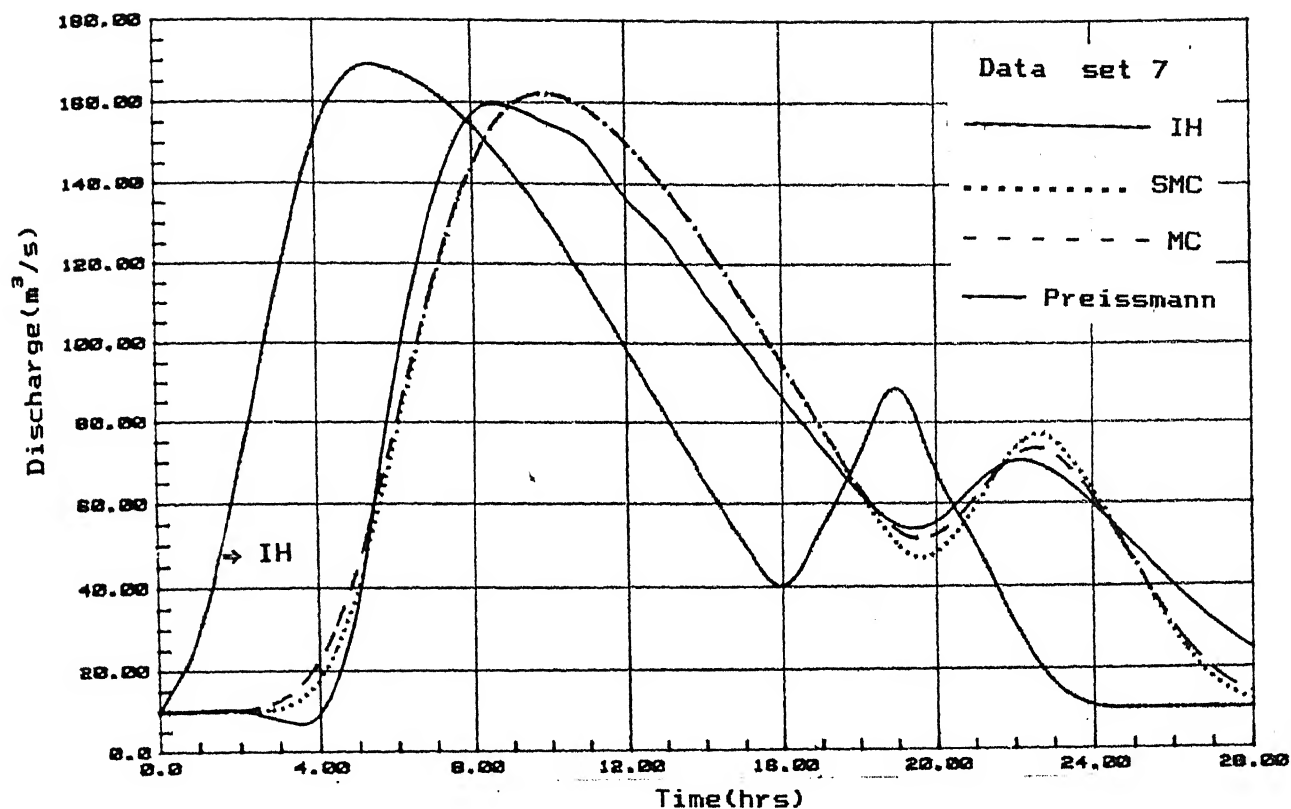


Fig. 4.11 Comparison of SMC model with the MC and Preissmann models --- Complex IH

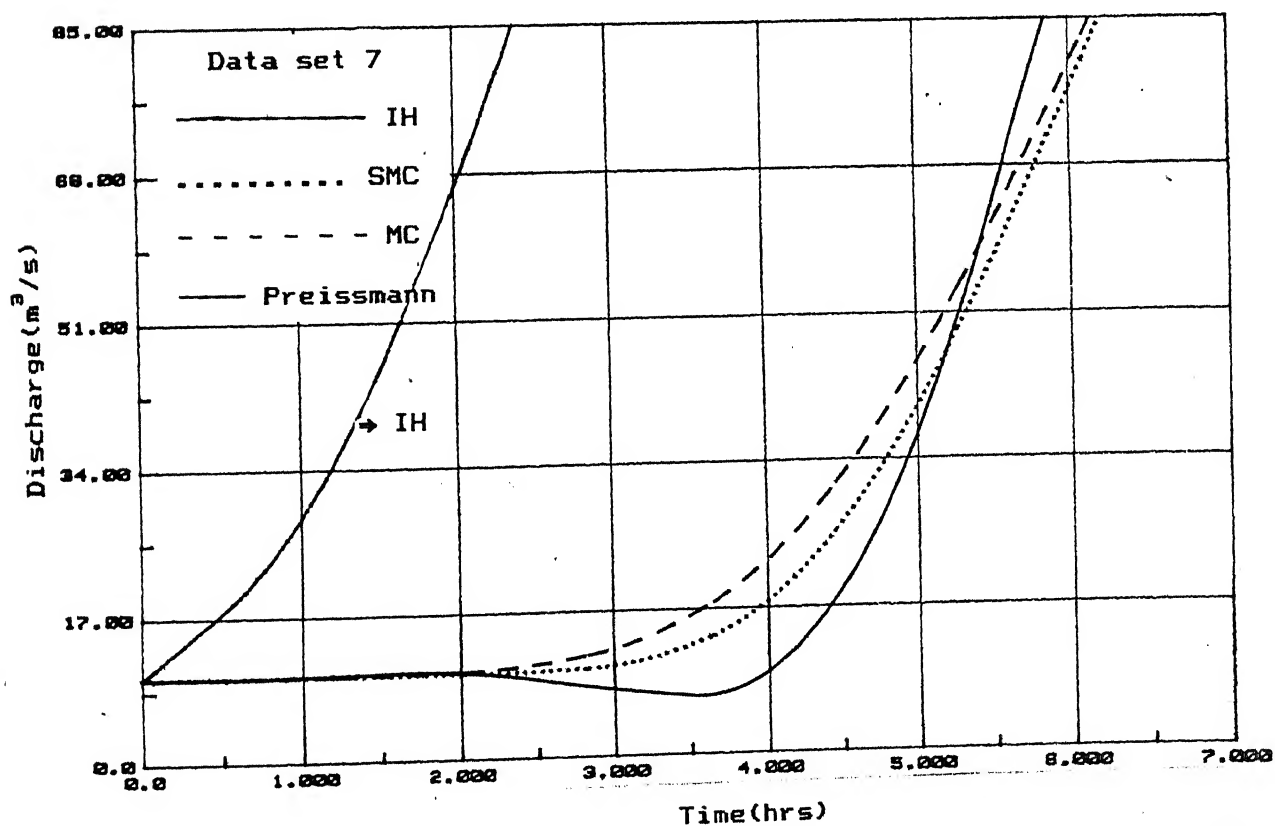


Fig. 4.12 Flows up to Q_{50} in the SMC, MC and the Preissmann models ---- Complex IH

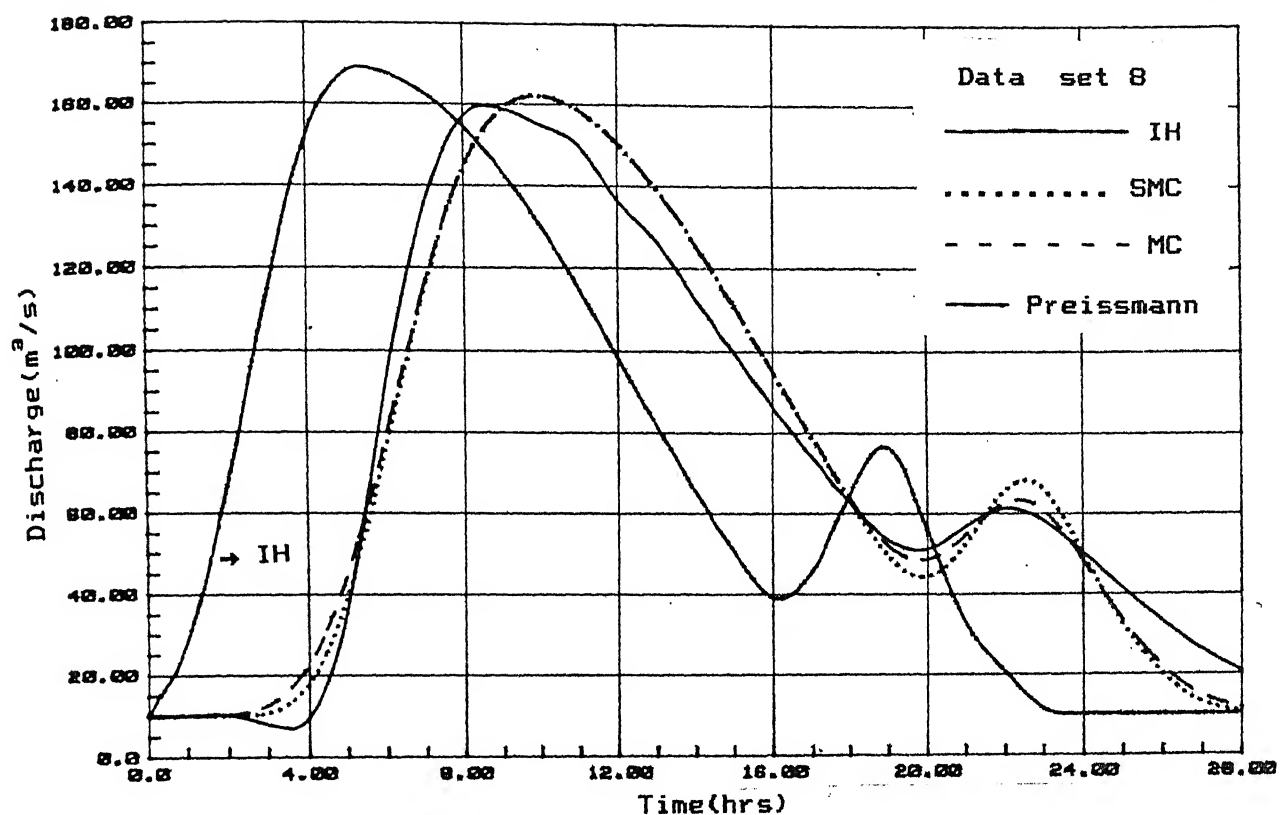


Fig. 4.13 Comparison of SMC model with the MC and Preissmann models --- Complex IH

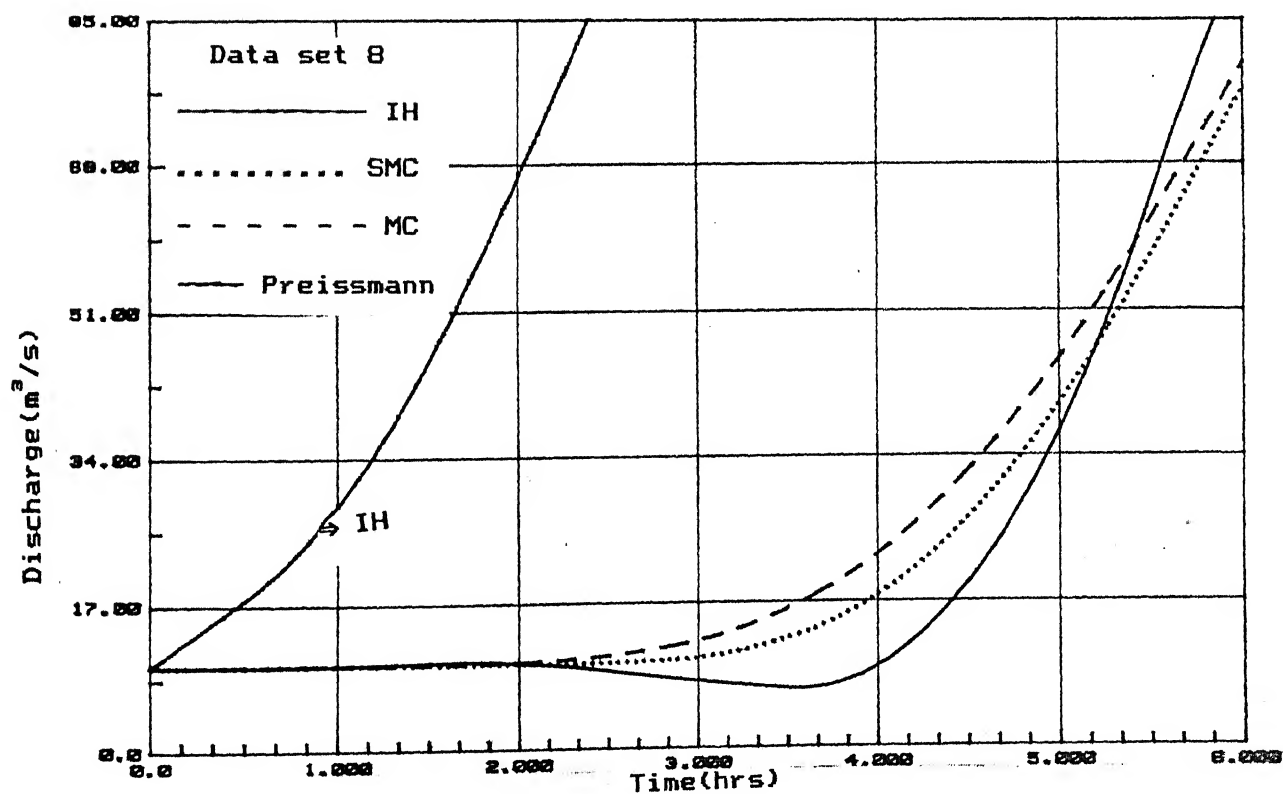


Fig. 4.14 Flows up to Q_{50} in the SMC, MC and the Preissmann models ---- Complex IH

20.0	55.75			49.83
20.28		48.64	44.07	
21.90		62.91	65.53	
22.0	20.60			62.44
24.0	10.00			50.20
24.33		42.95	43.06	
25.96		21.72	19.97	
26.0	10.00			33.08
28.0	10.0			20.56
28.39		10.86	10.24	

* represents peak value.

From Figs. 4.13 and 4.14 and Table 4.4, it is seen that:

The first three conclusions arrived in Case 1 (and also in Case 2 and Case 3) also hold good here. Further,

1. The predicted magnitude of second peak by the SMC method is slightly more in comparison to the Preissmann method and the MC methods.
2. The second peak predicted by the MC method lies between those of the SMC and Preissmann methods. However, the percentage over prediction by the SMC relative to the Preissmann is less than 5 % , and relative to the MC method is than 4 % .

4.4 CONCLUSION:

A method of Segregating the IH and using MC method, called as SMC is proposed.

1. This method predicts in all type of hydrographs , the flows upto Q_{50} more accurately than the MC method.
2. When the IH is a single peaked normal hydrograph , the flows beyond Q_{50} are predicted to the same accuracy as

the MC method.

3. When the IH is a complex hydrograph with double peaks , SMC method gives the outflow hyrograph values comparable to that one predicted by the MC method with errors less than 5 % .

However, when there is a second peak, , both the SMC and the MC methods over predict slightly ($\leq 10\%$) magnitude of the second peak in comparison to the results of the Preissmann method.

CHAPTER-5

LAPLACE TRANSFORM METHOD

5.0 INTRODUCTION:

An approach for routing the flood by a lumped model is developed by making use of the solution to a step input function of Muskingum equation with the boundary condition $Q(0^+) = 0.0$. The parameters are estimated as in the Muskingum-Cunge(MC) method, by relating them to the physical and morphological characteristics of the channel. The relative accuracies of the proposed model, is compared with the MC method and as well as with the implicit Preissmann scheme.

5.1 ROUTING OF A STEP INPUT :

The Muskingum method of flood routing is based on the following two equations.

$$\frac{dS}{dt} = I - Q \quad (5.1)$$

$$\text{and} \quad S = K [\theta I + (1-\theta)Q] \quad (5.2)$$

where S , K , θ are the usual Muskingum parameters.

Eliminating S in Eq(5.1) and (5.2) gives

$$Q + K(1-\theta) \left(-\frac{dQ}{dt} \right) = I - K\theta \left(\frac{dI}{dt} \right) \quad (5.3)$$

Kulandaiswamy [15] and Diskin [7] have solved Eq(5.3) for a step input by the instantaneous unit hydrograph technique of Nash

with the initial conditions

$$I(0) = Q(0) = I_0$$

and obtained the solution as

$$Q = I_0 \left\{ 1 - (1-\theta)^{-1} \exp \left[-\frac{t}{K(1-\theta)} \right] \right\} \quad (5.4)$$

Gill [10] obtained the solution to the step input by applying the Laplace transform to Eq(5.3) to get

$$\bar{Q} + K(1-\theta)[p \bar{Q} - Q(0^+)] = \bar{I} - K \theta [p \bar{I} - I(0^+)] \quad (5.5)$$

in which \bar{Q} and \bar{I} denote the Laplace transform of $Q(t)$ and $I(t)$ respectively. Here, p is a variable used in transforming $F(t)$ in the time domain into $F(p)$ in the Laplace transform domain and $Q(0^+)$ and $I(0^+)$ are the initial values. Q and I approach the origin ($t = 0$) from the positive side of the axis. The specification of the initial conditions in this manner is crucially important for situations in which a discontinuity exists at $t = 0$; Eq(5.5) is then solved by Gill[10] to give

$$\bar{Q} = \frac{\bar{I} - K \theta [p \bar{I} - I(0^+)] + K(1-\theta) Q(0^+)}{1 + Kp(1-\theta)} \quad (5.6)$$

Inversion of Eq.(5.6) leads to solution of $Q(t)$.

For a step input at $t = 0$, mathematically

$$\begin{aligned} I(t) &= 0, \quad t < 0 \\ I(t) &= I_0, \quad t > 0 \end{aligned} \quad (5.7)$$

There is a discontinuity in the value of $I(t)$ at $t = 0$, and it should be noted that $I(0^+) = I_0$. The discontinuity at the upstream end is progressively diffused and at the downstream end the flow can be taken equal to zero at $t = 0$ so that $Q(0^+) = 0$.

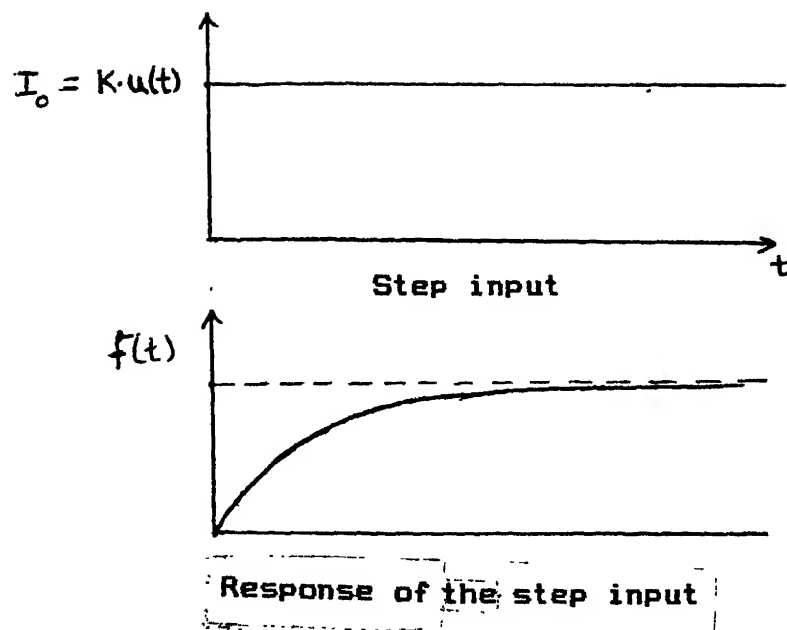


Fig. 5.0 Definition Sketch

Also, the Laplace transform of unit step of I_o at $t = 0$ is given by

$$\bar{I} = \frac{I_o}{p}.$$

Substituting \bar{I} , $I(0^+)$ and $Q(0^+)$ values in Eq(5.6), we obtain

$$\bar{Q} = \frac{I_o}{p[1 + Kp(1-\theta)]} \quad (5.8)$$

Eq(5.8) is solved directly to give

$$Q = I_o \left\{ 1 - \exp \left[- \frac{t}{K(1-\theta)} \right] \right\} \quad (5.9)$$

The Fig. 5.0 shows the definition sketch of a step input and the obtained output for the boundary conditions of $I(0^+) = I_o$ and $Q(0^+) = 0$.

Perumal[17], Dooge et. al [9] have taken the initial condition for Eq. (5.7) as

$$Q(0^+) = - \frac{\theta}{1-\theta} I_o \quad (5.10)$$

and obtained the solution in the same form as Eq.(5.4), viz

$$Q = I_o \left\{ 1 - (1-\theta)^{-1} \exp \left[- \frac{t}{K(1-\theta)} \right] \right\} \quad (5.4)$$

The solution proposed by Gill [10] with $Q(0^+)=0$ is considered superior, even though the boundary condition at $t = 0$ could be disputed [9,17].

The Gill solution for step input as

$$Q = I_o \left\{ 1 - \exp \left[- \frac{t}{K(1-\theta)} \right] \right\} \quad (5.9)$$

is used in this Chapter to develop a model for routing an inflow hydrograph(IH).

5.2 ROUTING OF INFLOW HYDROGRAPH(IH) BY STEP INPUT FUNCTIONS:

The given IH is approximated by a stair case function as in Gille et. al [11].

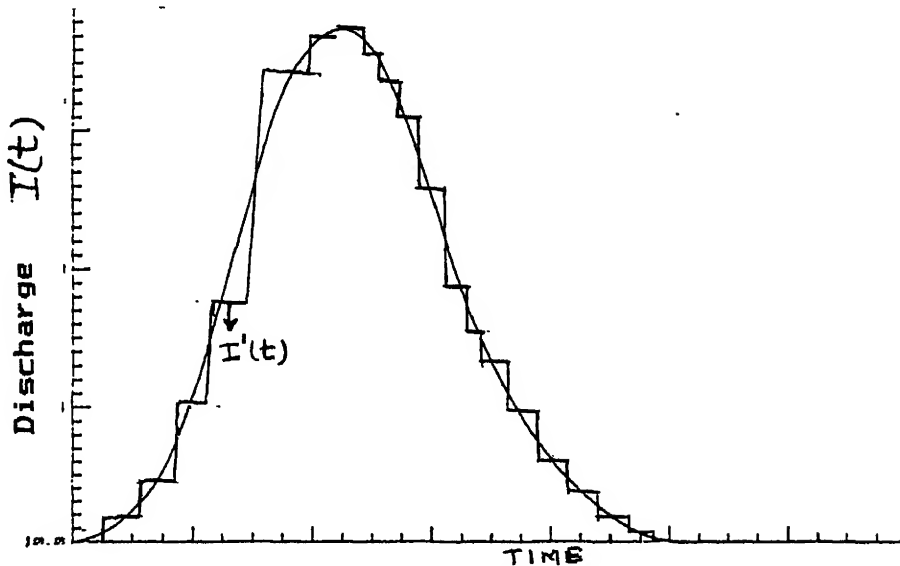


Fig. 5.1 Stair case approximation of a IH

Consider an $I'(t)$ in Fig. 5.1 an approximation of $I(t)$.

The IH at any time can be split and written as

$$I'(t) = I(0) + [I(1) - I(0)] u(t - \Delta t) + [I(2) - I(1)] u(t - 2\Delta t) + \dots$$

$$= I(0) + \sum_{j=1}^N [I(j) - I(j-1)] u(t - j\Delta t) \quad (5.11)$$

where $u(t)$ is a unit step function.

The transfer function

$$H(I_0) = I_0$$

$$H[M u(t - n\Delta t)] = M [1 - \exp(-\frac{(t - n\Delta t)}{K(1-\theta)})] u(t - n\Delta t)$$

where M is an appropriate constant, which is the differences between the two adjacent step input functions.

Since the Muskingum method assumes linear relationship between the storage, input and output hydrographs, the principle of superposition theorem can be used to get:

$$\begin{aligned}
H[I'(t)] = & I(0) + [I(1)-I(0)] \left[1 - \exp\left(-\frac{(t-\Delta t)}{K(1-\theta)}\right) \right] u(t-\Delta t) \\
& + [I(2)-I(1)] \left[1 - \exp\left(-\frac{(t-2\Delta t)}{K(1-\theta)}\right) \right] u(t-2\Delta t) \\
& + [I(3)-I(2)] \left[1 - \exp\left(-\frac{(t-3\Delta t)}{K(1-\theta)}\right) \right] u(t-3\Delta t) + \dots
\end{aligned}$$

The output hydrograph at any time t is calculated as

$$Q(t) = I(0) + \sum_{j=1}^N [I(j) - I(j-1)] \left[1 - \exp\left(-\frac{(t-j\Delta t)}{K(1-\theta)}\right) \right] u(t-j\Delta t). \quad (5.13)$$

Eq. 5.13 is the output for the given input stair case function $I'(t)$. Knowing the MC parameters K and θ , for any given IH the output $Q(t)$ can be explicitly determined by using Eq.(5.13).

The proposed model, which is routed with series of step inputs on the basis of Muskingum equation is designated as Muskingum-Laplace-Transform (MLT) model in rest of the Chapter.

5.3 ESTIMATION OF PARAMETERS K AND θ :

5.3.1. When the input hydrograph and physical characteristics of channel are known:

The rectangular channel has a breadth B units and a longitudinal bed slope of s_o . The Manning's roughness coefficient n is known. The IH has a peak discharge Q_p . The IH was routed by MLT method through a reach length of L units. In the MLT method, to ensure the continuity equation to be linear, it is assumed that $c \propto F(t)$ and is a constant irrespective of the discharge. To route an IH by MLT method the MC coefficients K and θ are proposed to be used.

Thus by MC method, (Eqs 2.30 and 2.31)

$$K = \frac{L}{c}, \text{ where } K \text{ has units of time.}$$

and $\theta = 0.5 \left(1 - \frac{Q}{B S_o C L} \right)$ and $0 < \theta < 0.5$.

The value of wave celerity c , could be further assumed by either of the following two methods:

1. Assume a celerity of c value and then iterating as per Raudikivi's algorithm given in Section 2.3.2(Chapter 2, page 13).
2. The wave celerity c , can be calculated by the Kleitz -Seddon's law [Eq. (2.9)] as

$$c = \left(\frac{dQ}{dA} \right)_x = \frac{1}{B} \left(\frac{dQ}{dy} \right)_x$$

where $\left(\frac{dQ}{dA} \right)_x$ = slope of the stage-discharge curve at any section x .

In the absence of the stage-discharge relationship, Manning's formula may be used to estimate $\left(\frac{dQ}{dy} \right)_x$ and hence c .

5.3.2 When the Input and Output hydrographs are available:

When one or more sets of inflow and outflow hydrographs are available for the catchment, by the method of moments the different sets of parameters of K and θ are obtained for different inflow and outflow hydrograph sets (as explained in Section 2.2.2).

Thus $K = M_1^O(Q) - M_1^O(I)$

$$\theta = 0.5 \left\{ 1 - \frac{M_2(Q) - M_2(I)}{K^2} \right\}$$

where, $M_1^O(Q)$ and $M_1^O(I)$ are the first moments of the outflow and inflow hydrographs about the origin respectively.

$M_2(Q)$ and $M_2(I)$ are the second moments of outflow and inflow

hydrographs about their center of gravity respectively.

From these sets of K and θ , the appropriate K and θ are chosen for use in the MLT method depending on the range of IH values.

5.4 PROPOSED ALGORITHM OF MUSKINGUM-LAPLACE-TRANSFORM(MLT) :

The following procedure is adopted for routing a flood by MLT method.

Given : Rectangular channel of breadth = B , Slope = s_o .

Manning's roughness coefficient = n , Reach length = L

IH with ordinates at time interval DTG.

1. Choose a value of DT at which the IH of period DTG, can be represented by a staircase approximation function.
2. Obtain the values of the IH at an interval of chosen DT with a second order interpolation procedure.
3. From the interpolated IH values, obtain the peak discharge Q_p .
4. Calculate the normal depth y_n for the peak discharge Q_p .
5. Calculate the wave celerity c for the rectangular channel by Kleitz-Seddon's law as:

$$c = \frac{\beta Q_p}{B y_n}$$

where β is the exponent value for the discharge area relationship based on the resistance formula. For Manning's formula $\beta = 1.66$.

6. Calculate the routing parameters K and θ as :

$$K = \frac{L}{\langle c \rangle}$$

$$\theta = 0.5 \left(1 - \frac{Q_p}{B s_o \langle c \rangle L} \right)$$

7. The approximated IH is now routed by the using routing parameters K

and θ , to get the outflow hydrograph ordinate at any time t is obtained as :

$$Q(t) = I(0) + \sum_{j=1}^N [I(j) - I(j-1)] \left[1 - \exp\left(-\frac{(t-j\Delta t)}{K(1-\theta)}\right) \right] u(t-j\Delta t)$$

where $u(t)$ is a unit function.

5.5 NUMERICAL EXPERIMENTATION:

The efficacy of the proposed MLT method is compared with the implicit Preissmann scheme and the MC method through numerical experimentation, using four sets of data [set2-5]. For all sets of data, a value of $\alpha = 0.66$ is used in the Preissmann scheme and a Courant number of 0.85 is used in the MC method. The MLT model was approximated into a staircase function at a time step $DT = 100$ seconds ($DTG/DT = 36$). Each IH was routed by the MLT, MC and the Preissmann methods.

Case 1:

First, the normal IH of data set 3 (Fig 5.2) for a rectangular channel was considered. The channel has a width of 50 m and a longitudinal bed slope of 0.0005. The Manning's roughness coefficient was chosen as $n = 0.03$. The IH was routed over a reach length of 18000 m. A value of $\Delta x = 4500$ m was used in the MC method. The outflow hydrographs obtained by the MLT, MC and the Preissmann methods in this study are plotted in Fig. 5.2 along with the corresponding IH. Fig. 5.3 is enlarged plot to show the attenuation of the peak discharge in these three methods. The numerical error is calculated for the peak discharge and its time of occurrence as:

$$\% \text{ Error} = \frac{E - E_P}{E_P} \times 100$$

where E_p is the Preissmann peak discharge or its time of occurrence. For all the cases (case 1-4), these error percentages are tabulated in Table 5.5. Some of the salient routing data for the MLT, MC and the Preissmann scheme are presented in Table 5.1(a). The peak characteristics obtained by the MLT, MC and the Preissmann methods are tabulated in Table 5.1(b).

From the Figs. 5.2 and 5.3 and Table 5.1(b) it is seen that:

1. The attenuation of the peak discharge in the MLT method is slightly more (1.23%) in comparison to the Preissmann scheme.
2. The attenuation of the peak discharge in the MC method is slightly less (1.26%) in comparison to the Preissmann scheme.
3. The translation of the peak discharge in the MLT method is slightly less (6.62%) in comparison to the Preissmann scheme.
4. The translation of the peak discharge in the MC method is slightly more (3.69%) in comparison to the Preissmann scheme.
5. The absolute error in the prediction of the peak discharge by the MLT method is of the same order as that of the MC method.
6. The absolute error in the prediction of time of occurrence for the peak discharge is more in the MLT than the MC method.

Table 5.1(a)

SOME SALIENT ROUTING DATA FOR DATA SET 3

Time (hrs)	Ord.of Inflow (m ³ /s)	Ordinates of outflow hydrograph in m ³ /s		
		Preissmann	MLT	MC
0.0	10.00	10.00	10.00	10.00
2.0	12.00	9.97	12.82	
4.0	50.00	11.00	29.41	10.60 @ 2.28 hr
6.0	107.00	38.74	71.79	21.77 @ 4.56 hr
8.0	147.00	109.01	120.98	45.77 @ 6.08 hr
9.0	150.00*			105.10 @ 8.36 hr
10.0	146.00	144.21	142.09	
11.0	129.00	144.44*	142.66 @ 10.27hr*	
12.0	105.00	135.62	127.44	146.26 @ 11.406 hr*
14.0	59.00	99.66	86.78	142.93 @ 12.17 hr
16.0	33.00	65.04	52.72	102.51 @ 14.45 hr
18.0	17.00	41.89	29.59	68.95 @ 15.97 hr
20.0	10.00	26.71	15.96	35.92 @ 18.25 hr
22.0	10.00	17.12	11.37	22.14 @ 19.77 hr
24.0	10.00	12.12	10.32	11.47 @ 22.05 hr
26.0	10.00	10.51	10.07	10.03 @ 24.33 hr
28.0	10.00	10.10	10.01	10.00 @ 25.85 hr
				9.99 @ 28.13 hr

* represents peak discharge values.

Table 5.1(b)

PEAK CHARACTERISTICS FOR DATA SET 3

	Preissmann	MLT	MC
Peak discharge Attenuation (in m ³ /s)	5.56	7.34	3.74
Time to peak (in hrs)	11.0	10.27	11.406

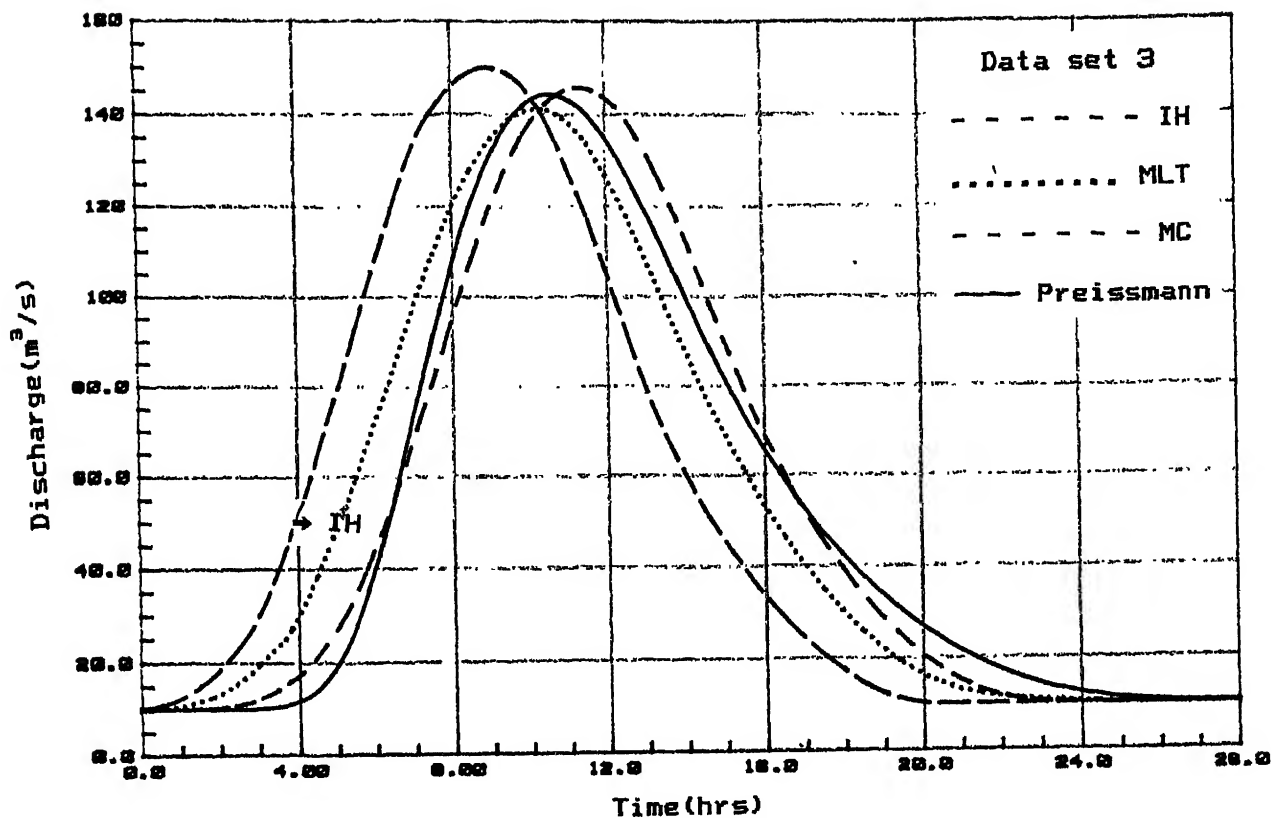


Fig. 5.2 Comparison of MLT model with the MC and the Preissmann models - Normal IH

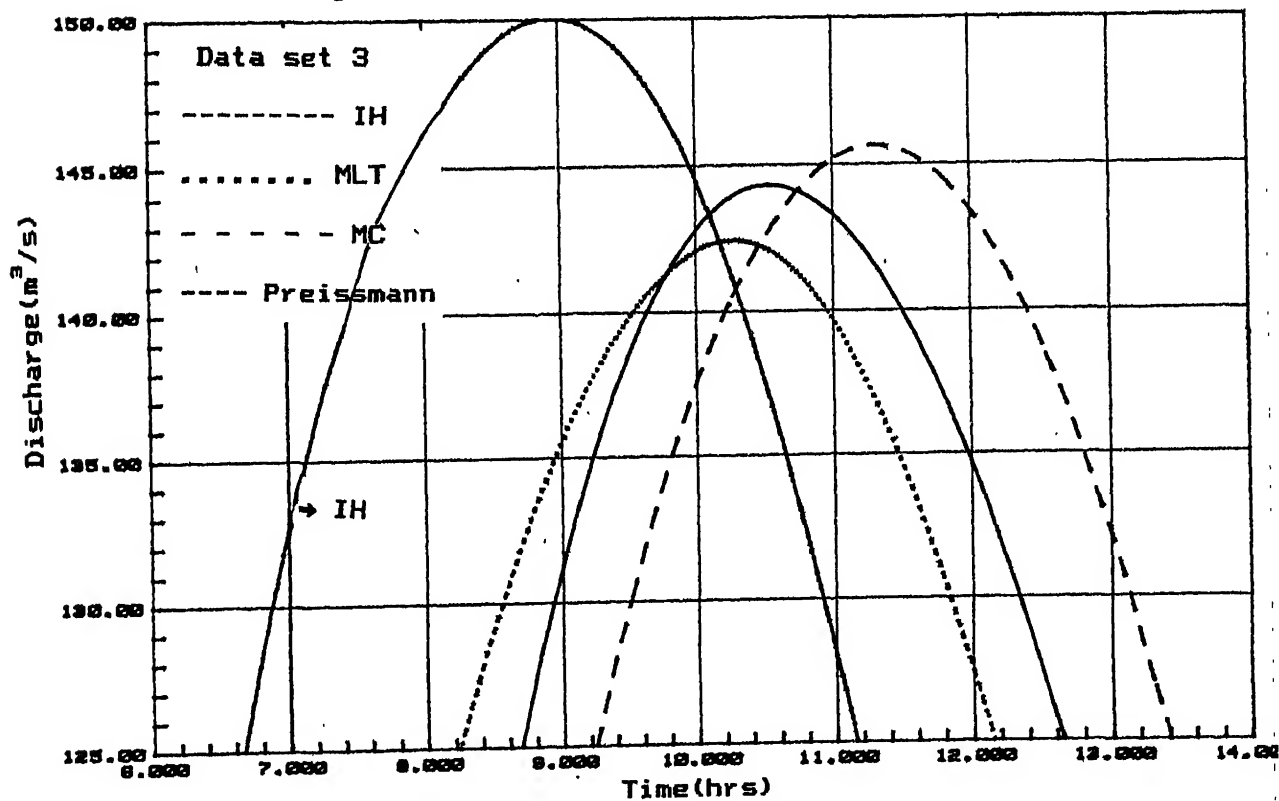


Fig. 5.3 Attenuation of peak discharge in MLT, MC and the Preissmann models - Normal IH

Case 2:

A steep rise IH(Fig. 5.4) of data set 4 for a rectangular channel was considered next. The physical characteristics of the channel are same as in case 1. a value of $\Delta x = 6000$ m is used for the MC method. The IH was routed by the MLT, MC and the Preissmann methods. The outflow hydrographs obtained by these methods are plotted in Fig. 5.4. Fig. 5.5 is an enlarged plot to show the attenuation of peak in the MLT, MC and the Preissmann methods. Some of the salient routing data are tabulated in Table 5.2(a). The peak characteristics are tabulated in Table 5.2(b).

From the Figs. 5.4 and 5.6 and Table 5.2(b) it is seen that:

1. The attenuation of the peak discharge in the MLT method is slightly more(3.33%) in comparison to the Preissmann method.
2. The attenuation of the peak discharge in the MC method is slightly less(1.27%) in comparison to the Preissmann method.
3. The translation of the peak discharge in the MLT method is slightly less(5.42%) in comparison to the Preissmann method.
4. The translation of the peak discharge in the MC method is slightly more(6.85%) in comparison to the Preissmann method.
5. The absolute error in the prediction of the peak discharge by the MLT method is more than that of the MC method.
6. The absolute error in the prediction of peak discharge by the MLT method is more than that of the MC method.

Table 5.2(a) SOME SALIENT ROUTING DATA FOR DATA SET 4

70

Time (hrs)	Ord. of Inflow (m ³ /s)	Ordinates of outflow hydrograph in m ³ /s		
		Preissmann	MLT	MC
0.0	10.00	10.00	10.00	10.00
2.0	52.00	9.78	24.58	11.62 @ 2.04 hr
4.0	141.0	38.14	88.94	47.51 @ 4.08 hr
5.0	150.0*			
6.0	144.0	133.13	134.04	
7.0		140.85*	136.16 @ 6.62hr*	122.75 @ 6.12 hr
				142.64* @ 7.48 hr
8.0	114.00	135.66	128.00	141.31 @ 8.16 hr
10.0	86.00	111.09	104.00	117.14 @ 10.26 hr
12.0	61.00	86.04	78.17	88.46 @ 12.25 hr
14.0	41.00	64.11	55.12	62.79 @ 14.29 hr
16.0	25.00	46.28	36.32	41.88 @ 16.32 hr
18.0	14.00	32.33	22.22	25.72 @ 18.37 hr
20.0	10.00	22.07	13.57	17.80 @ 19.73 hr
22.0	10.00	15.06	10.82	10.48 @ 22.45 hr
24.0	10.00	11.48	10.19	10.06 @ 23.81 hr
26.0	10.00	10.35	10.04	10.02 @ 25.85 hr
28.0	10.00	10.07	10.00	10.00 @ 27.89 hr

* represents peak discharge values.

Table 5.2(b) PEAK CHARACTERISTICS FOR DATA SET 4

	Preissmann	MLT	MC
Peak discharge Attenuation (in m ³ /s)	9.15	13.84	7.36
Time to peak (in hrs)	7.0	6.62	7.48

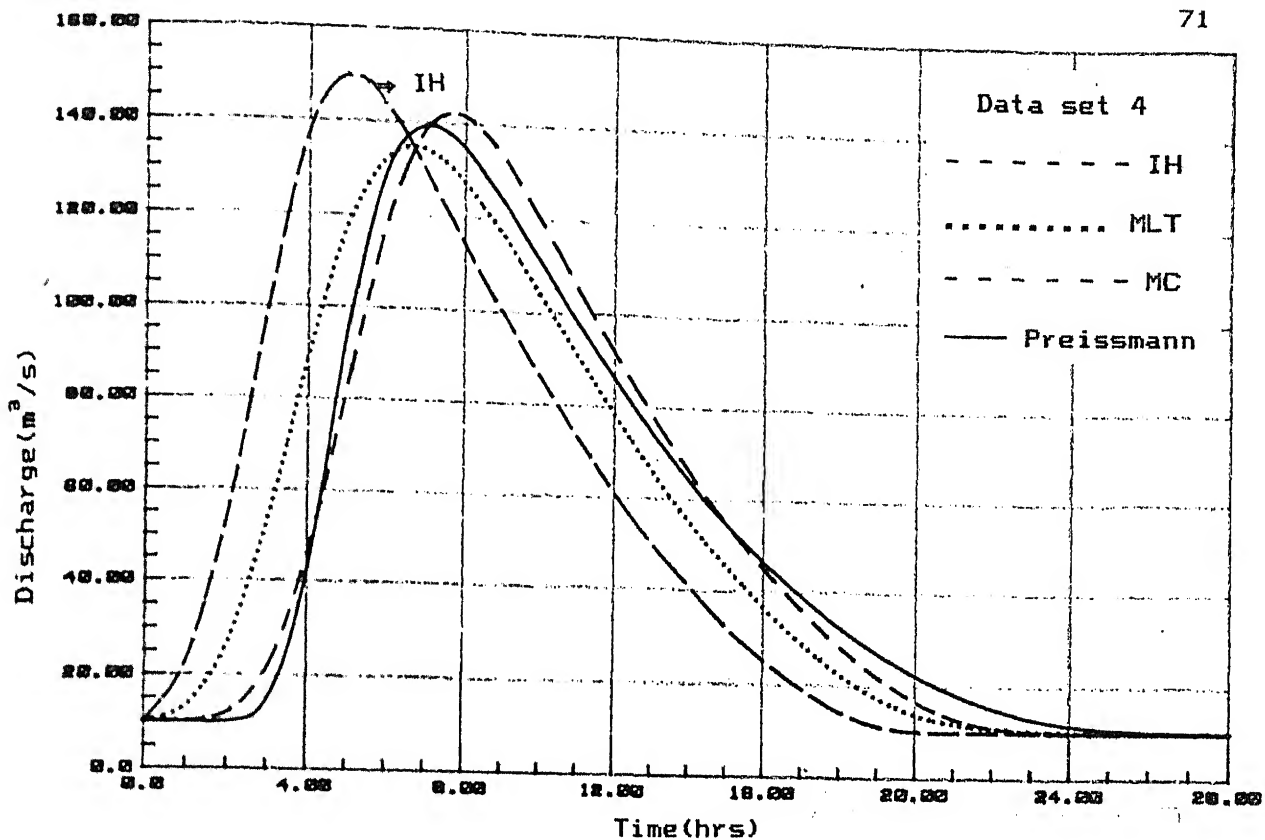


Fig. 5.4 Comparison of MLT model with the MC and the Preissmann models - Steep rise IH

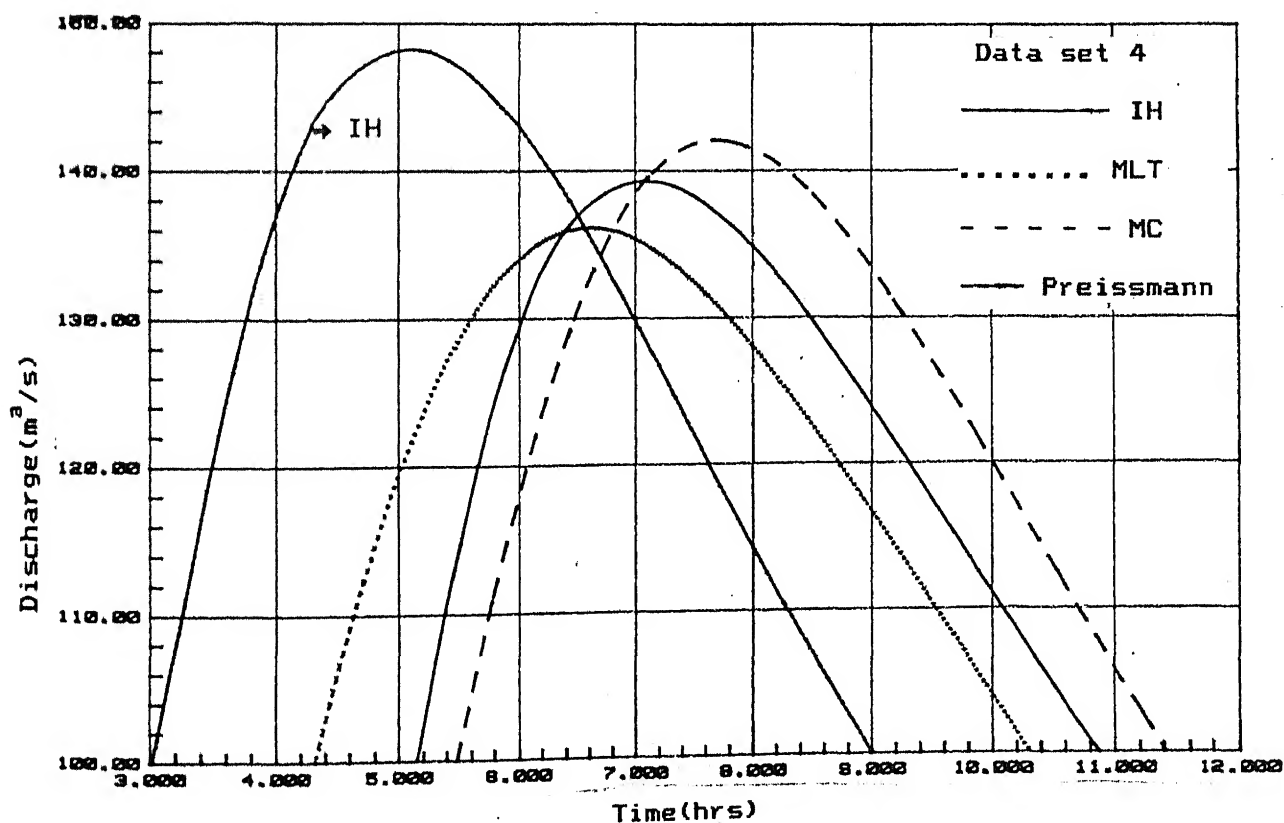


Fig. 5.5 Attenuation of peak discharge in MLT, MC and the Preissmann models - Steep rise IH

A triangular IH(Fig. 5.6) of data set 5 for a rectangular channel was considered. This IH of Fig. 5.6 has a peak discharge of $2000 \text{ m}^3/\text{s}$ occurring at 10.0 hrs. The channel has a width of 60 m and a longitudinal slope of 0.0015. The Manning's roughness coefficient $n = 0.02$ was chosen. The IH was routed by the MLT, MC and the Preissmann methods through a reach length of 30000 m. A value of $\Delta x = 7500 \text{ m}$ was used for the MC method. The outflow hydrographs obtained in the study by the MLT, MC and the Preissmann methods are plotted in Fig. 5.6 along with the corresponding IH. Fig. 5.7 is an enlarged portion of the plot to show the peak attenuation in the three methods. Some of the salient routing data are presented in Table 5.3(a). The peak characteristics are shown in Table 5.3(b).

From the Figs 5.6 and 5.7 and Table 5.3(b) it is seen that:

1. The attenuation of the peak discharge in the MLT method is slightly more (4.77%) in comparison to the Preissmann method.
2. The attenuation of the peak discharge in the MC method is slightly less (3.12%) in comparison to the Preissmann method.
3. The translation of the peak discharge in the MLT method is slightly less(1.69%) in comparison to the Preissmann method.
4. The translation of the peak discharge in the MC method is slightly more(11.77%) in comparison to the Preissmann method.
5. The absolute error in the prediction of the peak discharge by the MLT method is more than the MC method.

6. The absolute error in the prediction of the peak discharge by the MLT method is less than the MC method.

Table 5.3(a) SOME SALIENT ROUTING DATA FOR DATA SET 5

Time (hrs)	Ord. of Inflow (m ³ /s)	Ordinates of outflow hydrograph in m ³ /s		
		Preissmann	MLT	MC
0.0	50.00	50.00	50.00	50.00
2.0	80.00	49.89	60.61	50.00 @ 2.1 hr
4.0	110.00	51.42	82.99	51.11 @ 4.03 hr
6.0	140.00	78.48	109.98	75.88 @ 5.97 hr
8.0	170.00	115.52	138.80	107.37 @ 8.07 hr
10.0	200.00*	151.26	168.34	136.44 @ 10.01 hr
12.0	185.00	151.25	182.66	165.51 @ 11.95 hr 197.94 @ 14.53 hr*
13.0		191.97*	182.81 @ 12.78 hr	
14.0	170.00	190.41	178.77	195.75 @ 14.04 hr
16.0	155.00	177.47	168.15	187.02 @ 15.98 hr
18.0	140.00	163.29	154.67	171.22 @ 18.08 hr
20.0	125.00	149.15	140.54	156.69 @ 20.02 hr
22.0	110.00	135.12	125.81	142.15 @ 21.96 hr
24.0	95.00	121.23	110.91	126.41 @ 24.06 hr
26.0	80.00	107.52	95.95	111.87
28.0	65.00	94.03	80.97	96.13 @ 28.09 hr
30.0	50.00	80.85	65.97	81.59 @ 30.03 hr
32.0	50.00	68.03	56.14	67.06 @ 31.97 hr
34.0	50.00	55.94	52.42	51.79 @ 34.07 hr
36.0	50.00	51.45	50.94	49.98 @ 36.01 hr

* represents peak value.

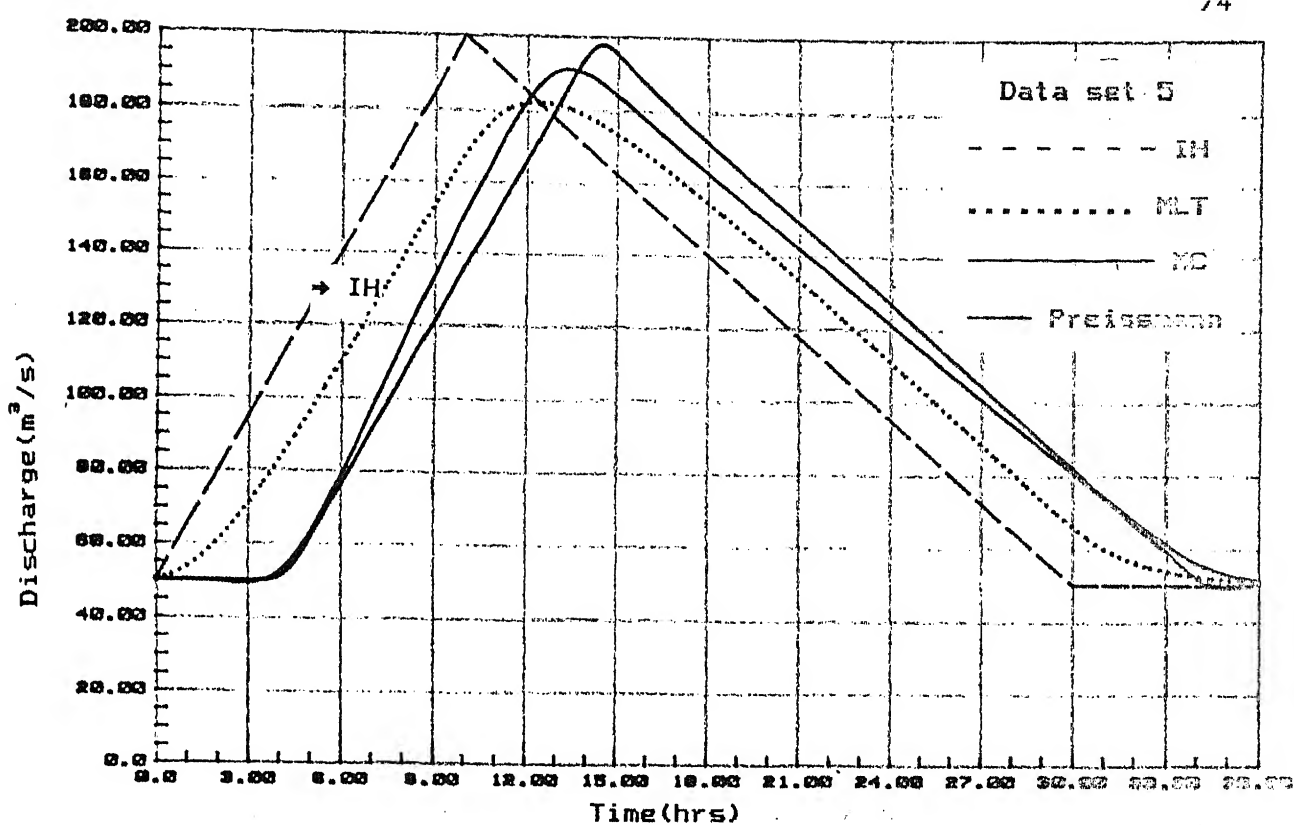


Fig. 5.6 Comparison of MLT model with the MC
and the Preissmann models - Triangular IH

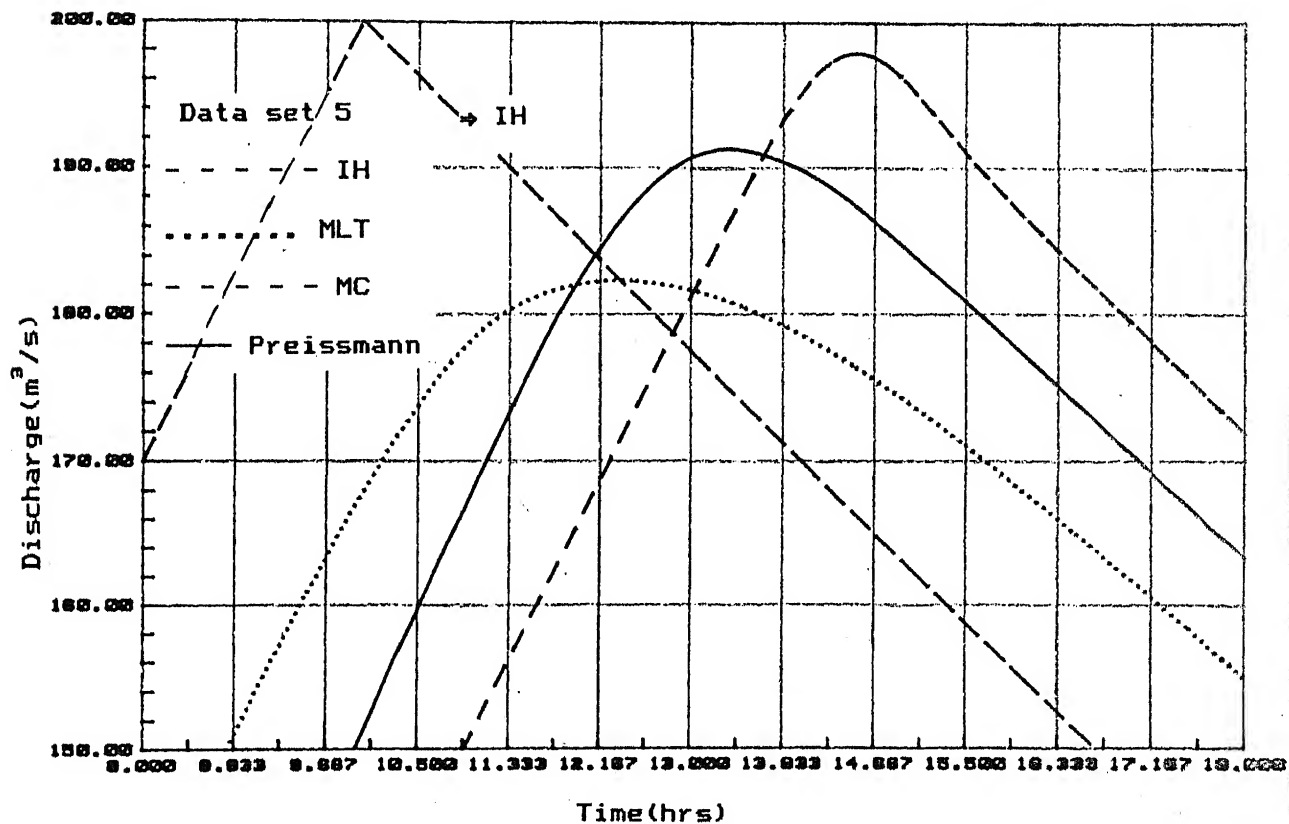


Fig. 5.7 Attenuation of peak discharge in MLT,
MC and the Preissmann models - Triangular IH

Table 5.3(b) PEAK CHARACTERISTICS FOR DATA SET 5

	Preissmann	MLT	MC
Peak discharge Attenuation (in m^3/s)	8.03	17.19	2.06
Time to peak (in hrs)	13.0	12.78	14.53

Case 4:

A Pearson type III hydrograph (data set 2) which has a stage hydrograph as shown in Fig. 5.8 for a rectangular channel was considered. The channel has a width of 5000 ft (1500 m) and a longitudinal bed slope of 0.000189. The Manning's roughness coefficient $n = 0.03$. This hydrograph was routed through reach length of 100 miles (160 Km) by MLT, MC and Preissmann methods. The outflow stage hydrograph obtained in this study are plotted in Fig. 5.8. Fig. 5.9 is an enlarged plot of Fig. 5.8 to show the attenuation of depth by the MLT, MC and the Preissmann methods. Some of the salient routing data are tabulated in Table 5.4(a). Peak characteristics are tabulated in Table 5.4(b).

Table 5.4(a) SOME SALIENT ROUTING DATA FOR SET 2

Time (hrs)	Initial (ft)	Final stage hydrograph in ft		
		Preissmann	MLT	MC
0.0	5.08	5.08	5.08	5.08 5.08 @ 5.07 hr
6.0	5.22	5.00	5.10	
12.0	7.21	5.00	5.66	5.15 @ 12.69 hr
18.0	12.04	4.98	8.09	5.64 @ 17.77 hr
24.0	18.02	5.00	12.42	8.72 @ 25.39 hr
30.0	23.49	5.51	17.51	12.46 @ 30.47 hr
36.0	27.57	2.86	22.29	16.85 @ 35.55 hr
42.0	29.95	10.20	26.04	23.15 @ 43.17 hr
48.0	30.68	21.62	28.47	26.42 @ 48.25 hr
54.0	30.06	26.85	29.51	28.67 @ 53.33 hr
60.0	28.43	29.01	29.585 @ 56 hr *	
64.5		29.4*	29.34	30.04 @ 60.94 hr *
66.0	26.15	29.36	28.20	29.78 @ 66.02 hr
72.0	23.52	28.57	26.36	28.04 @ 73.64 hr
78.0	20.80	27.06	24.09	26.26 @ 78.72 hr
84.0	18.15	25.17	21.62	24.20 @ 83.80 hr
90.0	15.70	23.09	19.12	20.88 @ 91.42 hr
96.0	13.51	20.99	16.73	18.69 @ 96.5 hr
102.0	11.62	18.97	14.54	15.62 @ 104.1 hr
108.0	10.05	17.07	12.60	13.80 @ 109.2 hr
114.0	8.77	15.34	10.93	12.17 @ 114.3 hr
120.0	7.76	13.79	9.53	10.76 @ 119.3 hr
126.0	6.99	12.41	8.40	9.03 @ 126.9 hr

132.0	6.41	11.20	7.50	8.12 @ 132.0 hr
138.0	5.99	10.14	6.85	7.38 @ 137.1 hr
144.0	5.70	9.23	6.30	6.55 @ 144.75 hr

* represents peak depth value.

Table 5.4(b) PEAK CHARACTERISTICS FOR DATA SET 2

	Preissmann	MLT	MC
Peak depth Attenuation (in ft)	1.28	1.095	0.64
Time to peak (in hrs)	64.5	56.0	60.94

From the Figs 5.8 and 5.9 and Table 5.4(b) it is seen that:

1. The attenuation of the peak depth in the MLT method is of the same order as the Preissmann method.
2. The attenuation of the peak depth in the MC method is slightly less (2.18%) in comparison to the Preissmann method.
3. The translation of the peak depth in the MLT method is slightly less (13.17%) in comparison to the Preissmann method.
4. The translation of the peak depth in the MC method is slightly less (5.52%) in comparison to the Preissmann method.
5. The absolute error in the prediction of the peak discharge by the MLT method is less than the MC method.
6. The absolute error in the prediction of the peak discharge by the MLT method is more than the MC method.

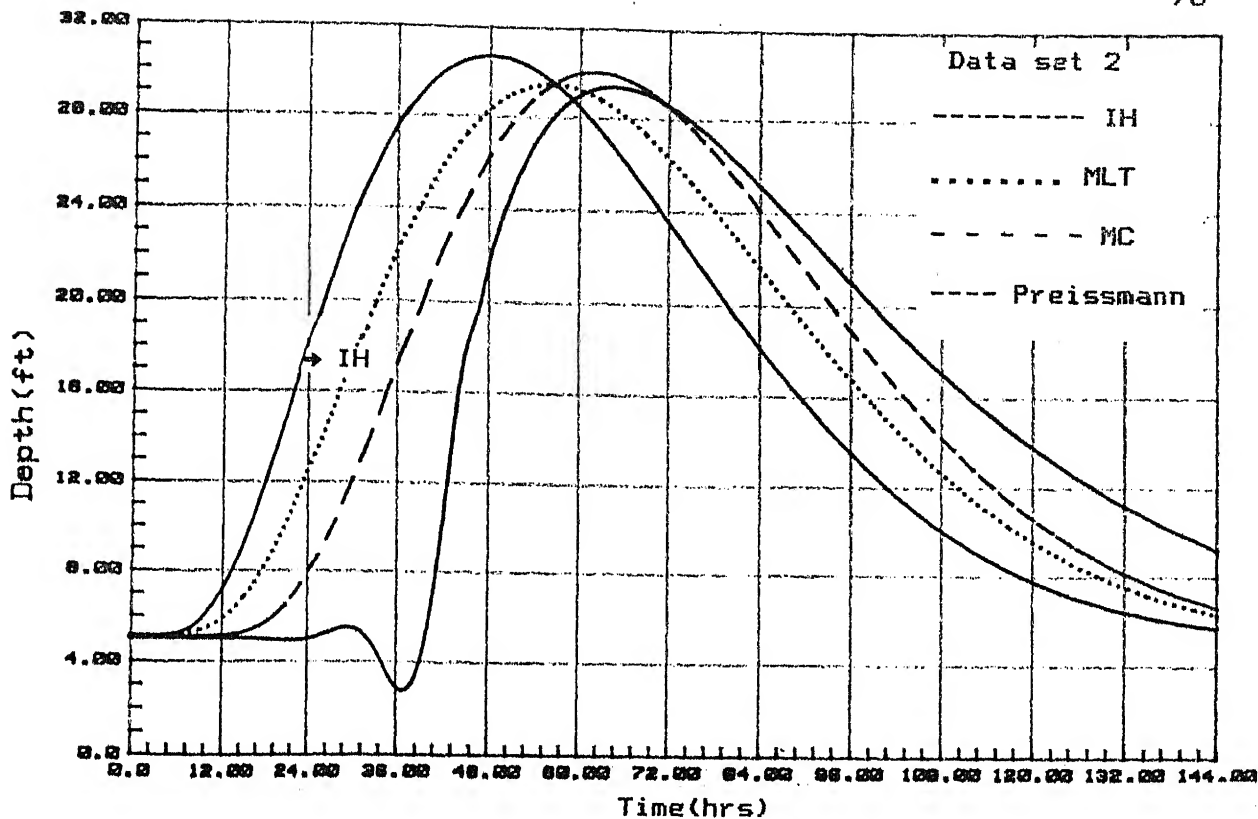


Fig. 5.8 Comparison of MLT model with the MC and the Preissmann models - Log Pearson Type III IH

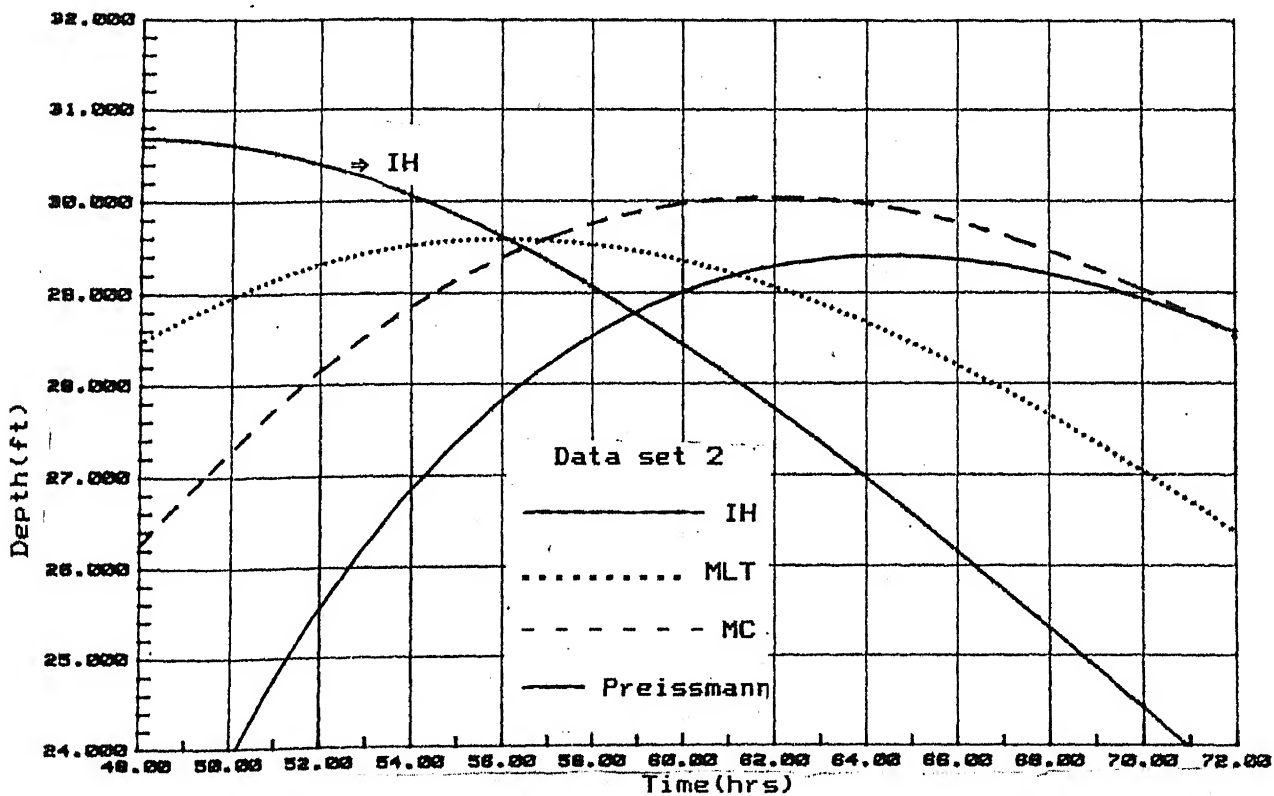


Fig. 5.9 Attenuation of peak depth in MLT, MC and the Preissmann models - Log Pearson type III IH

Case 5:

Out of Curiosity, the solution of Dooge.et.al[9] i.e. Eq.(5.4) was used instead of Eq.(5.9) in the MLT method. This method is referred as DMLT method. The results of case 1 are compared by routing the IH of case 1 by DMLT [Figs. 5.10, 5.11].

From the Figs. 5.10 and 5.11 it is seen that:

1. The output hydrograph values obtained in the DMLT method [Dooge.et.al's solution(Eq.5.4)] has negative flows in the initial region.
2. The outflow hydrographs values obtained by DMLT method Dooge.et.al's solution[Eq.5.4] do not match at all with the outflow values of either the Preissmann method or the MLT method.

As such, it is concluded that Gill's solution[Eq.5.9] is superior and relevant than the Dooge.et.al's solution[Eq. 5.4].

5.6 CONCLUSION:

Using Gill's solution [Eq.5.9] a method of routing the IH is proposed, called as MLT method. In the MLT method a stair case function is used to represent the given IH. An algorithm for the MLT method is given. The efficacy of the MLT method is compared with the implicit Preissmann and the MC method through numerical experimentation using four sets of data.

Table 5.5 gives an abstract of the relative performance of the MLT, MC and the Preissmann methods of routing for the four inflow hydrographs(data set 2- 4).

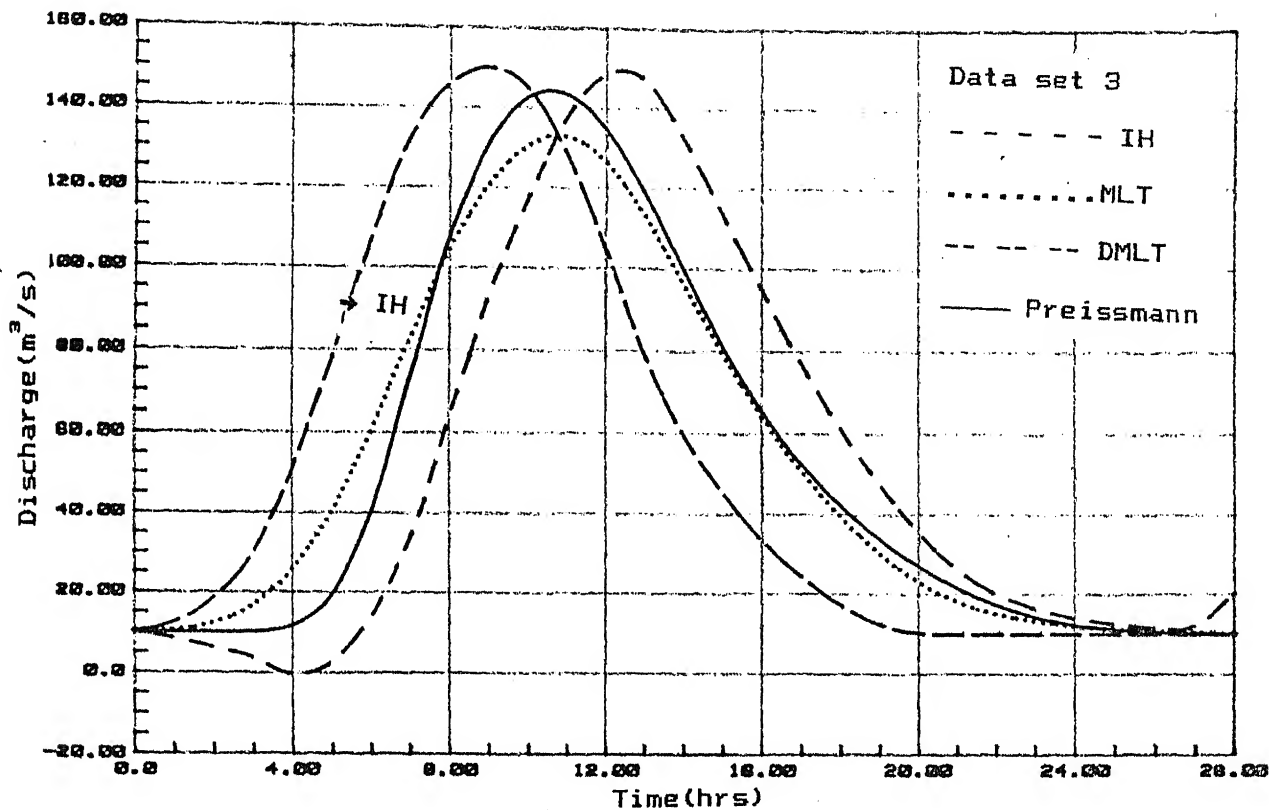


Fig. 5.10 Comparison of DMLT model with the MLT and Preissmann models - Normal IH

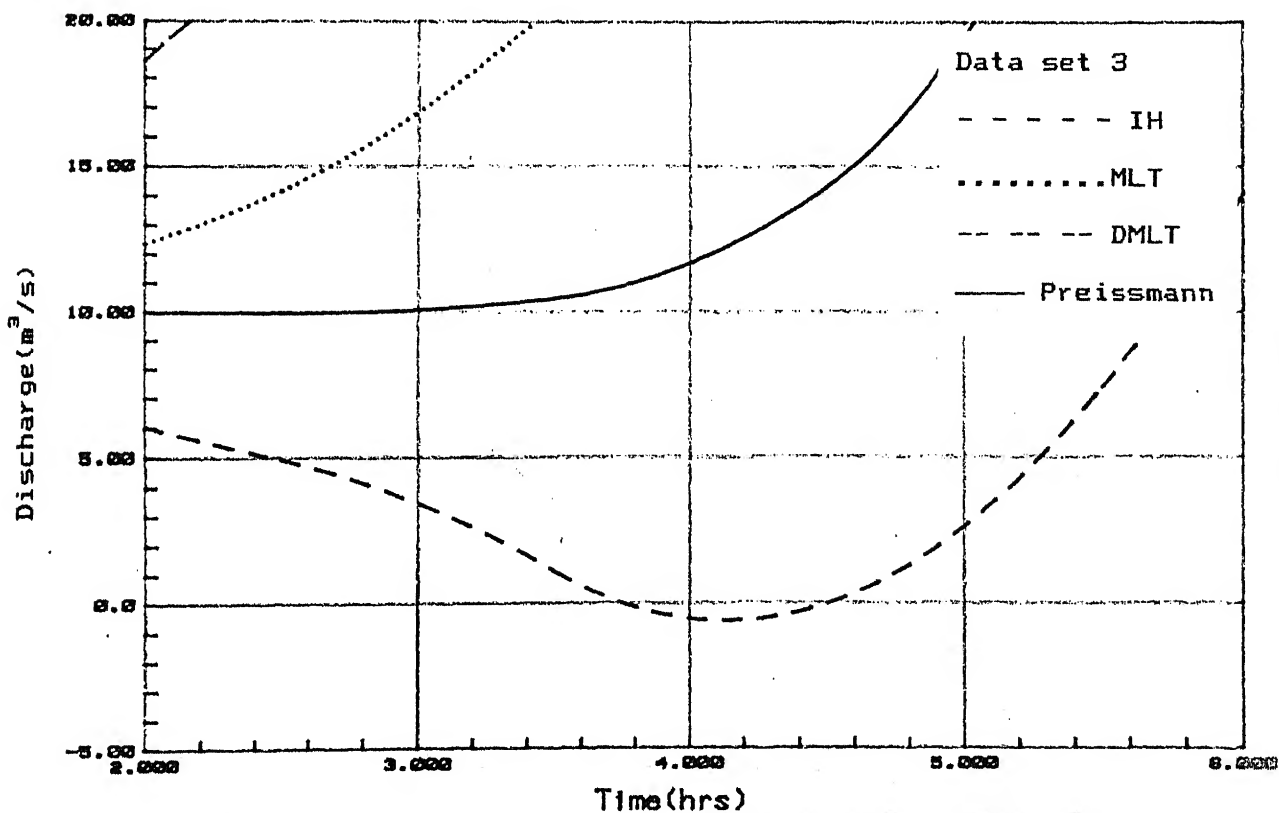


Fig. 5.11 Negative Flows in DMLT

Table 5.5

Data set#		Preissmann	MLT	MC	Error % For MLT	Error % For MC
For peak discharge(m^3/s)/depth(ft)						
2 (Normal)	Q	144.44	142.66	146.26	-1.23	1.26
3 (Steep)	Q	140.85	136.16	142.64	-3.33	1.27
5 (Triang.)	Q	191.97	182.81	197.94	-4.77	3.12
4.(Pearson)	H	29.401	29.585	30.042	0.63	2.18
Time of occurrence (in hrs)						
2 (Normal)		11.00	10.27	11.41	-6.63	3.69
3 (Steep)		7.00	6.62	7.48	-5.42	6.85
4 (Triang.)		13.00	12.78	14.53	-1.69	11.77
5 (Pearson)		64.50	56.00	60.94	-13.17	- 5.52

It is found that

1. The MLT method as proposed is a viable alternative to the MC method.
2. In general, the MLT method predicts peakflow to the same degree of accuracy as the MC method. However, while the MC method was found to over predict the peak (with errors of order of 3%) relative to the Preissmann scheme, the MLT method under predicts the peak (with errors of order of 5%) relative to the Preissmann scheme.
3. The time of occurrence in the peak is also predicted substantially to the same degree of accuracy as the MC method.

These results are for a wide range of IH's , having normal, steep, triangular and log pearson type III patterns. The MLT method gives comparable accuracies in a majority of cases to those of the MC method.

Special Features Of The MLT Method:

In addition to the above performance characteristics the following general advantages of the MLT method are worth noting:

1. In the use of the MC method, the IH has to be routed in through various sub reaches in between whereas in the MLT method, the IH is routed in a lumped manner over the full reach.
2. The MC method has to satisfy Courant stability condition whereas, the MLT method does not have any stability conditions to be taken care off.
3. The Programming and Computation efforts are considerably less in the MLT method when compared to the Preissmann and the MC methods.

CHAPTER-6

CONCLUSIONS AND RECOMMENDATIONS

6.1 The basic Muskingum method, the Muskingum-Cunge(MC) method and the various improvements of MC method are discussed in this study. The forward finite difference scheme is changed into a Leap frog finite difference scheme, called as the MCLF method. By segregating the IH and using the IH and using MC method a new model called SMC is proposed. An approach for routing the flood in a lumped manner, called as MLT method is proposed.

6.2 The following conclusions are drawn after comparing the MC method with the implicit Preissmann scheme:

1. The MC method over predicts the peak relative to the implicit Preissmann scheme.
2. The time of occurrence of the peak is also over predicted in the MC method relative to the implicit Preissmann scheme.
3. The MC method, predicts the initial flows more than the implicit Preissmann scheme.

6.3 The following conclusion is drawn after numerical experimentation on the MCLF model:

1. The higher order schemes are not desirable in the MC method and no improvement can be achieved by this way.

6.4 On comparing the SMC model with the MC and the Preissmann methods, by numerical experimentation on five sets of data the following conclusions are drawn:

1. The SMC model predicts the initial flows better than the MC method upto the chosen segregating discharge (Q_{50}) for all inflow hydrographs. Beyond Q_{50} , the SMC predicts the outflows to the same accuracy as the MC method.
2. Thus, with the SMC method, the efficacy of the MC method is generally improved.

6.5 The following significant conclusions are drawn after the numerical experimentation and comparison of the MLT model with the Preissmann methods:

1. The MLT model predicts outflow peak values and its time of occurrence to the same degree of accuracy as that of the MC method.
2. The MLT model has a distinction of being a lumped model and it can be programmed easily. There is no restriction of Courant conditions on the time step size as in MC method.
3. The MLT model is an alternate, viable to the MC method.

RECOMMENDATIONS:

1. Further studies are needed in the MC method to properly estimate the routing parameters K and θ .
2. To know the behavior of the SMC method for complex hydrographs, more experimentation is desirable.
3. As the MLT method is a viable alternative to the MC method, it is suggested that further work be carried out in the estimation of routing parameters K and θ applicable to the MLT method.

REFERENCES

1. Aldama A.A., "Least-Squares Parameter estimation for Muskingum flood routing," *Journal of Hydraulics Division, ASCE.*, Vol116 No.Hy4, April 1990, pp580-586.
2. Chaudhary, M.H., "Applied Hydraulic Transients," *Von Nostrand Reinhold Co.*, New York, N.Y., U.S.A. 1987.
3. Chow, V.T., "Open Channel hydraulics," *MacGraw hill Book co., Inc.*, New York, 1959.
4. Chow, V.T., Maidment, R.D., Mays, W.L., "Applied Hydrology," *MacGraw hill Book Co., Inc.*, 1988.
5. Cooley, R.L., and Moin, S.A., "Finite Element Solution of Saint-Venant equations," *Journal of Hydraulics Division, ASCE*, HY6, June 1976, pp759-775.
6. Cunge, J.A., "On the Subject of a Flood Propagation method (Muskingum method)," *Journal of Hydraulic Research, IAHR*, Vol17., No.2., 1969, pp205-230.
7. Diskin, M.H., "On the Solution of the Muskingum Flood routing Equation," *Journal of Hydrology*, Vol5, 1967, pp163-170.

8. Dooge, J.C.I., Strupczewski, W.G., and Napiorkowski, J.J., "Hydrodynamic derivation of Storage Parameters of the Muskingum model," *Journal of Hydrology*, Vol 154, 1984, pp 371-387.
9. Dooge, J.C.I., Perumal, M., Wang, Q.J., "Step Function response of Muskingum Reach," *Journal of Irrigation and Drainage Engg.*, ASCE, Vol 119, No. 2, April 1993, pp 410-415.
10. Gill, M.A., "Response of Muskingum equation to Step input," *Journal of Irrigation and Drainage Engg.*, ASCE, Vol 114 No. 4 pp 736-738.
11. Gille, J.C., Pelegrin, M.J., DeCaulline, P., "Feed back Control Systems Analysis, Synthesis, and Design" MacGraw hill Book co., Inc., Newyork, N.Y., 1959, pp 123-125.
12. Karmegam, M., "Stratified Muskingum Routing," *VIII Congress of APRD, IAHR, Proceedings Vol 1*, pp A66-A87.
13. Koussis, A., "Theoretical Estimation of Flood Routing Parameters," *Journal of the Hydraulics division*, ASCE, Vol 104, No. HY1, Jan 1978, pp 109-115.
14. Koussis, A., "Comparison of Muskingum method difference schemes," *Journal of the Hydraulics division*, ASCE, Vol 106, HY5, 1980, pp 925-929.

15. Kulandiaswamy, V.C., "A note on Muskingum method of Flood Routing," *Journal of Hydrology*, Vol4, 1966, 273-276.
16. Mahmood K., and Yevjevich., "Unsteady flow in Open Channels," *Water Resources publications*, P.O.Box 303, Fort Collins, Colorado, USA, 1975.
17. Perumal, M., Discussion of " Response of Muskingum Equation of Step Input," *Journal of Irrigation and division*, ASCE, Vol115, No.4, pp605-606.
18. Ponce, V.M., and Yevjevich, V., "The Muskingum-Cunge method with variable parameters," *Journal of Hydraulics division*, ASCE, Vol104, No.12, Dec1978, pp1663-1667.
19. Ponce, V.M., "Simplified Muskingum Routing Equation," *Journal of Hydraulics division*, ASCE, Vol105, NO.1, Jan1979, pp85-91.
20. Raudikivi., " Hydrology - An Advanced Introduction to Hydrological processes and modeling," *Pergamon press*, 1979.
21. Singh, V.P., and McCann, R.C., "Some notes on Muskingum method of Flood routing," *Journal of Hydrology*, Vol48, 1980, pp343-361.
22. Singh, V.P., "Hydrologic Systems-Rainfall Runoff Modeling," Vol1, *Prentice-Hall, Inc.*, Englewood Cliffs, N.J., 1988.

23. Subramanya.K., "Flow in Open Channels," Tata McGraw-Hill Publishing Co., Ltd., NewDelhi, 1991.
24. Subramanya.K., "Engineering Hydrology," Tata McGraw-Hill Publishing Co., Ltd., NewDelhi, 1988.
25. Wang Guange-Te, Singh.V.P., "Muskingum method with variable parameters for Flood Routing in Channels," *Journal of Hydrology*, Vol134, 1992, pp57-76.
26. Weinmann, P.E., and Laurenson, E.M., "Approximate Flood Routing Methods : a Review," *Journal of Hydraulics Division*, Vol105, No.12, pp1521-1536.

APPENDIX-1

PRIESSMANN SCHEME FOR NUMERICAL SOLUTION OF ST. VENANT EQUATIONS

For the hydrodynamic flows the governing Saint-Venant equations constitute a set of non-linear, first-order, hyperbolic partial differential equations. For the Saint-Venant equations, general analytical solutions are not available except for only a few idealized cases. Therefore, they are generally solved by using numerical techniques. In this section, one such scheme, originally developed by Preissmann(1961) is presented.

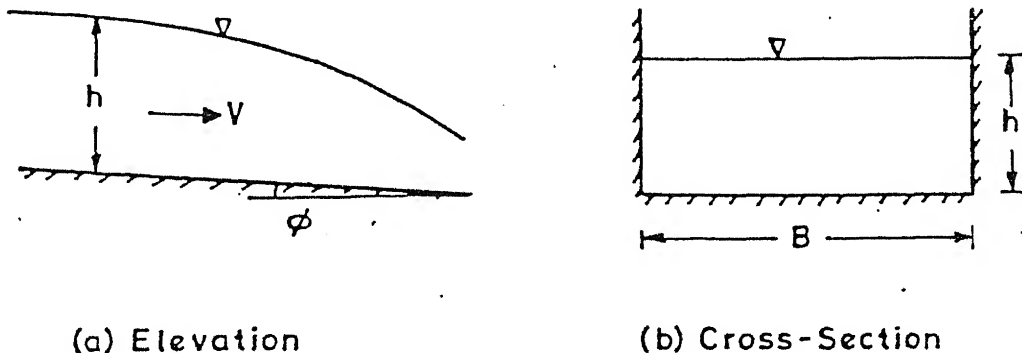


Fig. A.1 Definition Sketch

In a wide rectangular prismatic channel as shown in Fig. A.1, the Saint-Venant equations are derived using the following assumptions.

1. The flow is one-dimensional in the direction of channel.
2. The channel is straight and prismatic.

3. The pressure distribution is hydrostatic.
4. The velocity distribution at a channel section is uniform.
5. The transient-state friction losses may be computed using formulas for the steady state conditions.
6. The bed slope of channel bottom is small such that the cosine of the angle made by the averaged bed profile with the horizontal can be regarded as unity.

The Saint-Venant equations based on principles of mass and momentum to a differential control volume [2]. The conservative form of these equations are :

$$\frac{\partial A}{\partial t} + \frac{\partial Q}{\partial x} = 0 \quad (A1)$$

$$\frac{\partial Q}{\partial t} + \frac{\partial}{\partial x} \left(\frac{Q^2}{A} + g I \right) = g A (s_o - s_f) \quad (A2)$$

where

$$I = \int_0^{y(x)} (y - \zeta) o(\zeta) d\zeta$$

in which $o(\zeta)$ = width of cross-section

ζ = depth integration variable

The non-conservative form of Saint-Venant equations are:

$$\frac{\partial y}{\partial t} + v \frac{\partial y}{\partial t} + y \frac{\partial v}{\partial x} = 0 \quad (A3)$$

and

$$\frac{\partial v}{\partial t} + v \frac{\partial v}{\partial x} + g \frac{\partial y}{\partial x} = g(s_o - s_f) \quad (A4)$$

Where y is the depth of flow; v is the flow velocity, g is the acceleration due to gravity; s_o is the slope of channel bottom; s_f is the slope of energy gradient line; x is the distance measured downstream direction, and t is the time of computation. s_f is evaluated using Manning's formula for a wide rectangular channel.

$$s_f = \frac{n^2 v^2}{y^{4/3}}$$

where n is the Manning's roughness coefficient.

PREISSMANN SCHEME:

Preissmann scheme is basically a four-point weighted implicit finite difference scheme, used to transform the non-linear partial differential Saint-Venant equations into non-linear algebraic equations. Referring to Fig. A.2 a function $f(x,t)$ is represented by its values on a grid with f_j^n denoting the value at the j^{th} grid and n^{th} time interval. Δx_j is the non-dimensional grid spacing between the $(j+1)^{\text{th}}$ and j^{th} point. Non-dimensionalisation is explained in the next section. Then for a non-dimensional time step Δt , the four-point weighted difference approximations for the time and space derivatives f_t and f_x for a cell defined by the four points $(n,j), (n+1,j), (n,j+1), (n+1,j+1)$ are:

$$f_t = \frac{f_{j+1}^{n+1} - f_{j+1}^n + f_j^{n+1} - f_j^n}{2 \Delta t} \quad (\text{A5})$$

$$f_x = \alpha \left[\frac{f_{j+1}^{n+1} - f_j^{n+1}}{\Delta x_j} \right] + (1-\alpha) \left[\frac{f_{j+1}^n - f_j^n}{\Delta x_j} \right] \quad (\text{A6})$$

and

$$f(x,t) = \alpha \left[\frac{f_{j+1}^{n+1} + f_j^{n+1}}{2} \right] + (1-\alpha) \left[\frac{f_{j+1}^n + f_j^n}{2} \right] \quad (\text{A7})$$

where α is a weighing factor varying from 0.5 to 1.0.

Preissmann scheme is first order accurate in space and second-order accurate in time.

BOUNDARY CONDITIONS:

In the Preissmann scheme, from N nodes $(2N-2)$ algebraic equations are obtained from the Saint-Venant equations. The remaining two equations are obtained from boundary conditions. In the subcritical flows, only one boundary condition is sufficient.

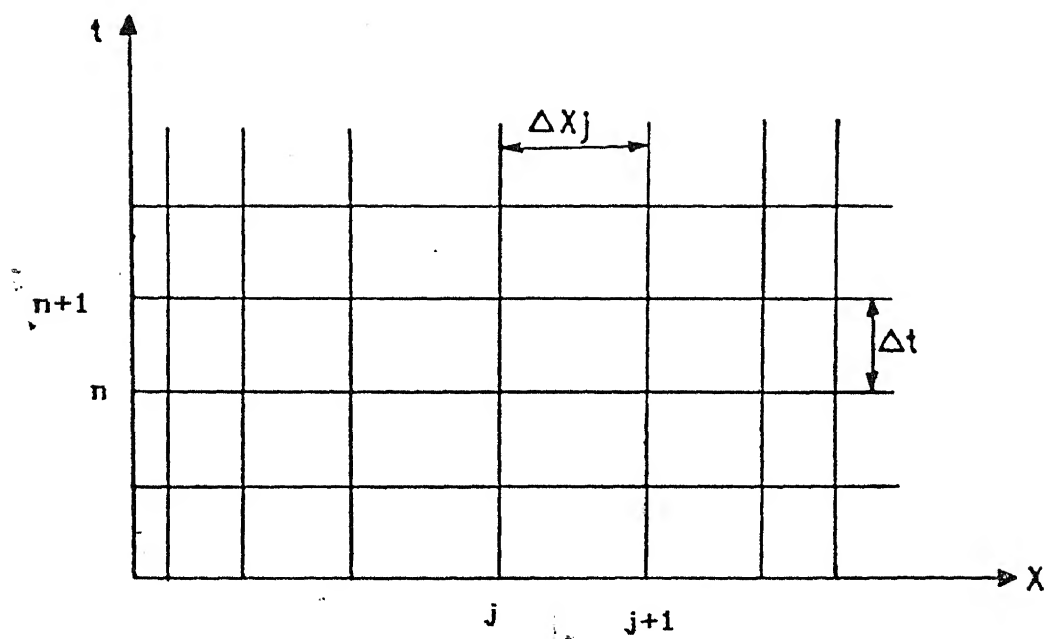


Fig. A.2 Computational grid

The downstream can be evaluated by second order extrapolation. The upstream boundary condition is specified by a hydrograph. At the downstream end it is extrapolated by a second-order extrapolation

$$\frac{\partial^2 h}{\partial x^2} = 0.0$$

These non-linear equations are solved using Newton-Raphson method[2].

NON-DIMENSIONALISATION:

The Saint-Venant equations are non-dimensionalised using channel length L_o as distance parameter and initial steady uniform flow depth Y_o as the depth scale parameter.

The initial steady state uniform flow velocity, v_o is taken as the velocity scale parameter and is obtained using Manning's equation

$$v_o = \frac{1}{n} Y_o^{2/3} S_o^{1/2} \quad (A8)$$

The time scale parameter, T_o is equal to the time required to travel a distance of L_o with a wave speed of $\sqrt{gY_o}$.

$$\text{i.e.} \quad T_o = \frac{L_o}{\sqrt{gY_o}} \quad (A9)$$

Various other dimensionless variables (shown with a bar) are defined as

$$\bar{x} = \frac{x}{L_o} \quad (A10)$$

$$\bar{t} = \frac{t}{T_o} \quad (A11)$$

$$\bar{y} = \frac{y}{Y_o} \quad (A12)$$

$$\bar{v} = \frac{v}{v_o} \quad (A13)$$

Substitution of all these Eqs(A8-A13) in Eqs A3 and A4, it results

$$a_o \frac{\partial \bar{y}}{\partial \bar{t}} + b_o \bar{v} \frac{\partial \bar{y}}{\partial \bar{x}} + c_o \bar{y} \frac{\partial \bar{v}}{\partial \bar{x}} = 0.0 \quad (A14)$$

and

$$d_o \frac{\partial \bar{v}}{\partial \bar{t}} + e_o \bar{v} \frac{\partial \bar{v}}{\partial \bar{x}} + f_o \frac{\partial \bar{y}}{\partial \bar{x}} = g_o (s_o - p_o \bar{s}_f) \quad (A15)$$

where a_o , b_o , c_o , d_o , e_o , f_o and g_o are dimensionless coefficients. But p_o is dimensionless constant and it becomes dimensionless when combined with

$$\bar{s}_f = \frac{n^2 \bar{v}^2}{\bar{y}^{4/3}} \quad (A16)$$

The best set of coefficients after non-dimensionalisation are:

$$a_o = 1.0 \quad (A17)$$

$$b_o = \frac{v_o T_o}{L_o} \quad (A18)$$

$$c_o = b_o \quad (A19)$$

$$d_o = \frac{v_o}{g T_o} \quad (A20)$$

$$e_o = \frac{v_o^2}{g L_o} \quad (A21)$$

$$f_o = \frac{y_o}{L_o} \quad (A22)$$

$$g_o = 1.0 \quad (A23)$$

$$\text{and } p_o = \frac{v_o^2}{y_o^{4/3}} \quad (A24)$$

PROGRAM: A value of $\alpha = 0.66$ is used in the Preissmann scheme. The Preissmann scheme is programmed and tested against Moin and cooley data[5]. The error between the Moin's data and the outflow values obtained by the Preissmann scheme are in permissible limits. This implicit Preissmann scheme is used as a benchmark to compare the proposed models in this study.

APPENDIX-2

INPUT DATA

The following data sets were used in this study for the numerical experimentation.

Set # 1. (Cooley and Moin, 1976).

A rectangular channel 20ft(6.1m) wide and 2 miles(3.2km) long carrying a steady uniform discharge of 833.49 cfs(23.34 m³/s) at 6ft (1.83m) depth is subjected to an upstream flood wave with a peak of 2000 cfs (56m³/s) increasing linearly in a period of 20 min. This upstream flow decreases linearly from its peak of 2000cfs to 833.49cfs(57m³/s to 23.34 m³/s) in 40 min. Additional properties given by Veismann .et.al are $s_o = 0.0015$ ft/ft and $n=0.02$. The problem is to follow the translation of the flood wave down the stream.

Set # 2. (Cooley and Moin, 1976)

A hydrograph described by the Pearson Type III distribution is routed down a wide [5000 ft(1500 m) was used herein]. Open channel having length of 100 miles(160 km). $s_o = 1/5280$ ft/ft, and $n = 0.03$. The initial depth and discharge are 5 ft(1.5m) and 49766 cfs (1390m³/s) respectively, and all subsequent discharges are given by

$$Q(t) = Q_o \left[1 + (\rho - 1) \left(\frac{t}{\tau} \right) \right]^{[1/(\gamma - 1)]} e^{[1 - (t/\tau)][1/(\gamma - 1)]}$$

in which $\rho = Q_{\max}/Q_0 = 20$; $\gamma = 1.2$; τ = the time at which the maximum occurs; and Q_0 , the initial upstream discharge.

Set # 3 (Raudikivi, 1979)

The hydrograph at the upstream end of a river reach ($x=0$) is as follows:

t hours:	0	1	2	3	4	5	6	7	8	9
$Q \text{ m}^3/\text{s}$:	10	12	18	28.5	50	78	107	134.5	147	150

t hours:	10	11	12	13	14	15	16		17
$Q \text{ m}^3/\text{s}$:	146	129	105	78	59	45	33		24

t hours:	18	19	20	21	22	23	24		25
$Q \text{ m}^3/\text{s}$:	17	12	10	10	10	10	10		10

t hours:	26	27	28
$Q \text{ m}^3/\text{s}$:	10	10	10.

Length of reach is 18000 m, $s_0 = 0.0005$. Manning's roughness coefficient = 0.02. Breadth of channel = 50 m. Assume the channel is rectangular in cross-section.

Set # 4 (Raudikivi, 1979)

The hydrograph at the upstream end of a river, reach ($x=0$) time $t=0$ is as follows:

t hours:	0	1	2	3	4	5	6	7	8	9
$Q \text{ m}^3/\text{s}$:	10	20	52	100	141	150	144	130	114	100

t hours:	10	11	12	13	14	15	16	17
Q m ³ /s :	86	73	61	50	41	32	25	19

t hours:	18	19	20	21	22	23	24	25
Q m ³ /s :	14	11	10	10	10	10	10	10

t hours:	26	27	28
Q m ³ /s :	10	10	10.

Length of reach is 18000 m, $s_o = 0.0005$. Manning's roughness coefficient = 0.02. Breadth of Channel is 50 m. Assume a rectangular cross-section.

Set # 5

A rectangular channel 60.0 wide and 30 Km long carrying a steady uniform discharge of 50.0 m³/s is subjected to upstream flood wave with a peak of 2000 m³/s increasing linearly in a period of 10 hours. This upstream flow decreases linearly from its peak of 2000 m³/s ^{to} 50 m³/s in 20 hours. Additional properties are $s_o = 0.0015$ and $n = 0.02$.

Set # 6

The hydrograph at the upstream end of a river reach ($x=0$) is as follows:

T hours	Discharge(m^3/s)	T hours	Discharge(m^3/s)
0	10.00	15	60.24
1	25.28	16	43.48
2	65.28	17	28.28
3	114.72	18	17.92
4	154.72	19	11.75
5	170.00	20	10.00
6	168.25	21	10.00
7	163.08	22	10.00
8	154.72	23	10.00
9	143.53	24	10.00
10	130.00	25	10.00
11	114.72	26	10.00
12	140.63	27	10.00
13	123.30	28	10.00
14	85.28		

Length of reach is 30000 m, $s_o = 0.0005$. Manning's roughness coefficient = 0.02. Breadth of Channel is 50 m. Assume a rectangular cross-section.

Set # 7

The hydrograph at the upstream end of a river reach($x=0$) is as follows:

T hours	Discharge(m^3/s)	T hours	Discharge(m^3/s)
0	10.00	15	50.00
1	25.28	16	36.47

2	65.28	17	53.78
3	114.72	18	70.90
4	154.72	19	95.43
5	170.00	20	65.75
6	168.25	21	51.00
7	163.08	22	30.60
8	154.72	23	15.23
9	143.53	24	10.00
10	130.00	25	10.00
11	114.72	26	10.00
12	98.36	27	10.00
13	81.64	28	10.00
14	65.28		

Length of reach is 30000 m, $s_o = 0.0005$. Manning's roughness coefficient = 0.02. Breadth of Channel is 50 m. Assume a rectangular cross-section.

Set # 8

The hydrograph at the upstream end of a river reach ($x=0$) is as follows:

T hours	Discharge(m^3/s)	T hours	Discharge(m^3/s)
0	10.00	15	50.00
1	25.28	16	36.47
2	65.28	17	43.78
3	114.72	18	65.90
4	154.72	19	81.43

5	170.00	20	55.75
6	168.25	21	31.00
7	163.08	22	20.60
8	154.72	23	10.00
9	143.53	24	10.00
10	130.00	25	10.00
11	114.72	26	10.00
12	98.36	27	10.00
13	81.64	28	10.00
14	65.28		

Length of reach is 30000 m, $s_o = 0.0005$. Manning's roughness coefficient = 0.02. Breadth of Channel is 50 m. Assume a rectangular cross-section.